



UNIVERSITÀ DEGLI STUDI DI SALERNO



UNIVERSITÀ DEGLI STUDI DI SALERNO
Dipartimento di Farmacia

Dottorato di Ricerca
in **Scienze del Farmaco**
Ciclo XXIX — Anno accademico 2016/2017

Tesi di Dottorato in

***Chronotherapeutic Drug Delivery in Early
Morning Pathologies: Design and
Production of new NSAIDs/SAIDs
polysaccharide-based systems***

Dottorando

Tutore

Dott. *Andrea Cerciello*

Chiar.ma Prof.ssa *Paola Russo*

Coordinatore: Chiar.mo Prof. *Gianluca Sbardella*

TABLE OF CONTENTS

LIST OF PUBLICATIONS

AIM AND OUTLINE OF THE PhD PROJECT	I
INTRODUCTION.....	1
1. Chronobiology and Chronotherapy.....	2
1.1 Diseases affected by circadian rhythms	3
1.2 Early morning pathologies (EMPs): Rheumatoid Arthritis	5
1.2.1 Conventional drugs used in RA treatment	7
1.3 Innovative oral treatments of RA: Chronotherapeutics	10
2. Drug-delivery technology for chronotherapeutics	11
2.1 Oral controlled Drug Delivery Systems	12
2.2 Natural polysaccharides/carbohydrate polymers	13
2.3 Advantages and opportunities of polysaccharides-hydrogel based beads for the design of ChDDS	17
2.4 Prilling technique for the production of hydrogel based beads.....	18
RESULTS AND DISCUSSION	21
SECTION A:	23
Design and development of chronotherapeutic systems loaded with short half-life NSAIDs.....	23
SECTION A PART 1:.....	25
Ketoprofen loaded alginate beads: <i>in vitro/in vivo</i> characterization	25
SECTION A PART 2:.....	39
Core-shell beads for delayed ketoprofen oral delivery	39
SECTION A PART 3:.....	51
Ketoprofen lysine salt controlled release systems: Alginate vs ALM-pectin ..	51
SECTION B:	63
Design and development of ChDDS loaded with prednisolone as model SAIDs	63
SECTION B PART1:	67
Study of the effect of divalent cation and their combination on alginate beads loaded with prednisolone	67
SECTION B PART 2:	81
Study of the effect of alginate concentration as well as drug/polymer ratio on alginate beads	81
SECTION B PART 3:.....	95
Design and formulation of floating alginate beads and their <i>in vitro/in vivo</i> characterization and performances.....	95
SECTION C:	105
Design and development of chronotherapeutic systems loaded with long half-life NSAIDs.....	105
Gastroretentive systems to sustain piroxicam release: <i>in vitro</i> and <i>in vivo</i> characterization	107
MATERIALS & METHODS	123

Materials	123
Methods	123
REFERENCES	133

LIST OF PUBLICATIONS

Papers, Chapter books, Conference Proceedings and Communications

Papers:

A. Cerciello, G. Auriemma, S. Morello, R.P. Aquino, P. Del Gaudio, P. Russo. “Prednisolone delivery platforms: Capsules and Beads Combination for a Right Timing Therapy”, *PLoS ONE*, **2016** 11(7): e0160266. doi:10.1371/journal.pone.0160266.

A. Cerciello, G. Auriemma, P. Del Gaudio, M. Cantarini, R.P. Aquino. “Natural polysaccharides platforms for oral controlled release of ketoprofen lysine salt”, *Drug development and industrial pharmacy*, **2016**, dx.doi.org/10.1080/03639045.2016.1195401.

A. Cerciello, G. Auriemma, P. Del Gaudio, F. Sansone, R. P. Aquino, P. Russo. “A novel core–shell chronotherapeutic system for the oral administration of ketoprofen”. *Journal of Drug Delivery Science and Technology*, **2016**, 32, 126-131.

A. Cerciello, G. Auriemma, S. Morello, A. Pinto, P. Del Gaudio, P. Russo, R.P. Aquino. “Design and In Vivo Anti-Inflammatory Effect of Ketoprofen Delayed Delivery Systems”, *Journal of Pharmaceutical Sciences* **2015** Feb; DOI 10.1002/jps.24554 Epub 2015 Jun 18.

Submitted Papers:

G. Auriemma, **A. Cerciello**, A. Pinto, S. Morello, R. P. Aquino. “Floating gastroretentive system for piroxicam sustained release: design, characterization and in vivo prolonged anti-inflammatory effect”. *Submitted 2016*.

A. Cerciello, P. Del Gaudio, V. Granata, M. Sala, R. P. Aquino, P. Russo. “Synergistic effect of divalent cations in improving technological properties of cross-linked alginate beads”. *Submitted 2016*.

Chapter book

G. Auriemma, **A. Cerciello** and R. P. Aquino. “NSAIDs: design and development of innovative oral delivery systems”. Part of the Book “Nonsteroidal Anti-inflammatory Drugs”. *Submitted 2017* to InTech Open.

Proceedings with ISBN:

A. Cerciello, G. Auriemma, P. Del Gaudio, F. Sansone, R. P. Aquino, P. Russo, “A novel core-shell chronotherapeutic system for the oral administration of ketoprofen.”, CRS, Università Federico II, Napoli, 12-14 Novembre 2015.

ISBN:978-88-941404-0-8.

Proceedings with ISSN:

A. Cerciello, M. Pellegrino, P. Del Gaudio, R.P. Aquino, P. Russo, “Improved technological properties of cross-linked alginate microspheres: the synergistic effect of divalent cations.”, 11th Central European Symposium on Pharmaceutical Technology, Belgrado, Serbia 22 – 24 Settembre 2016.

ISSN 2217-8767.

List of communications:

P. Del Gaudio, F. De Cicco, P. Russo, **A. Cerciello**, E. Reverchon, R. P. Aquino. “A combined technique based on prilling and supercritical drying for the production of doxycycline loaded aerogel beads”, Third International Seminar on AEROGELS Synthesis – Properties – Applications, Sophia Antipolis, Francia, 22 – 23 Settembre 2016.

F. De Cicco, **A. Cerciello**, P. Russo, R. P. Aquino, P. Del Gaudio “Combination of co-axial prilling and supercritical drying for the formulation of doxycycline particles for wound healing.”, 20th International Symposium on Microencapsulation, Northeastern University, Boston, MA, USA 1-3 Ottobre 2015.

A. Cerciello, F. De Cicco, M.C Pellegrino, R. P. Aquino, P. Del Gaudio, P. Russo “Prilling as a versatile technique for the development of controlled delivery systems containing anti-inflammatory drugs.”, 20th International Symposium on Microencapsulation, Northeastern University, Boston, MA, USA 1-3 Ottobre 2015.

Oral communication

A. Cerciello, G. Auriemma, R. P. Aquino, P. Russo “Strategie formulative per il rilascio controllato di farmaci anti-infiammatori nelle early morning pathologies”, XV Edizione Summer School per la formazione avanzata in discipline Tecnologico-Farmaceutiche, Università degli Studi di Salerno, Fisciano 9-12 Settembre 2015.

G. Auriemma, **A. Cerciello**, S. Morello, A. Pinto, P. Russo, P. Del Gaudio, R. P. Aquino “Novel NSAIDs controlled delivery systems obtained by prilling: design, in vitro characterization and in vivo effects”, XXIII National Meeting on Medicinal Chemistry, Università degli Studi di Salerno, Fisciano 6-9 Settembre 2015.

A. Cerciello, P. Russo, G. Auriemma, R. P. Aquino “Alginate-prednisolone controlled delivery systems: design and in vitro characterization”, 9th A.It.U.N. Annual Meeting, Università di Milano, Milano 25-27 Maggio 2015.

A. Cerciello, G. Auriemma, S. Morello, A. Pinto, P. Russo, P. Del Gaudio, R. P. Aquino “Time-specific controlled release dosage formulations of NSAIDs: design, in vitro and in vivo characterization”, XIV Corso Permanente di

Aggiornamento per i Dottorandi del Settore Tecnologico Farmaceutico,
Università della Calabria, Cosenza 22-26 Settembre 2014

AIM AND OUTLINE OF THE PhD PROJECT

In the last few years there is a continuous research in the development of processes and techniques that allow to transform active pharmaceutical ingredients (APIs) into new dosage forms (Buttini, Colombo et al. 2012). The so-called “new drug delivery systems” are able to modify biopharmaceutical and pharmacokinetic properties of the API, to control its release rate, and to obtain a time specific delivery, reducing side effects. All these aspects may increase the therapeutic efficacy and the safety of both new and old drugs allowing an optimal use in clinical practice (Tiwari, R. et al. 2012). Particularly, in the field of modified release dosage forms, there has been a growing interest in time specific oral delivery, which generally refers to the pre-programmed release of drugs following administration to achieve improved therapeutic efficacy. These systems constitute a relatively new class of devices, the importance of which is especially connected with the recent advances in chronopharmacology (Roy and Shahiwala 2009; Bethke, Huennemeyer et al. 2010; Ohdo, Koyanagi et al. 2010). Chronopharmacology demonstrating the importance of biological rhythms in drug therapy, has led to a new approach to the development of drug delivery systems which are required to enable the drug release timing and control. In fact, treating diseases affected by the circadian rhythms, such as “early morning pathologies”, requires a desired concentration of drug available at expected times (Smith, Neutel et al. 2001; Ambedkar Sunil, Venkata Srikanth et al. 2013). This effect may be assured by device releasing no drug within the time gap and delivering the optimal amount at certain point correspondent to symptoms peak (Lemmer 1991; Youan 2004; Lévi and Okyar 2011). Diseases with established circadian cycle show day-night patterns in the onset and symptoms exacerbation, usually with peaks in the morning and decrease throughout day. Moreover, the plasma concentration of C-reactive protein and interleukin-6 has been shown to follow a circadian rhythm in chronic inflammatory-based diseases such as rheumatoid

arthritis (Arvidson, Gudbjörnsson et al. 1994). The conventional treatment of these pathologies consists of daily administrations of non-steroidal or steroidal anti-inflammatory drugs (NSAIDs or SAIDs), which are often unable to coordinate drug release with clinical symptoms onset resulting in inefficient therapy and poor patient compliance.

Moreover, as reported elsewhere, in the case of the management of chronic inflammation (rheumatoid arthritis) and associated pain, NSAIDs may be very effective if the drug is administered at least 4-6 hours before the pain reaches its peak (Gazzaniga, Palugan et al. 2008; Tavares, Wells et al. 2010). Therefore, many approaches have been used to design pharmaceutical dosage forms tailored to follow the human chronobiological rhythm (Hermida, Ayala et al. 2007; Smolensky and Peppas 2007; Lévi F and A. 2011) and, in the last few years, micro-technologies have been applied as innovative and efficient tool in drug delivery (Singh, Hemant et al. 2011)

Several methods and techniques are potentially useful for the preparation of polymeric microparticles, such as spray drying, fluid bed coating, solvent evaporation, coacervation phase separation, prilling etc. The choice of a specific microencapsulation technology is related to the polymer nature, the chemical features of drug, the desired particles size as well as to the reproducibility and ease to scale ability of the method (Dalmoro, Barba et al. 2012).

In particular, design and production of hydrophilic mono- or multi-layered microparticles like hydrogel based beads thanks to their biocompatibility and ability to control drug release may be one of the most versatile strategies to produce chronotherapeutic drug delivery systems (ChDDS).

The last decade has seen a shift from empirical formulation efforts to an engineering approach based on a better understanding of particle formation in the various microencapsulation techniques. The research group in Pharmaceutical Technology of the University of Salerno has developed

various advanced drug delivery systems that can dose orally, being less expensive and more compliant for the patients and at the same time extremely effective considering the specificity of early morning pathologies. In particular, the group has acquired competence in particle design of polymeric hydrogel microparticles (gel-beads) able to control rate, period of time and targeting of delivery. The processing method of choice is the relatively new and effective laminar jet break-up/prilling, using vibrating technology, which allows the production of microparticles, in mild operative conditions, by breaking apart a laminar jet of polymer solution into a row of mono-sized drops under the influence of a superimposed vibration. The fall of the droplets into a polymer gelation solution produce solidified beads.

Prilling has the capability to produce mono-dispersed, homogenous-shaped microparticles, with a narrow size distribution, using a short production time and it is easy to scale. However, particle engineering requires large experimental research into parameters that influence particle formation for a deeper understanding of particle formation process.

In this context, this PhD project focused on the development by prilling of hydrogel based beads as controlled/delayed drug delivery systems for the chronotherapeutic treatment of rheumatoid arthritis with specific emphasis on the underlying particle formation mechanisms and design concepts. The beads were designed for a range of functions such as stabilization of the active, transport and targeting of the dose and mainly for release modulation achieving early morning pathologies requirements. Generally biodegradable and with excellent biocompatibility natural polymers are very attractive materials in microencapsulation and also are relatively inexpensive.

Carbohydrate polymers, such as alginate and amidated low methoxyl (ALM) pectin were selected as polymeric carriers thanks to their ability to form hydrogels in mild operative conditions. It is well known that these polymers have gelling properties mainly due to the carboxyl groups able to engage in

coordination bonds with divalent cations forming a so called “egg-box” structure at ambient temperature. This property opens the possibility of encapsulating drugs, cells, proteins and other bioactive compounds under mild conditions, while maintaining their full biological activity. However, polymer type and its concentration, as well as cross-linking conditions are key parameters strongly affecting gelled microparticles performance. Therefore, influence of feed composition, cross-linking ions (Ca^{2+} , Zn^{2+}), gelation times and gelling bath temperature on beads characteristics were investigated.

Moreover, prilling process was deeply studied to optimize the final production conditions (polymeric solution flow, viscosity at nozzle, frequency and amplitude of the vibration, distance between the vibrating nozzle and the gelling bath), because of the many process and formulation variables that need to be tuned correctly to achieve the desired results, to link feed materials properties and process parameters to the resultant particle properties.

Engineered beads were used as carrier for anti-inflammatory drugs with different chemical/pharmacological (NSAIDs or SAIDs) and pharmacokinetic characteristics (with short or long half-life), as well as different biopharmaceutical features in terms of solubility and permeability in accordance with the Biopharmaceutical Classification System (BCS).

Particularly, the first part of the project was aimed to produce ChDDS loaded with ketoprofen and ketoprofen lysine salt as models of short half-life NSAIDs with different biopharmaceutical classification (Results Section A). Based on the acquired know-how, during the second part the research moved to the design and the development of ChDDS loaded with prednisolone as model SAID (Results Section B). The third part of the PhD project focused on the development of ChDDS containing piroxicam as model long half-life NSAID (Results Section C).

According to the features of the selected drugs, different experiments were conducted in order to set the optimal formulation and prilling operative

conditions. In this way, gel-beads with proper morphological characteristics, good drug content (DC) and encapsulation efficiency (EE) values as well as controlled and delayed drug release profiles were produced. Formulations showing the best *in vitro* performances were selected as starting material for the preparation of more complex drug delivery technology platforms enabling an improved delayed delivery of the selected drugs. To design “smart” and efficient oral platforms for drug delivery, starting from comprehensive knowledge of the pharmacological and pharmaceutical properties of the drugs and polymers, different creative manufacturing processes were proposed:

- Charge of drug-carrying beads into specific DR[®] capsules to obtain final dosage form further delaying the drug release,
- Core/shell microparticles consisting of a core (Zn-pectin ALM beads) and a gastro-resistant shell formed by methacrylic acid - methyl methacrylate copolymer (Eudragit S100),
- Floating beads which maximizing the gastric emptying process are able to prolong residence time in the stomach, obtained producing beads with specific excipients (gas-generating agent or low density/foaming polymers) able to confer floating ability to the final dosage form.

All the platforms showed high effectiveness in sustaining the release over several hours and the potential to provide a viable alternative to conventional anti-inflammatory formulations.

Moreover, the *in vivo* anti-inflammatory effect of optimized beads and platforms was studied using a modified protocol of carrageenan induced oedema in rat paw. The possibility to correlate the delayed and sustained drug release profiles evaluated *in vitro* with *in vivo* performance (slow release of NSAIDs and SAIDs in rats) is essential in the pharmaceutical development in order to reduce development time and optimize the final formulation.

INTRODUCTION

1. Chronobiology and Chronotherapy

The Chronobiology is the study of biological rhythms and their mechanisms and it's clearly relevant in the fields of medicine, pharmacology, and drug delivery (Smolensky and Peppas 2007).

Particularly, the term "chrono" basically refers to the study that every metabolic happening follows rhythmic changes in time (Surve, Sapakal et al. 2013). Circadian rhythms (CRs) are, endogenous oscillations that occur with a periodicity of about 24 h and regulate many body functions like-metabolism, sleep pattern, hormone production etc. (Neeharika and Jyothi 2015)

CRs are generated by suprachiasmatic nuclei located in the hypothalamus. This latter receives daily inputs from environmental cycles and generates rhythmic physiological outputs such as rest-activity, body temperature and hormonal secretions (Lévi and Okyar 2011).

Several physiological processes in humans change in a rhythmic manner, in synchrony with the internal biological clock (Neeharika and Jyothi 2015).

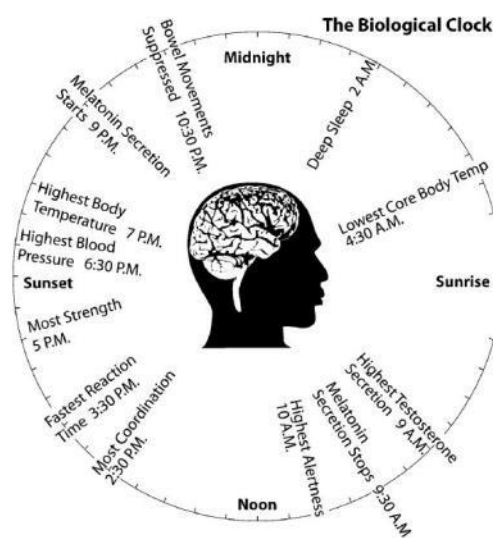


Figure.1 Human circadian time structure

(<https://goinggentleintothatgoodnight.com/tag/circadian-rhythm/>).

In addition to many biological functions, different diseases show rhythmic changes with time. Therefore, in view of this considerations based on chronobiology, in the recent years researches focus their attention on chronotherapy and chronopharmacology.

Chronotherapy refers to a treatment method in which *in vivo* drug availability is timed to match rhythms of disease in order to optimize therapeutic outcomes and minimize side effects (Surve, Sapakal et al. 2013). It's based on the observation that there is a relationship between the peak of disease symptoms and risk factors, pharmacologic sensitivity and pharmacokinetic of many drugs. Chronopharmacology is a branch of chronotherapy that applies the principles of circadian rhythms to determine the best timing of drug administration, which can affect the absorption, distribution, metabolism, and excretion of administered substances (Ferrell and Chiang 2015).

Chronotherapy does not only involve new medicines but uses also old ones in a different approach. In fact, chronopharmacology evaluates person's circadian rhythm in determining the timing and sometimes the right quantity of an active pharmaceutical ingredient (API) to optimize the therapeutic efficacy and minimize undesirable side-effects.

Hence, revising the dosing schedule, reformulating a drug in a suitable form, or using programmable dosage forms delivering an API at precise intervals, significant improvements could be achieved (Peppas and Leobandung 2004).

1.1 Diseases affected by circadian rhythms

Circadian disruption has been significantly linked to chronic jet lag and sleep disturbances and to increased incidence of cardiovascular events, gastrointestinal diseases, and metabolic syndrome. On the other hand, many chronic and acute disorders have a prominent circadian pattern of symptom appearance and severity and some of these are listed below.

Asthma

Symptoms of asthma occur mainly in the night than during the day (Bohadana, Hannhart et al. 2002; Wagh and Kalshetti 2011). This effect is related to many circadian-dependent factors: for example cortisol levels are lowest in the middle of the night and histamine (a mediator of bronchoconstriction) liberation peak occurred at 4.00 am (Sajan, Cinu et al. 2009).

Gastroesophageal reflux disease

Gastroesophageal reflux disease that occurs during wakefulness is usually postprandial and rapidly cleared. Nocturnal gastroesophageal reflux events occur less frequently than during the daytime but are associated with longer acid clearance time due to sleep and/or circadian-related decreases in swallowing, saliva production, peristalsis (Orr, Allen et al. 1994; Litinski, Scheer et al. 2009).

Alzheimer Disease

Alzheimer disease (AD) affects about 15 million people worldwide, and is most commonly seen after age of 50, with progressive cognitive decline, circadian rhythm disturbances and sleep disturbances, including insomnia. “Sundowning” is a feature of AD, characterized by a late afternoon/evening predominance of activity, which some authors attribute to insufficient melatonin production (Cohen-Mansfield, Garfinkel et al. 2000; Hu, Van Someren et al. 2009).

Epilepsy

Epilepsy is another disorder that often exhibits a day/night variation in clinical presentation. Patients with epilepsy have seizures during the day only, or the night only, although some may have a more random pattern (Pavlova, Shea et al. 2004; Peppas and Leobandung 2004; Durazzo, Spencer et al. 2008; Cho 2015).

Cardiovascular pathologies

Cardiovascular disorders exhibit differences in patterns of illness between day and night (Hermida, Ayala et al. 2007; Wagh and Kalshetti 2011). For example, there exists robust epidemiological evidence that the peak incidence of cardiac ischemic events, including angina, acute myocardial infarction and sudden cardiac death occurs around 9-11 am (Shea, Hilton et al. 2007; Litinski, Scheer et al. 2009). The peak incidence of the arrhythmias occurred between 10 and 11 am, with a nadir between 2 and 3 am. Arterial blood pressure (BP) generally falls during sleep and rises during activity, contributing to a day/night pattern in BP in most normotensive people as well as those with uncomplicated essential hypertension (Litinski, Scheer et al. 2009).

Cancer

Epidemiological data indicate a link between various physiologic parameters having well-established day/night rhythms and carcinogenesis. For example, Rafnsson et al. found a higher rate of breast cancer in shift working and flight attendant females (Rafnsson, Tulinius et al. 2001). Severely disrupted rest/activity cycles in patients with metastatic colorectal cancer is accompanied by decreased survival compared with patients with a well-preserved rest/activity pattern (Mormont, Waterhouse et al. 2000).

1.2 Early morning pathologies (EMPs): Rheumatoid Arthritis

The phrase "early morning pathologies" relates to pathologies, diseases, or other illnesses in which symptoms are typically more pronounced, aggravated or acute during the last hours of sleeping-time (4-6 am) or after the patient awakens from sleep (6-8 am) (Busetti and Crimella 2006).

Between various disorders with pronounced early morning symptoms (ischemic heart diseases, arrhythmias, allergic rhinitis), this project focused on chronic inflammatory based diseases such as rheumatoid arthritis (RA).

RA is an autoimmune disease that is associated with progressive disability, systemic complications and early death. The cause of this pathology is unknown, and the prognosis is serious, the patient is acutely ill with a questionable outlook and a small chance for improvement. Rheumatoid arthritis is characterized by synovial inflammation and hyperplasia, autoantibody production, cartilage and bone destruction, and systemic complications, including cardiovascular, pulmonary, psychological, and skeletal disorders (McInnes and Schett 2011).

Rheumatologists agree that RA patients show joint pain, morning stiffness, and functional disability in the early morning hours (Straub and Cutolo 2007; Gibbs and Ray 2013). This variation in symptoms expression is due to daily oscillations in plasma concentrations of hormones, disease-mediating cytokines, and other endogenous substances (Straub and Cutolo 2007; Perry, Kirwan et al. 2009).

Hormones

The differences in circadian rhythm fluctuations in healthy people compared to RA patients of some hormones have been studied.

First of all, cortisol is the strongest endogenous anti-inflammatory substance and, in healthy subjects, its cycle shows a maximum in the early morning hours (8.00 am) and the lowest secretion point at midnight. This rhythm is highly disturbed in RA patients when the disease is very active with low cortisol levels at the early morning (Straub and Cutolo 2007).

Besides cortisol two other hormones, melatonin and prolactin, exhibit a circadian rhythm. Both of them are correlated to stimulation of the immune system, that may lead to an increase in pro-inflammatory conditions in RA (Walker and Jacobson 2000; Maestroni, Sulli et al. 2002).

The conventional circadian rhythm of melatonin and prolactin display a maximum at 3.00 am. Several researches revealed that in RA patients

melatonin and prolactin levels were significantly higher compared to normal subjects (Chikanza, Petrou et al. 1993; Sulli, Maestroni et al. 2002). This anomalous concentration induces a strong immune response and enhances inflammatory cytokine and nitric oxide production involved in immune and inflammatory response in RA at the early morning.

Disease-mediating cytokines

Cytokines like Tumor Necrosis Factor (TNF) and interleukin-6 (IL-6) exhibit a marked rhythmicity, in serum levels. In healthy subjects, the peak value of TNF is reached at ~3:00 am and that of IL-6 at ~6:00 am. In patients with RA, the peak level of TNF has been reported to appear at 6:00 am and that of IL-6 at 7:00 am (Straub and Cutolo 2007).

For both cytokines, a time shift of the peak value toward the morning is observed. In healthy people, TNF and IL-6 levels are ~2–5 pg/ml whereas in RA patients these levels are 20–50 pg/ml. In addition for healthy people, serum levels of TNF and IL-6 have already begun to decrease at 6:00 am and 9:00 am, respectively, whereas in RA patients these levels remain elevated until 10:00 am and 11:00 am, respectively (Straub and Cutolo 2007).

Hence, there is a well-established up and down-regulation of cytokines (IL-6, TNF) and hormones that implicates fluctuations in immune and inflammatory response in RA. These data suggest that increasing levels of cytokines, melatonin and prolactin as well as inadequate low secretion of cortisol contribute to symptoms exacerbation in the early morning hours in patients with RA (Straub and Cutolo 2007).

1.2.1 Conventional drugs used in RA treatment

The main goals of RA therapy involve: stop inflammation, relieve symptoms, prevent joint and organ damage, improve physical function and overall well-being, reduce long-term complications.

There are different drugs used in the treatment of rheumatoid arthritis. Some are used primarily to soothe RA symptoms and others are used to slow or stop the course of the disease and to inhibit structural damage.

Disease-modifying antirheumatic drugs (DMARDs) target inflammation and reduce structural damage progression. Non-steroidal anti-inflammatory drugs (NSAIDs), reduce pain and stiffness and improve physical function, but do not interfere with joint damage and are thus not disease modifying. Steroidal anti-inflammatory drugs (SAIDs) offer rapid symptomatic and disease-modifying effects but are associated with serious long-term side-effect (Smolen, Aletaha et al. 2016).

DMARDs

DMARDs represent the basis of pharmacologic treatment for RA (Clements 2011). These drugs are classified on the basis of their “biologic” or “non-biologic” activity.

DMARDs therapy should be initiated within 3 months of RA diagnosis, allowing for aggressive treatment of the disease. Based on severity of the disease, particular DMARDs may be recommended and prescribed for an individual or specific patient. DMARDs without biologic activity include methotrexate, hydroxychloroquine, sulfasalazine, and leflunomide. These agents do not target a specific component of the immune system involved in the pathophysiology of RA but have been shown to improve clinical outcomes. Later, thanks to an enhanced understanding in the pathophysiology of RA, more specific therapies (with biologic activity) have been developed to target a specific component of the immune system. DMARDs with biologic activity include TNF antagonists (etanercept, infliximab, adalimumab), IL antagonists (anakinra, tocilizumab), T-cell modulator (abatacept), and B-cell modulator (rituximab).

NSAIDs

NSAIDs have been used in the management of RA for several decades. NSAIDs inhibit cyclooxygenase (COX) and prevent further formation of prostaglandins and other related inflammatory mediators. Based on their mechanism of action, NSAIDs are useful adjuvant therapy for the symptomatic management of RA, reducing joint swelling, tenderness, and pain. Most commonly used NSAIDs, include aspirin, diclofenac, ibuprofen, ketoprofen, piroxicam, sulindac and many others.

The majority of these drugs are taken orally but, because of their short half-life need multiple daily administrations leading to toxicity and poor patient compliance. In fact, long term NSAIDs therapy includes several side effects such as gastrointestinal disorders, nephrotoxicity, anaemia and cardiovascular problems (Clements 2011).

SAIDs

SAIDs possess anti-inflammatory and immunosuppressive properties. Similar to NSAIDs, corticosteroids such as prednisone, prednisolone or methylprednisolone are commonly used for symptomatic management of RA. Corticosteroids may be used in combination therapy with DMARDs to avoid long-term adverse events. With long-term therapy, the lowest dose of corticosteroid is recommended to control symptoms and reduce the risk of adverse events (Clements 2011).

Commonly, anti-inflammatory drugs (NSAIDs and SAIDs) employed to relieve symptoms, are administered to RA patient at different moments of the day (after awakening, after lunch, during the night) in immediate-release formulations. In this way, drugs are absorbed rapidly and explicate their action independently from the circadian rhythms of hormones and cytokines responsible of RA symptomatology. This conventional approach, usually leads to ineffective therapy because of drug liberation from the dosage form is not

synchronized with symptoms peak determining an increase of side effects and consequently poor patient compliance.

1.3 Innovative oral treatments of RA: Chronotherapeutics

In the last years some researches focused on the possibility to treat RA with a chronotherapeutic approach via oral route enhancing both patient compliance and therapeutic efficacy.

Chronotherapy using glucocorticoids has achieved interesting outcomes. A modified-release tablet of prednisone has been developed able to release the drug ~4 hours after its ingestion; therefore, patients with RA do not need to take the drug during the night (2–3 am). A double-blind, randomised controlled trial showed that the prednisone modified-release tablet had better control of joint morning stiffness compared with the immediate release tablet (Buttgereit, Doering et al. 2008; To 2016). Moreover, studies of Alten et al. have demonstrated the safety and effectiveness of these tablets in that chronotherapy do not reduce hypothalamic–pituitary–adrenal axis function or the secretion of endogenous glucocorticoids (Alten, Döring et al. 2010; Alten, Holt et al. 2015). Therefore, chronotherapy using modified-release SAIDs formulations may be expected to become useful in RA therapy .

Moreover, the formulations of several available NSAIDs (ie, indomethacin, aceclofenac, ketoprofen, flurbiprofen, lornoxicam) have been recently modified, and some of them have been designed in order to obtain chronotherapeutic effects in RA (Cutolo 2016).

Levi F. et al., found that an evening once daily scheduling of 75 mg (indomethacin formulation 25 mg immediate-release combined with 50 mg controlled-release) resulted in much greater control of morning symptoms compared to once-daily morning (breakfast time) or once-daily midday (lunchtime) schedules (Levi, Louarn et al. 1985).

A pH-responsive dual pulse multiparticulate dosage form containing ketoprofen was tested in RA and was found to be able to relieve circadian symptoms during midnight and early morning (Lotlikar, Kedar et al. 2010).

2. Drug-delivery technology for chronotherapeutics

The aim of Chronotherapeutic Drug Delivery System (ChDDS) is to synchronize drug delivery with circadian rhythms of a specific disease in order to optimize therapeutic efficacy and minimize side effects.

An ideal ChDDS may be non-toxic, biocompatible and biodegradable, be easy to manufacture at economic cost and be easy to administer to patients in order to enhance compliance to dosage regimen (Devdhawala Mehul and Seth Avinash 2010).

In particular advantages of ChDDS could be summarized as established by Neeharika and Jyonthi (Neeharika and Jyothi 2015):

- Less inter-and intra-subject variability
- Flexibility in design
- Reduced frequency in dosage schedule
- Improved bioavailability
- Limited risk of local irritation
- Unique release pattern

Hence, a ChDDS must release the drug at predetermined rates and time to achieve optimal drug levels at the site of action when the therapeutic action is needed. Regarding RA, as previously reported, the symptoms exacerbation occurs at the early morning hours (4.00-6.00 am) therefore a ChDDS must release maximum anti-inflammatory dose at this time. The optimal goal may be the production of oral controlled ChDDS releasing the maximum of the dose at the early morning hours after single daily administration prior to go bed.

2.1 Oral controlled Drug Delivery Systems

The oral administration is the most versatile, convenient and commonly employed route of drug delivery. Gastrointestinal physiology offers more flexibility in dosage form design than other routes, that is the reason why for controlled release systems, oral route of administration has received the most attention in developing controlled release systems (Tagde, Jain et al. 2012).

Oral modified release delivery systems are most commonly used for:

- Extended release,
- Delayed release,
- Pulsatile release;
- Time or site specific release

Oral programmed release (e.g., delayed, gastroretentive or time-specific release, etc.) and time-dependent delivery are main and primary aims of pharmaceutical technology research which would ideally enable the chronotherapy of various pathologies with night or early-morning symptoms such as RA (Maroni, Del Curto et al. 2012).

Controlled release systems are based on polymers widely used in pharmaceutical dosage forms as release modifiers and release controllers of API via oral route. Depending upon the nature of polymer or a combination of polymers used in formulations, they play an important role in inducing a delayed, and/or sustained, and/or time-specific drug delivery as well as in forming gastroretentive/floating formulations.

Particularly, natural polymers resulted greater to the synthetic ones in respect of their highly organized macroscopic and molecular structure. This adds to their strength and biocompatibility. Moreover, their low toxicity and excellent biodegradability have also attracted researchers to pay attention towards the widespread application of natural polymers (Singh, Sharma et al. 2011).

2.2 Natural polysaccharides/carbohydrate polymers

Natural polymers include proteins (collagen, albumin etc.) and polysaccharides or their derivatives. They are especially attractive because of their stability, availability, renewability and low toxicity. Moreover, the usual biocompatibility and biodegradability of these natural polymers, coupled with the possibility to tailor their physicochemical properties by chemical modification on the chain backbone structure, make them ideal excipients for the development of controlled drug release systems.

From a chemical point of view, polysaccharide term includes different type of carbohydrates that can be composed of only one kind of repeating monosaccharide (homopolysaccharides) or made up by two or more different monomeric units (heteropolysaccharides) (Alvarez-Lorenzo, Blanco-Fernandez et al. 2013).

In nature, polysaccharides have various resources from algal origin (e.g. alginate), plant origin (e.g. pectin, guar gum), microbial origin (e.g. dextran, xanthan gum), and animal origin (chitosan, chondroitin).

Furthermore, polysaccharides can be classified into polyelectrolytes and non-polyelectrolytes, the latter can be further divided into positively charged polysaccharides (as chitosan, polylysine, etc.) and negatively charged polysaccharides (alginates, hyaluronic acid, pectins, etc.) (Liu, Jiao et al. 2008).

2.2.1 Alginate

Alginate, is a naturally occurring linear anionic polysaccharide extracted from brown seaweed, composed by β -D-mannuronic acid (M) and α -L-guluronic acid (G) residues linked by α -(1,4)-glycosidic bond. The blocks are composed of consecutive G residues (GGGGGG), consecutive M residues (MMMMMM), and alternating M and G residues (GMGMGM) (Fig. 2). Alginates extracted from different sources differ in M and G contents as well

as the length of each block, and more than 200 different alginates are currently being manufactured (Lee and Mooney 2012).

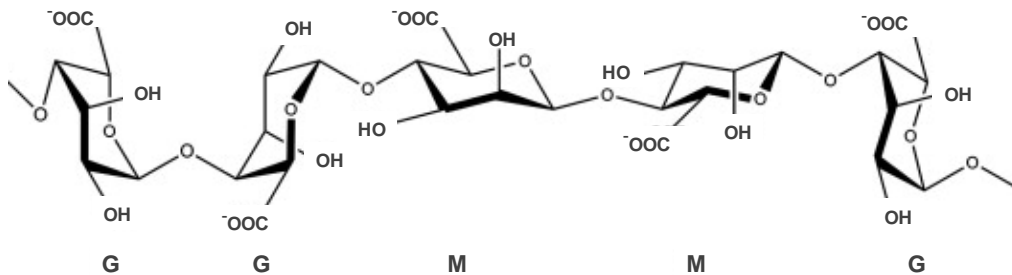


Figure. 2 Representative structure of alginate.

Most of the commercially available alginates are in the form of the salt, that is, sodium alginate (SA). Sodium alginate is able to move from sol to gel state by ionotropic gelation under mild conditions through interactions between blocks of G residues and bivalent or trivalent cations resulting in the formation of an elastic hydrogel with good mechanical strength commonly referred as “egg-box” model (Aquino, Auriemma et al. 2012).

The chelation at the G-residue of the alginate molecules results in ionic interaction between the G groups while the van der Waal forces between alginate segments result in a three-dimensional gel network (Gaumann, Laudes et al. 2000).

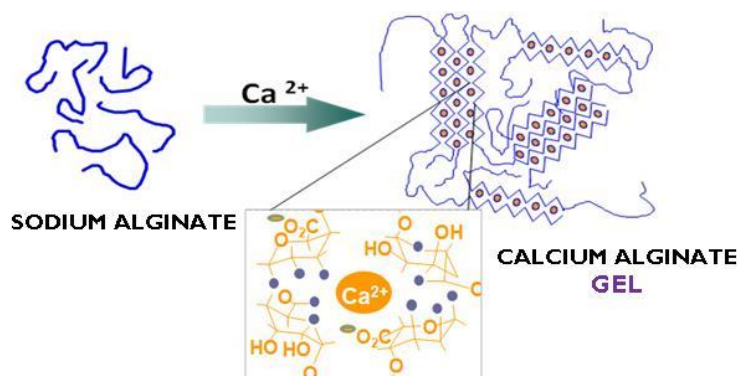


Figure 3. Alginate gel formation via G blocks.

In general, divalent cations (Cd^{2+} , Co^{2+} , Cu^{2+} , Mn^{2+} , Ni^{2+} , Pb^{2+} and Zn^{2+}) are suitable crosslinking agents (Chan, Jin et al. 2002) but not monovalent cations or Mg^{2+} (Goh, Heng et al. 2012). Literature survey confirms that calcium is the most used gelling agent to form alginate hydrogels (Agarwal, Narayana et al. 2015; Zhang, Zhang et al. 2016). Ca^{2+} ions, preferentially interact with G units of alginate in a planar two-dimensional manner, while producing the so-called “egg-box” structure (Goh, Heng et al. 2012). However, other divalent cations like Zn^{2+} , are less selective and interact with both G and M residues of alginate moieties producing more extensive cross-linking hydrogels (Chan, Jin et al. 2002) and seem to be more suitable for controlled drug delivery.

Alginate hydrogels are useful as a matrix for cell immobilization, as well as entrapment of bioactive compounds and drugs for oral administration. These biomedical applications are mainly due to pH-sensitive characteristic of alginate beads (swells especially in neutral- and basic aqueous media, but sink in acidic aqueous solutions) able to protect drugs from environmental stress and from chemical/enzymatic digestion in gastric fluids as well as to prolong the drug release, based on swelling properties.

The material encapsulated within the inert alginate environment could be delivered at a desired rate in a controlled release system. Encapsulated drugs are released from alginate beads by diffusional processes through pores and the release is facilitated by the degradation of the polymeric network. In general, the release of water-soluble drugs is controlled predominantly by diffusion while that of water insoluble drugs is largely dependent on gel erosion (Goh, Heng et al. 2012).

2.2.2 Pectin

Pectin is a linear polysaccharide of α -linked anhydrogalacturonic acid with a certain degree of methyl esterification of carboxyl groups (Fig.4) (degree of

esterification) depending on the polysaccharide quality and source (Brejnholt 2009).

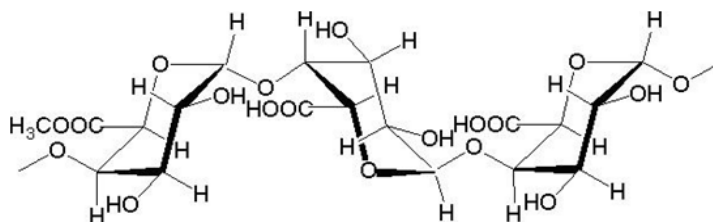


Figure 4. Representative structure of pectin.

The most attractive property of pectin for industrial application is its gelling activity. Pectinate gel is water insoluble (water resistant), while still enzymatically degradable. For this reason, it can be used as an effective vehicle for drug delivery. Pectin can move from sol to gel state by thermal, acidic or cationic treatment. The choice of the pectin source as well as the gelation mechanism significantly influences the resulting gel nanostructure (Sriamornsak 2003). Indeed, the degree of esterification and the distribution of methoxyl-esters of each pectin type determine the main interactions between the polymer chains (hydrogen bonding, hydrophobic and ionic interactions) and the extent of chains alignment (Brejnholt 2009; García-González, Alnaief et al. 2011).

Thermal treatment (heating) promotes the dissolution of pectin in water and, upon cooling below the so-called setting temperature, gelation takes place by hydrogen bonding between free carboxyl groups on the pectin molecules as well as the hydroxyl groups of the molecules. Acidic gelation promotes the hydrolysis of the methyl esters inducing a pectin structure predominantly composed of galacturonic acid (White, Budarin et al. 2009). Moreover, low methyl-esterified pectins require the presence of divalent cations for proper gel formation through ‘egg-box’ model mechanism by interaction of the cations (e.g., calcium, zinc, etc.) with galacturonic acid residues (Grant, Morris et al. 1973; El-Nawawi and Heikal 1995; García-González, Alnaief et al. 2011). The

presence of sugar (10–20 wt.%) may also contribute to the decrease of shrinkage of the gel, as well as to confer firmness to the gel (García-González, Alnaief et al. 2011). Various reports suggest that Ca or Zn-pectinate systems may be viable carriers for controlled drug delivery to the colon due to digestion by specific enzymes produced by bacteria present exclusively in the colon. Unfortunately, their solubility and swelling ability in aqueous fluid cause premature drug release before the delivery system is able to reach the colon. First of all, this phenomenon can be controlled through proper selection of pectin type and its concentrations, as well as gelation agent and cross-linking conditions (time, pH, conc. and nature of gelling solutions) (Sriamornsak and Nunthanid 1998; Das, Ng et al. 2010). Moreover, pectin beads could be used as starting material for the development of a final dosage forms through the combination with gastro-resistant excipients (Eudragit, cellulose acetate phthalate etc.) or through the insertion into specific capsules able to protect pectin beads from the acidic medium.

2.3 Advantages and opportunities of polysaccharides-hydrogel based beads for the design of ChDDS

Hydrogels are three-dimensional systems composed of hydrophilic polymers that can absorb water. They are not soluble in aqueous mixtures but swell due to the presence of chemical or physical crosslinks (Khan, Ullah et al. 2016). The degree of crosslinking, which is dependent on formulation conditions, is the most important factor affecting the properties of hydrogels. In fact, highly crosslinked hydrogels have a generally more compact structure and reduced dissolution rate and swelling ability.

By controlling the swelling properties and other characteristics (solubility at different pH, mucoadhesion, etc.) in biological fluids, hydrogel based beads can be a useful tool for releasing drugs in a controlled manner at desired times

and sites as required for a chronotherapeutic system (Smolensky and Peppas 2007).

Different microencapsulation techniques have been studied for the development of hydrogel based beads as carrier for drugs, peptides, proteins or for cells delivery. Many of these involve the use of organic solvents enhancing the possibility of adverse effects in the treatment of chronic diseases. For this reason, more interesting are biodegradable natural polysaccharides such as alginate, pectin, chitosan which do not require organic solvents for the production of gel-beads and are potentially qualified for a number of chemical modifications (Patil, Kamalapur et al. 2010).

One of the most common method used for the production of crosslinked beads is ionotropic gelation based on the ability of polyelectrolyte polymers (alginate, pectin, chitosan, gellan gum) to cross-link in the presence of counter ions (Ahirrao, Gide et al. 2014).

Generally, hydrogel beads are produced with a syringe, dropping the polymer/drug solution into a specific gelling medium (divalent cation, sodium tripolyphosphate) (Das, Ng et al. 2010; Mandal, Kumar et al. 2010; Vino, Paryani et al. 2012). However, the simple dripping method is often unable to produce beads with homogenous size and morphology resulting in poor process control and reproducibility.

2.4 Prilling technique for the production of hydrogel based beads

Prilling or laminar jet breakup is an emerging microencapsulation technique able to produce microparticles or beads with very narrow dimensional range and high encapsulation efficiency. It is a vibration-based technology consisting in breaking apart a laminar jet of polymer solution into a row of mono-sized drops by means of a vibrating nozzle device (Del Gaudio, Russo et al. 2009; Tran, Benoît et al. 2011). Once the droplets are formed, the gelation/consolidation step follows in order to prevent either the aggregation

of polymer droplets or the undesired leakage of encapsulated drugs. The chemical nature of the droplets (dispersed phase) determines the consolidation step, in which the droplets are transformed into solids microparticles known as gel-beads: this procedure can involve temperature modification, chemical reactions and mainly ionic cross-linking (ionotropic gelation).



Figure 5. Vibrating nozzle device Nisco Encapsulator Unit, Var D.

Several variables in prilling can affect droplet size and size distribution as polymer concentration and flow rate (Berkland, Kim et al. 2001; Mazzitelli, Tosi et al. 2008). Moreover, frequency of vibration as well as falling distance also affect particles characteristics, In fact, the longer the wavelength of the jet break-up, and the shorter the distance to the impact plane of the hardening solution, the less likely is drop coalescence. Thus, smaller nozzle diameters and higher frequencies increase the possibility of coalescence (Tran, Benoît et al. 2011). The frequency is usually kept as low as possible in order to avoid the formation of satellite droplets leading to a broader size range (Del Gaudio, Russo et al. 2009).

The production of microparticles by the vibrating nozzle device is highly reproducible, time-saving, can be performed under aseptic and scaled-up conditions (Zvonar, Kristl et al. 2009). The acoustic jet excitation process involved in prilling was patented for production of uniform microspheres of alginate (Brandau 1995), collagen (Dumas, Tardy et al. 1992) and PLGA (Berkland, Pack et al. 2003b; Kim, Seo et al. 2008). The scale-up of the vibration process is easily done by using a multi-nozzle system (Fig. 6)

without changing other process parameters such as flow rate and the vibration frequency (Brandenberger and Widmer 1998). The most important element is about the arrangement of the nozzles which must ensure equal jet formation and equal pressure drops between the nozzles (Brandenberger and Widmer 1998). The pilot apparatus using this technique is now being sold by Brace GnbH (Germany), Nisco Inc. (Switzerland) and Inotech AG (Switzerland) (Brandau 2002; Tran, Benoît et al. 2011).



Figure 6. Multi-nozzle system *BRACE GMBH* (Brandau 2002).

RESULTS AND DISCUSSION

SECTION A:
**Design and development of
chronotherapeutic systems loaded
with short half-life NSAIDs**

SECTION A PART 1:

Ketoprofen loaded alginate beads: *in vitro/in vivo* characterization

Based on the article: **A. Cerciello**, G. Auriemma, S. Morello, A. Pinto, P. Del Gaudio, P. Russo, R.P. Aquino. “Design and In Vivo Anti-Inflammatory Effect of Ketoprofen Delayed Delivery Systems”, *Journal of Pharmaceutical Sciences* **2015** Feb; DOI 10.1002/jps.24554Epub 2015 Jun 18.

3-A 1.1 Scientific background and research aim

Ketoprofen is a nonsteroidal anti-inflammatory drug (NSAID) with analgesic and antipyretic properties indicated for the symptomatic treatment of pain and inflammation in osteoarthritis and rheumatoid arthritis. However, its efficacy is countered by a large number of side effects, especially those related to gastrointestinal complications. Moreover, its short biological half-life ($t_{1/2} = 2.1$ h) and high frequency of dosing (2–4 times daily) increase health risks precluding a long-term use, as required in chronic inflammations and namely to relieve early morning pain in the management of osteoarticular pathologies (Arvidson, Gudbjörnsson et al. 1994). For these reasons, ketoprofen is a good candidate for the development of controlled release formulations, able to provide drug release at predetermined rate and time, targeting intestine, with the potential of reducing the well-known adverse effect of NSAIDs (Del Gaudio, Russo et al. 2009; Della Porta, Del Gaudio et al. 2013).

Among different technologies proposed for the development of controlled and delayed drug delivery systems (Kamada, Hirayama et al. 2002; Stigliani, Aquino et al. 2013), prilling producing gel beads through vibrating nozzle extrusion was chosen as time-saving technique, offering several advantages compared with other microencapsulation technologies such as mild operative conditions (i.e., aqueous feed solutions, ambient temperature, and pressure) and an easy scale-up process (Del Gaudio, Colombo et al. 2005; Auriemma, Mencherini et al. 2013).

In this work, a gel beads formulation was designed for delayed delivery of ketoprofen using alginate as a polymer carrier with emphasis on stabilization of the active, delivery and targeting of the API and mainly on drug release modulation achieving early morning pathologies requirements that is to treat chronic inflammation and pain showing a circadian pattern with symptoms exacerbation in early morning (Lemmer 1991).

To achieve this goal, the main critical variables of the prilling process, i.e., composition of the aqueous feed solutions (sodium alginate and ketoprofen in different ratio), cross-linking conditions, frequency of vibration and flow rate, as well as beads micromeritics, were studied. *In vitro* dissolution/release performances were assessed in conditions simulating the gastrointestinal environment (USP 36). To demonstrate that delayed and sustained *in vitro* drug release profiles correlate with slow release *in vivo*, the delayed anti-inflammatory effectiveness was evaluated using a modified carrageenan-induced acute oedema in rat paw (male Wistar rats) protocol.

3-A 1.2 Gel-beads production and characterization

Different experiments were conducted for the optimization of process parameters in order to obtain ketoprofen gel beads with desired size and high drug EE. Process parameters such as frequency of vibration and flow rate have been set according to Cross model equation to control the diameter of the drops coming out of the nozzle, producing hydrated beads with narrow size distribution (Aquino, Auriemma et al. 2012; Del Gaudio, Auriemma et al. 2013). A 400 μm nozzle, frequency of vibration at 350 Hz (100% amplitude) and a feed flow rate of 5 mL/min were used; moreover composition of the aqueous feed solutions (e.g., polymer concentration and drug–polymer ratio) was also a critical parameter. As the successive ionotropic gelation of the formed droplets, behaviour of curing cross-linking divalent cations (Zn^{2+}) by inducing ionotropic gelling of the polymer/drug drops, as well as pH of the gelling solution and cross-linking time were studied.

This systematic study led to optimized operative conditions: sodium alginate of 2.0% (w/w), Zn^{2+} aqueous solution (10% w/v) as a gelling agent with gelling time around 2 min, and pH of the gelling solution set at 1.5.

Particularly, Zn^{2+} was selected as a cross-linker cation because its antioxidant properties may boost the efficacy of the anti-inflammatory drug encapsulated

in the polymeric matrix (Gaweł, Librowski et al. 2013; Abbas, Schaalán et al. 2014). Formulations F5, F10, and F20 with different drug/polymer mass ratios (from 1:20 to 1:5, as shown in Table I) were obtained in a few minutes by prilling. As control, blank Zn–alginate beads (F) were produced too. The drying process of all the hydrated beads was conducted overnight by exposing hydrated beads to standard room conditions (22°C; 67% RH) for 12–18 h until constant weight was reached.

Table I. Zn-Alginate-based beads loaded with K. Composition, theoretical and actual drug content, encapsulation efficiency, mean diameter and sphericity coefficient of Zn-alginate beads manufactured by prilling; blank (F) and loaded with ketoprofen (F5, F10 and F20).

Formulation code	K/Alg Mass ratio	TDC (%)	ADC (%± SD)	EE (%± SD)	Dried beads diameter (µm± SD)	SC
F	-	-	-	-	2386 ± 119	0.93 ± 0.01
F5	1:20	4.8	2.3 ± 0.2	48.2 ± 5.0	1813 ± 84	0.88 ± 0.02
F10	1:10	9.1	4.3 ± 0.2	47.0 ± 1.9	1672 ± 52	0.91 ± 0.01
F20	1:5	16.7	8.9 ± 0.2	53.0 ± 1.1	1770 ± 59	0.91 ± 0.01

Analysis of the ADC and EE showed satisfying values for all dried formulations (EE ranging from 47% to 53%, as reported in Table I). However, it is interesting to point out that ADC and EE were related to the drug/polymer ratios. This result suggests that the loading of high amount of drug into feed solutions may promote, during the gelling phase, the formation of a more compact cross-linked matrix via intermolecular interactions, such as hydrophobic or hydrogen bonding, which stabilize the well-known “egg-box” structure (Lin and Metters 2006; Hoffman 2012). This phenomenon led to tough polymer beads and reduced the leaching of the drug from the drops into the gelling medium; accordingly, F20 formulated at the highest ketoprofen content (ketoprofen–alginate = 1:5) showed the highest entrapment of the drug within the matrix (EE = 53.0%).

With regard to the morphology, all ketoprofen-loaded beads exhibited a remarkable reduction in mean diameter in comparison to blank beads. In fact, F5, F10, and F20 displayed diameters in the range of 1672 μm (F10)–1813 μm (F5), whereas F showed dimension greater than 2 mm ($d = 2386 \mu\text{m}$).

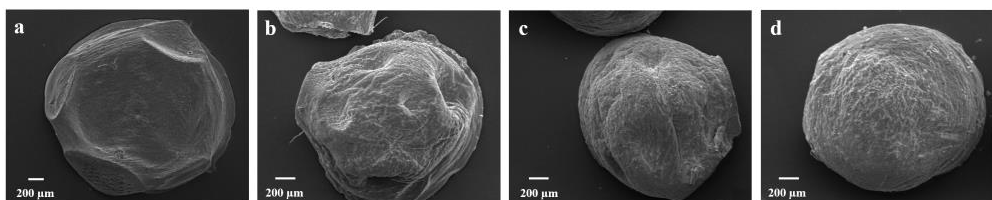


Figure 7. Zn-Alginate-based beads loaded with K.SEM microphotographs of dried Zn-alginate beads formulations: F (a), F5 (b), F10 (c) and F20 (d).

Stabilization of the polymer matrix influenced beads shape after the drying process. In fact, SEM analyses confirmed that ketoprofen-loaded beads (both F10 and F20) had almost spherical shape, whereas F5 presented less regular contour with craters on the surface (Fig. 7). According to the ketoprofen loading, SC values were higher for drug-loaded beads value (>0.90), whereas F5 presented SC value around 0.88. Overall results from particle size and SC analysis suggest the formation of more compact cross-linked matrix according to the content of drug into the gel polymeric network.

To better understand the influence of drug content on polymeric matrix structure, beads were cryo-fractured and successively analysed by both SEM and FM.

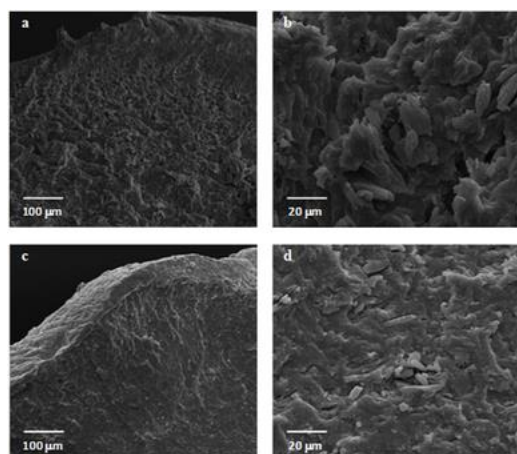


Figure 8. Zn-Alginate-based beads loaded with K. SEM microphotographs at different magnifications of cryo-fractured beads: F10 (a-b) and F20 (c-d).

Results from SEM showed that F20 had a more compact polymeric matrix than other formulation (Figs. 8c and 8d).

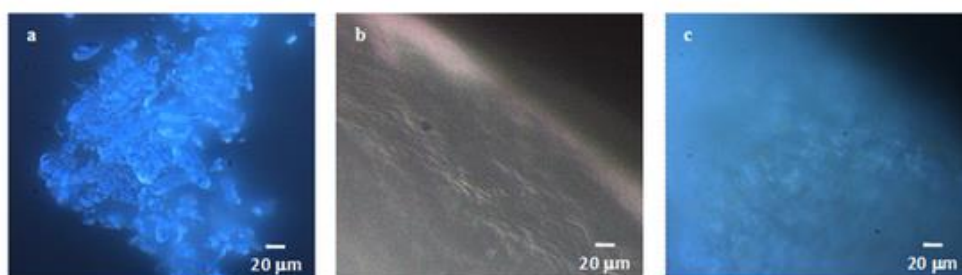


Figure 9. Zn-Alginate-based beads loaded with K. Fluorescent microscopy images of K raw material (a), cryo-fractured blank Zn-alginate beads F (b), and cryo-fractured K loaded formulation F20 (c).

Pure ketoprofen arose as a crystalline material with blue fluorescence consisting of small crystals ($d_{50} = 3.1 \mu\text{m}$) forming aggregates with large size ($d_{50} = 20.5 \mu\text{m}$) (Fig. 9a), while blank particles cross-sections (F) showed a pale yellow and off-white fluorescence (Fig. 9b). FM images of F20 (cryo-fractured ketoprofen loaded beads) displayed fluorescent spots due to ketoprofen crystals homogeneously embedded within the Zn–alginate matrix

(Fig. 9c). As highlighted by FM images (Fig. 8), ketoprofen seems to keep its crystallinity after prilling and drying process, and crystal clusters of the drug were homogeneously embedded within the polymeric Zn–alginate matrix (Figs 8d and 9c).

Moreover, to complete the technological characterization, DSC experiments on ketoprofen raw material and Zn– alginate beads, both blank (F) and ketoprofen loaded (F5–F20) were performed and the thermograms are shown in Figure 10.

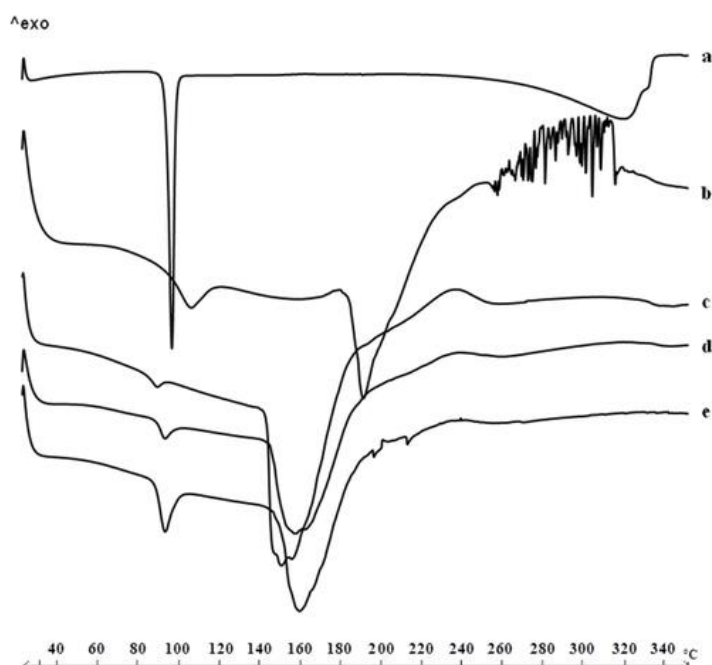


Figure 10. Zn-Alginate-based beads loaded with K. Differential scanning calorimetry thermograms of K raw material (a) and Zn-alginate beads, both blank F (b) and K loaded F5 (c), F10 (d) and F20 (e).

According to previous observations (Del Gaudio, Auriemma et al. 2013), thermal profile of crystalline ketoprofen raw material (Fig. 10a) exhibited a very narrow melting peak at 97°C with an intensity of -13.88 mW. The thermogram of blank beads F (Fig. 10b) showed two endothermic events, well

separated in temperature values, at 107°C and 190°C. The first event exhibited its onset at 84°C typical of the loss of hydration water from the polymer matrix (Pillay and Fassihi 1999; Atassi, Mao et al. 2010) and an intensity of -9.54 mW; the second event at 190°C was related to the endothermic melting process of the Zn-alginate matrix and had an intensity of -20.81 mW. This peak is followed by a ramp-like event ranging from 230°C to 252°C referable to polymeric matrix degradation.

All ketoprofen-loaded beads (Figs. 10c–9e) showed a similar thermal trend with the endothermic events shifted at lower temperature. In fact, the first endothermic peak was found between 91°C and 94°C, for F5 and F20, respectively. The intensity of this peak increased with drug content and has been related to two simultaneous events overlapping in this range, namely, the loss of water and the melting of residual ketoprofen crystals, which were not encapsulated in the egg-box structure. The second endothermic melting process, between 155°C and 160°C, also showed an increased intensity related to ketoprofen content. Results suggest the establishing of a physical interaction, which occurs between the polymer and the drug after loading into the polymeric matrix.

Drug Release studies

Pilot dissolution tests of all formulations were performed by conventional vessel methods (USP Apparatus 2, paddle) (Yang, Chu et al. 2002) using a classic pH change method, providing essential information and recommended in various guidelines (Rockville 1997) as a first choice for the *in vitro* dissolution testing of controlled/ modified release formulations (Wen and Park 2011).

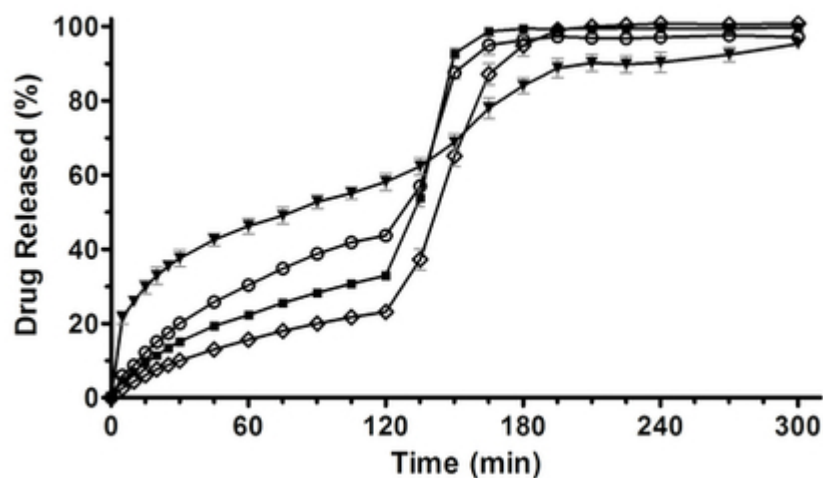


Figure 11. Zn-Alginate-based beads loaded with K. Release profiles of K raw material (full triangle) and K loaded formulations F5 (empty circle), F10 (full square), F20 (empty diamond), performed by USP Apparatus 2 using a pH change assay. Mean \pm SD; (n=6).

Results showed that during the permanence of the formulations in acidic medium (2 h), F5 and F10 released 43.7% and 32.8% of the loaded ketoprofen, respectively. After the pH change the drug release rate increased very rapidly, leading to a complete release of ketoprofen in simulated intestinal fluid (SIF) in about 1 h, whereas pure ketoprofen exhibited lower release rate (Fig. 11). Interestingly, ketoprofen release from F20 was greatly reduced (around 20%) in simulated gastric fluid (SGF) in 2 h. Thus, F20 acts as a gastro-resistant oral dosage form; complete drug release was achieved in SIF after pH change in about 1.5–2 h, with a dissolution rate lower than those observed for F5 and F10.

Although previous papers reported no significant effects on drug release under simulated gastrointestinal environment by varying the ketoprofen concentration in Ca–alginate beads (Del Gaudio, Russo et al. 2009; Tous, Fathy et al. 2014), we observed that ketoprofen *in vitro* release rate from Zn–alginate beads resulted strongly influenced by the amount of drug loaded. F20, formulated with the highest amount of ketoprofen, exhibited a gastro-resistant

profile followed by a slow and extended release of the drug in SIF (100% ketoprofen release at about 3.5 h, Fig. 11). These data matched with SEM microphotographs analyses of the cryo-fractured F20 beads (Figs. 8c and 8d). In fact, the loading of high amount of drug into feed solutions promote intermolecular interactions between the polymeric chains enhancing polymer entanglement during the gelling phase. This effect combined to the high cross-linking degree due to zinc ions provides tougher polymer matrix, especially in F20, leading to a stronger resistance to drug diffusion.

F20 dissolution behaviour was further investigated using the USP apparatus 4 (flow-through, open-loop configuration), which is reported to closely mimic *in vivo* hydrodynamics and thus to better predict *in vivo* performance of solid oral dosage forms (Gao 2009; Fotaki 2011).

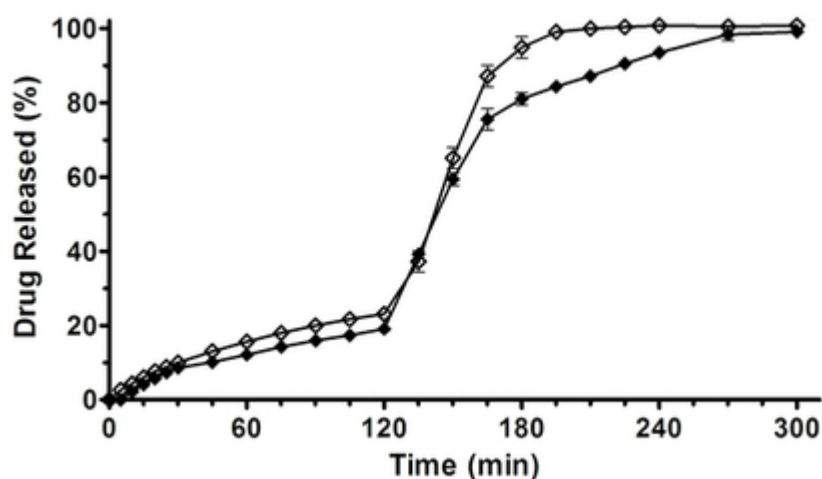


Figure 12. Zn-Alginate-based beads loaded with K. Release profiles of F20 formulation, performed by USP Apparatus 2 (empty diamond) and USP Apparatus 4 (full diamond), using a pH change assay. Mean \pm SD; (n=6).

As shown in Figure 12, the apparatus 4 confirmed that F20 had enteric release behaviour (19% of the drug released in 2 h at pH 1) and in SIF showed a slower rate than that obtained using the USP paddle method. Differences between the two apparatus may be explained by the different hydrodynamic

conditions that characterize the flow-through cell system, where no agitation mechanisms occur and the dosage form is continuously exposed to a uniform laminar flow, similar to the natural environment of the gastrointestinal tract (Hu, Kyad et al. 2005; Medina, Salazar et al. 2014).

F20 performance may be explained by considering the selected formulation factors affecting the drug release and which can potentially influence oral absorption and bioavailability, namely alginate pH-dependent solubility, zinc cross-linking properties, and the obtained high structural density of matrix in F20.

It is well known that drug release from alginate-based hydrogel beads depends upon the extent of crosslinking within the polymer, the polymeric composition and morphology, the size and density of the beads, as well as the physicochemical properties of the incorporated drug. *In-vitro* drug release also depends upon pH and the used dissolution media. The release of drug from these beads involves the:

- desorption of the surface bound for the small amount of drug entrapped in the surface layer of the beads,
- diffusion through the bead polymeric matrix which comprises three steps, 1) water penetrates into the polymeric system of beads causing swelling of the matrix. 2) the conversion of glassy polymer into rubbery matrix 3) the diffusion of drug from the swollen rubbery matrix,
- bead polymeric matrix erosion or -combined erosion /diffusion process.

Our results indicated that F20 beads did not erode in SGF and still keep intact matrix, whereas in SIF (at pH 6.8) the main mechanism may be swelling/diffusion and successive erosion due to the ion exchange (Caballero, Foradada et al. 2014).

***In Vivo* experiments**

The anti-inflammatory activity of the formulation F20 in rats was evaluated by a carrageenan-induced oedema model and compared with the activity of pure drug. Rat paw oedema reached the maximum value (paw volume, mL) between 2 and 4 h after carrageenan injection, as shown in Figure 13.

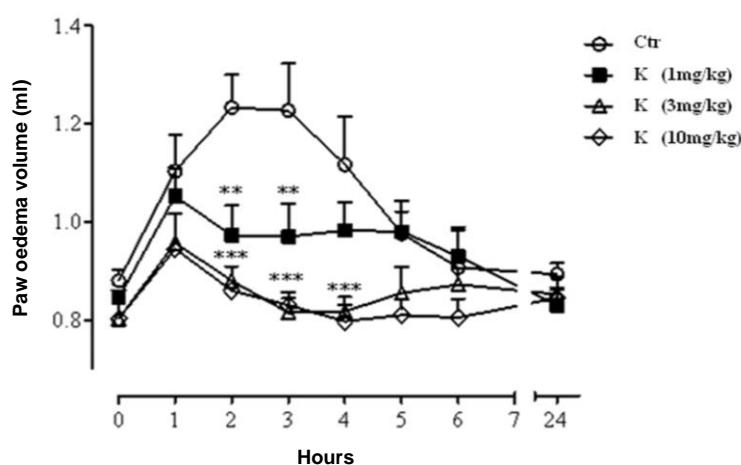


Figure 13. Zn-Alginate-based beads loaded with K. Dose-response curves of pure ketoprofen (1, 3 and 10 mg/kg doses) administered *per os* to rats 0.5h before carrageenan injection; mean \pm SD (n=8). **P \leq 0.01, ***P \leq 0.001 compared with control.

First, a dose–response curve of pure ketoprofen (1, 3, and 10 mg/kg *per os* doses) was performed following a conventional protocol, which prescribes drug administration 0.5 h before the injection of the phlogistic agent. As expected, the administration of pure ketoprofen caused a significant reduction of oedema after the first hour from carrageenan injection, compared with control at all tested doses. The anti-inflammatory effect of pure ketoprofen persisted even in the late phase of carrageenan induced rat paw oedema (24 h). These preliminary experiments suggest to select the dose of 3 mg/kg of ketoprofen as it achieved optimal anti-inflammatory effects (Fig. 13).

With the aim to verify a potential delayed *in vivo* anti-inflammatory effect, corresponding to the *in vitro* delayed drug release, F20 (ketoprofen equivalent

dose of 3 mg/kg) was administered orally following the same protocol at different time points (5, 3, or 0.5 h) before oedema induction.

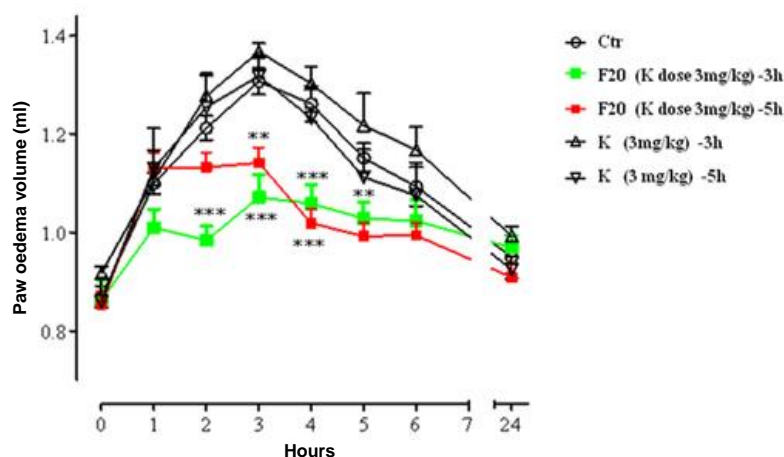


Figure 14. Zn-Alginate-based beads loaded with K. Oedema volume reduction obtained administering F20 and pure ketoprofen per os to rats 5 and 3h before carrageenan injection compared to control; mean \pm SD (n=8). **P \leq 0.01, ***P \leq 0.001 compared with control.

Interestingly, F20 showed a prolonged anti-inflammatory effect in terms of paw oedema inhibition after oral administration to rats compared with control. Pure ketoprofen (3 mg/kg) was efficient in reducing rat paw oedema only at t = 0 (0.5 h before phlogistic agent injection) (Fig. 13), whereas no response was observed when it was administered at 3 or 5 h before carrageenan injection. Blank Zn–alginate beads (F) did not significantly affect the paw oedema when administered to rats at the same time points before oedema induction (data not shown), thus, indicating that Zn–alginate matrix do not interfere with the inflammatory process. It is interesting to point out that F20 administered 3 h or 5 h before oedema induction still showed a significant anti-inflammatory activity by reducing maximum paw volume (3–4 h) in response to carrageenan injection, therefore reflecting an *in vivo* delayed release (Fig. 14).

The strong delay in drug anti-inflammatory activity appreciated *in vivo* may be due to a combination of the low gastric release of ketoprofen from F20

demonstrated *in vitro* and a further lowering of ketoprofen absorption in the GIT as an effect of the mucoadhesive properties of alginate beads (Aquino, Auriemma et al. 2013), which may guarantee a much more intimate and sustained contact with the absorption site (Moogooee, Ramezanzadeh et al. 2011).

3-A 1.3 Conclusions

In many inflammatory-based pathologies, clinical symptoms are commonly most severe in the early morning, closely following the circadian rhythm of the pro-inflammatory mediators such as cytokines and interleukins. A delayed release dosage form administered prior to sleep and able to deliver NSAID several hours after oral administration may be optimally effective to treat early morning symptoms.

The present study suggested that prilling by the accurate selection of biopolymers, the opportune set-up of process parameters and gelling conditions allows to produce interesting delayed drug delivery systems. Particularly, Zn^{2+} as gelling/curing cross-linker seems to affect physicochemical characteristics and *in vivo* performance of beads by a combination of effects. Technological properties of Zn–alginate-based beads, such as morphology, hardness of cross-linked matrix, mucoadhesion and, consequently, *in vitro* and *in vivo* release behaviour resulted strongly influenced by the amount of loaded ketoprofen.

The optimized formulation F20 may be proposed as a chronotherapeutic system that is able to slow and delay *in vivo* ketoprofen release and absorption to 6–7 h. By opportunely timing the administration of the oral dosage form, it is possible to match the disease rhythms and to better control early morning symptoms, particularly in rheumatoid arthritis therapy.

SECTION A PART 2:

Core-shell beads for delayed ketoprofen oral delivery

*Based on the article: **A. Cerciello**, G. Auriemma, P. Del Gaudio, F. Sansone, R. P. Aquino, P. Russo. “A novel core–shell chronotherapeutic system for the oral administration of ketoprofen”. *Journal of Drug Delivery Science and Technology*, **2016**, 32, 126-131.*

3-A 2.1 Scientific background and research aim

As reported in the part 1 of this section, ketoprofen may be encapsulated into a Zn-alginate matrix system with a quite satisfactory EE (higher than 50% for formulation F20). The Zn-alginate beads carrying ketoprofen resulted able to delay K release *in vitro* and prolong its anti-inflammatory effect up to 5h *in vivo* (Cerciello, Auriemma et al. 2015).

Although results are quite good, beads overall performance leaves room for improvement both in the encapsulation efficiency of K and in a further delay of drug release.

In order to further improve the beads loading capacity and the drug release rate control, a more complex drug delivery technology platforms was designed consisting of:

- Core/shell microparticles made up by:
 - ❖ a core of a different natural biocompatible polymeric carrier (pectin-based beads carrying ketoprofen)
 - ❖ and a gastro-resistant shell formed by gastro-resistant methacrylic acid - methyl methacrylate copolymer.

To achieve this goal, amidated low methoxyl (ALM) pectin was selected as alternative natural polysaccharide for the production of gel-bead core.

ALM pectins ensure high hydrophobic interactions between pectin chains and additional internal hydrogen bonding between amide groups, thus, better stabilizing the egg-box structure (Auriemma, Mencherini et al. 2013). Zinc was selected as crosslinking agent; in fact, as reported in the literature zinc-pectinate beads compared to calcium-pectinate beads are more able to resist in the upper gastro-intestinal tract and to refrain drug from premature release (El-Gibaly 2002; Das, Ng et al. 2010; Dhalleine, Assifaoui et al. 2011).

Considering that pectin usually exhibit poor stability in acidic conditions, the core-shell structure was designed as a monolayer system (K-Zn-ALM-pectin core) coated by an enteric shell, methacrylic acid methyl methacrylate

copolymer (Eudragit S100[®]). This synthetic polymer should protect the pectin-based core from a premature acidic degradation thanks to its property to dissolve only at pH close to 7 (Dai, Guo et al. 2015).

K-Zn-ALM-pectin core was produced by prilling deeply studying the process and formulation variables with special attention to ALM-pectin concentration, K/polymer ratio and gelling conditions (crosslinking agent concentration, pH and temperature) to optimize the production conditions and their effect on resultant particle properties (morphology, micromeritics, encapsulation efficiency) and performance (drug release).

Beads micromeritics, as well as solid state characteristics were studied using established method (SEM, DSC). *In vitro* dissolution/release tests were assessed in conditions simulating the gastrointestinal environment (USP 36) by means of a pH change method.

3-A 2.2 Pectin beads production and characterization

Ketoprofen loaded gel beads with desired size and high drug EE were obtained using a ALM-pectin feed of 6.00% (w/w) in aqueous solution. Different amounts of ketoprofen were suspended into the polymer solution and stirred for 2 h in order to obtain 3 different drug/polymer ratios in the pectin solution (1:20, 1:10 and 1:5 w/w). Prilling operative conditions were set as for the production of alginate loaded K beads (Section1_Part1): 400 μ m nozzle, frequency of vibration at 350 Hz (100% amplitude) and a feed flow rate of 5 mL/min;

The droplets produced by the laminar jet break up were collected into an aqueous solution of Zn (CH₃COO)₂×2H₂O (10% w/v, pH= 1.5) where they were gelled under gentle stirring. The gelation time was maintained between 5-10 min at room temperature then, the produced microparticles were recovered with a sieve and thoroughly rinsed with deionized water. Finally, the beads were dried at room temperature by exposure to air (22 °C; 67% RH)

for several hours (12-18 h) until constant weight was reached. In addition, blank beads of gel zinc pectinate (F) were produced as a control.

The actual drug content (ADC) and encapsulation efficiency (EE) of dried beads were determined by UV-VIS spectroscopy and the results obtained are shown in table II.

Table II. Zn-ALM-pectin-based beads loaded with K. Composition, theoretical drug content, actual drug content, encapsulation efficiency, mean diameter and sphericity coefficient of Zn-pectinate beads manufactured by prilling; blank (F) and loaded with ketoprofen (F20, F10 and F5).

Batch	Drug/polymer ratio (w/w)	TDC (%)	ADC (%± SD)	EE (%± SD)	Mean diameter (mm± SD)	SC
F	-	-	-	-	2.02 ± 0.08	0.91 ± 0.01
F20	1:20	4.8	3.9 ± 0.3	77.6 ± 2.6	2.51 ± 0.12	0.88 ± 0.04
F10	1:10	9.1	7.4±0.3	81.3 ± 3.0	2.76 ± 0.12	0.89 ± 0.04
F5	1:5	16.7	14.5 ± 0.3	86.7 ± 1.7	2.16 ± 0.10	0.99 ± 0.01

As reported in table II, also in the case of pectin based beads, ADC and EE were related to the drug/polymer ratio and EE increased with ADC increasing. This effect can be explained by assuming that the loading of larger quantity of K in the feed solution may promote the formation of a more compact polymeric matrix during the gelation process (Lin and Metters 2006; Hoffman 2012). Hydrophobic interactions between the ketoprofen and the ALM-pectin are able to stabilize the egg-box structure reducing drug leaking from liquid drops to the gelling bath, and thus, allowing a best entrapment of ketoprofen. As a result, beads F5, formulated with the greatest amount of drug (drug/polymer ratio 1:5), showed the highest EE (86.7 %). This effect was

previously observed also for alginate based beads loaded with K suggesting that the drug and its amount play an important role in the gel matrix formation and the derived technological features (Cerciello, Auriemma et al. 2015).

In order to study the main morphological characteristics of the produced gel beads formulations, SEM analyses combined to image J software elaboration were employed. Results revealed that K loaded microparticles have a mean diameter between 2.2 (F5) and 2.8 mm (F20), with F5 beads having highest sphericity coefficient (0.99).

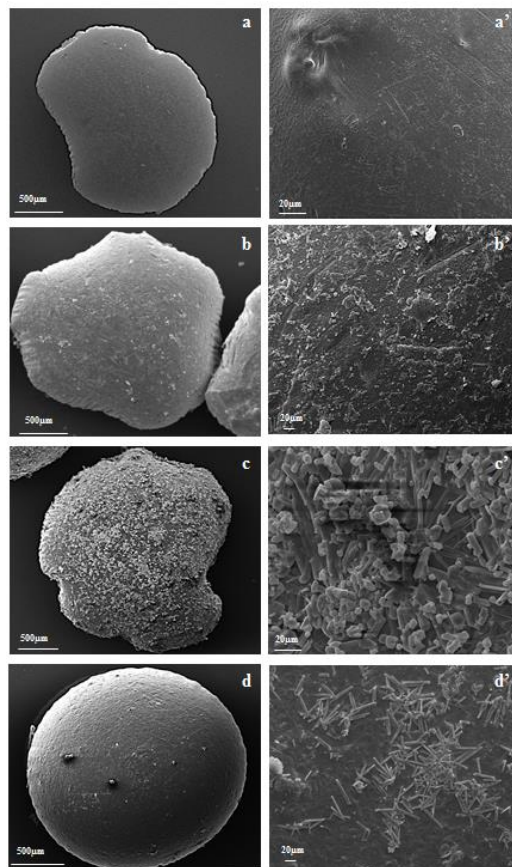


Figure 15. Zn-ALM-pectin-based beads loaded with K. SEM pictures of dried beads (left side) and of their surface (right side): F (a); F20 (b); F10 (c) and F5 (d).

F5 resulted spherical in shape and showed an uniform surface (Figure 15), while beads F (control blank), F20 and F10 (Fig. 15 a-c) presented a less regular geometry. The morphology results confirm that the loading of larger

amount actively contributes to the formation of a high structural density matrix, able to give to gel beads a well-defined morphology. Moreover, as evidenced by higher magnification photographs (Fig. 15, right side), showing the distribution of drug crystals on the surface of beads, F5 showed the lowest quantity of ketoprofen crystals on the surface (Fig. 15 d'), confirming the highest encapsulation efficiency.

With the aim to study the solid state of the drug before and after the encapsulation process and to highlight potential drug-polymer interactions, a series DSC experiments were performed (on ketoprofen raw material, on developed formulations and on blank beads (F) as control).

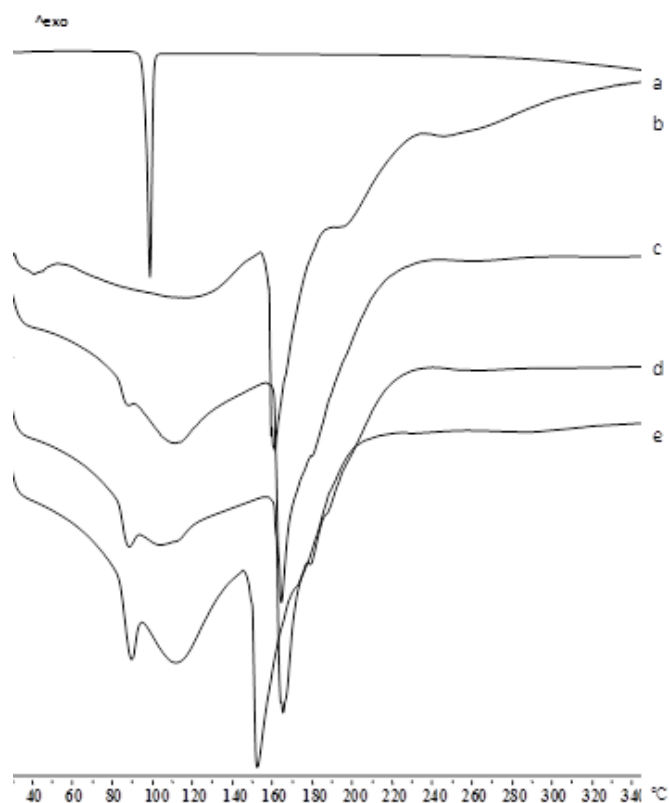


Figure 16. Zn-ALM-pectin-based beads loaded with K. DSC thermograms of: ketoprofen raw material (a); F (b); F20 (c); F10 (d) and F5 (e).

As reported in figure 16, ketoprofen raw material shows the typical thermal profile of a crystalline compound, with a melting peak at 98 °C (Auriemma, Del Gaudio et al. 2011). The thermogram of F beads (Fig 16b) shows two endothermic events in the range of 90 -120 °C and at 170 °C. The first signal corresponds to the loss of water adsorbed on the surface and entrapped into the gel matrix (Pillay and Fassihi 1999), the second at 170° C is due to the melting of zinc pectinate matrix. These events are followed by an exothermic signal ranging from 200 °C to 250 °C with a ramp-like trend, attributable to the degradation of cross-linked matrix. Drug loaded beads, F20 and F10, obtained with 1:20 and 1:10 drug/polymer ratio exhibit a thermal behaviour comparable to F beads (Fig. 15 c-d). The thermogram of F5 (Fig 16e), with the highest drug content, shows the melting endothermic peak of zinc pectinate slightly shifted at lower temperatures (155 °C vs 170 °C). This behaviour may be due to physical interactions between the polymer and the encapsulated drug (Liu and Guo 2006), Moreover, drug charged beads showed the melting peak of ketoprofen shifted at lower temperatures related to the presence of aliquots of drug embedded into the matrix and close to the surface.

Drug release studies

In order to have an indicator of performance, *in vitro* drug release assessment was carried out evaluating ketoprofen dissolution profile from ALM-pectin formulations, through a USP apparatus II using a classic pH change method (2 h in 0.1 M HCl, and then in 0.2 M of Na₃PO₄ at pH 6.8). The dissolution profiles are shown in Figure 17.

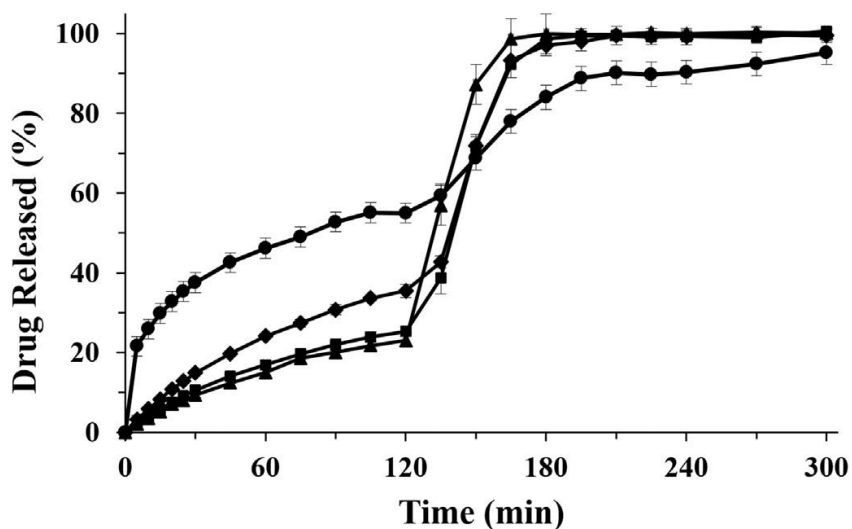


Figure 17. Zn-ALM-pectin-based beads loaded with K. Drug Release profiles of pectin based beads F20 (◆), F10 (■) and F5 (▲) compared to K raw material (●).

Results demonstrated that the beads drug content may affect the amount of drug released especially in SGF. In fact, #F5, formulated with the greatest amount of ketoprofen, released into the gastric simulated fluid only 22.2% of the loaded drug and reached the complete release of the drug in SIF after 1 hour from pH change. The lower percentage of drug released in gastric environment from F5 compared to F10 and F20 was related, firstly, to the lower quantity of drug crystals on beads surface as evidenced by SEM photographs (Fig. 15). Moreover, this result supported the hypothesis that the loading of higher amounts of drug contributes to produce a tougher polymeric matrix able to better encapsulate the drug during the ionotropic gelation process as well as to retain the drug when it is in contact with biological fluids. The tough polymeric matrix also deriving from the high degree of crosslinking caused by zinc ion, increased the structural density of the F5 polymeric matrix after drying process, contributing to delay the release of ketoprofen. After changing the pH, a rapid swelling and erosion process in SIF takes place, pectin chains are hydrolysed and complete the drug release in about 1 hour;

the phosphate ions in simulated intestinal fluid (SIF) determined, in fact, the capture of zinc ions from the cross-linked polymeric matrix, causing its dissolution with consequent prompt release of the encapsulated drug.

Design and production of core-shell microparticles

Considering the rapid swelling and erosion process in SIF, monolayer pectin based beads are able to delay K release only up to 180 min and, this lag time, was inadequate for a chronotherapeutic treatment of RA, whereby, beads were coated with Eudragit S100[®], an anionic copolymer of methacrylic acid and methyl methacrylate insoluble in acid pH (de Arce Velasquez, Ferreira et al. 2014; Maghsoodi 2014; Dai, Guo et al. 2015), to obtain core-shell system.

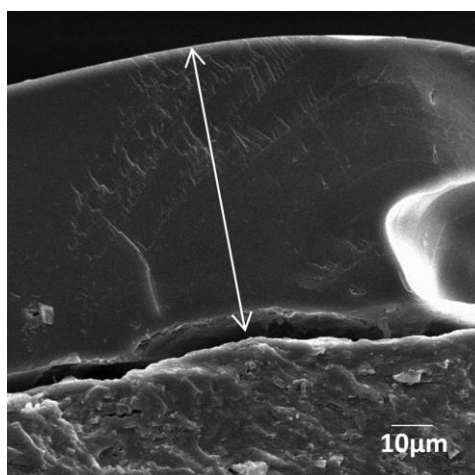


Figure 18. Zn-ALM-pectin-based beads loaded with K. SEM picture of cryo-fractured (F5)-shell (40% w/w Eudragit S100[®]) system, with magnification of the core-shell structure.

In preliminary experiments, the covering level of F5 beads was varied between 10 and 60% w/w. A uniform coating of about 100 µm was achieved with the addition of 40% w/w of enteric polymer, as shown in figure 18, while with a 20% w/w Eudragit S100[®] content the shell cannot cover the entire particles surface and a 60%w/w of Eudragit S100[®] produced adhesive particles that tended to aggregate.

The *in vitro* dissolution performance of final technological platforms F5/ES100 is reported in figure 19.

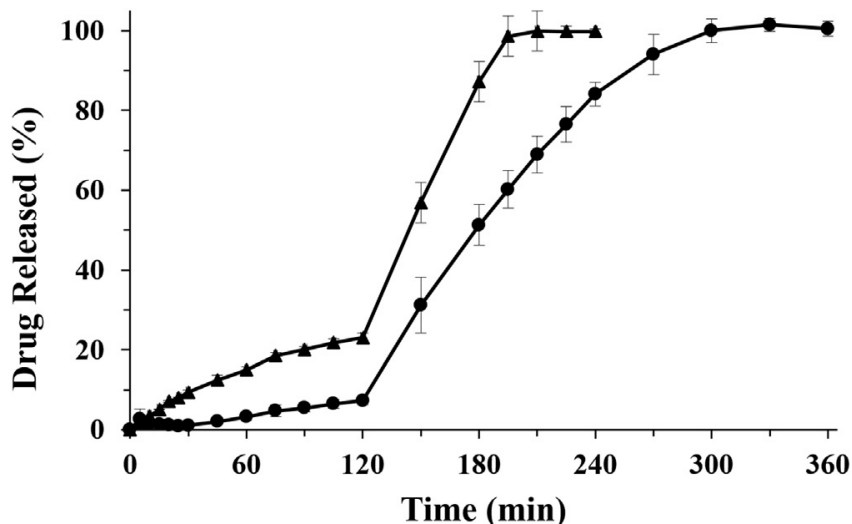


Figure 19. Zn-ALM-pectin-based beads loaded with K. Drug Release profiles of core shell microparticles F5/ES100 (●) compared to monolayer formulation F5 (▲).

Interestingly, the core (F5)-shell (40% w/w Eudragit S100[®]) system showed a strong delay of ketoprofen release in SGF followed by a slow and controlled release in SIF. The core-shell system is able to significantly reduce the release of ketoprofen in acid pH from 22.2% (monolayer F5) up to 7.3% and extend its release in simulated intestinal environment. After the pH change, in fact, the drug release was completed in about three hours (t = 300 min) rather than in one hour (t = 180) as for F5.

Only after the dissolution of the Eudragit S100[®] shell in SIF, the pectin/drug core was exposed to the fluid and pectin chains started later the hydrolysis process, releasing slowly the encapsulated drug.

3-A 2.3 Conclusions

The present study suggested that prilling may produce core-beads of pectin showing narrow size distribution and high drug content and encapsulation efficiency. ALM-pectin beads opportunely gelled with Zn ions revealed as an

alternative polymeric carrier to alginate for ketoprofen oral delivery. In particular, the loading of larger amounts of drug in the feed solution (1:5 drug/polymer ratio as in F5) may promote, as previously observed for Zn-alginate beads, the formation of a compact cross-linked matrix, allowing high encapsulation efficiency (87%) and reducing drug release in simulated gastric fluid (22%). The core-shell system may be obtained applying a gastro-resistant polymer, Eudragit S100[®] as a shell (40% w/w) to F5 core. The core-shell system developed was able to dramatically increase the retain of ketoprofen in the acid simulated environment (7.3% drug released in SGF) and to prolong the release in simulated intestinal environment until 5 h. This optimized technology platform appears, therefore, feasible and potentially effective as a dosage form suitable for the chronotherapy of RA. The control and strong delay in the NSAID release suggests a drug products to be taken at bed time and able to act in the early morning.

SECTION A PART 3:

Ketoprofen lysine salt controlled release systems: Alginate vs ALM-pectin

*Based on the article: **A. Cerciello**, G. Auriemma, P. Del Gaudio, M. Cantarini, R.P. Aquino. “Natural polysaccharides platforms for oral controlled release of ketoprofen lysine salt”, *Drug development and industrial pharmacy*, **2016**, dx.doi.org/10.1080/03639045.2016.1195401.*

3-A 3.1 Scientific background and aim

In the first part of my PhD project (Section A, part 1-2), the work was aimed to encapsulate a poor soluble NSAID, ketoprofen K (BCS class II), optimizing formulation and operative conditions of prilling technique accordingly to the physic-chemical characteristics of the selected drug.

In this part of the PhD program, the versatility of prilling technique for the production of engineered microparticles was evaluated loading an highly soluble NSAIDs Ketoprofen lysinate (KL), using Zn-alginate and Zn-ALM-pectin as release controllers.

Particularly, KL, the water soluble lysine salt of ketoprofen (K), is commonly used in the symptomatic treatment of various chronic inflammatory diseases such as RA (Gentile, Boltri et al. 1999) and it is frequently used in paediatric therapy for its analgesic efficacy.

Furthermore, compared to K, L-lysine salt has shown better pharmacokinetics and tolerability, enhancement in the rate of absorption, reduction of the onset of therapeutic effect as well as improvement of the gastric tolerance (Cimini, Brandolini et al. 2015).

Although several studies have been reported on polysaccharide hydrogels entrapping the non-soluble form of K (Del Gaudio, Russo et al. 2009; Prajapati, Patel et al. 2012; Cerciello, Auriemma et al. 2015), few or no researches are available on L-lysine salt. In fact, the high KL solubility is the limiting step for the formulation of delivery systems with high drug encapsulation efficiency and, above all, controlled release properties.

To achieve this goal, many formulation and prilling process variables have been investigated to find the optimal ones. Moreover, due to the high KL solubility in simulated biological fluids, the optimized formulation was selected as starting material for the preparation of an advanced delivery platform charging drug loaded beads in specific acid-resistant capsules. A similar platform may be potentially able to guarantee a delayed and sustained

drug release. Different types of capsules were taken into account and finally DR[®] capsules were selected as the proper ones (Cerciello, Auriemma et al. 2016).

3-A 3.2 Gel-beads production and characterization

Two series of KL hydrogel-based beads were prepared by prilling using alginate or ALM-pectin as carrier material.

All beads formulations were prepared using Zn as gelling agent and optimizing cross-linking conditions in terms of temperature (4-5 °C), pH (1.5) and gelling time (2 min) in order to limit drug leaking during the ionotropic process accordingly to the high KL solubility. In fact, as reported elsewhere, temperature as well as pH are key parameters to properly set (Sriamornsak 2003) in order to improve the gelling properties of pectin or alginate and, consequently, limit drug leaking typical of high solubility API. In fact, as reported for pectin beads, at high temperature (or pH increase), a chain cleavage process starts and results in very rapid loss of viscosity and gelling properties (Sriamornsak 2003). In addition the gelling time was maintained as low as possible to obtain a compact hydrogel reducing the potential drug leaking.

Six formulations, namely F2-F8, as shown in Table III, were produced using 2.0% and 6.0% w/w polymer concentrations for alginate or pectin, respectively, and varying drug-polymer ratio from 1:20 to 1:5. As control, blank beads (F1, alginate and F5, pectin) were also produced. Drying process of the hydrated beads was conducted by exposing beads to standard room conditions (22 °C; 67% RH) for 12–18 h until constant weight was reached.

Results reported in Table III showed that actual drug content (ADC) and encapsulation efficiency (EE) values were related to the specific polymeric material used to manufacture the beads and drug polymer ratio. The higher the drug polymer ratio, the higher the EE. KL encapsulation process was more

efficient in pectin than in alginate with EE values ranging from 39.0% to 49.7% for zinc-alginate beads (F2, F3, F4) and from 81.8% to 93.5% for pectin-based beads (F6, F7, F8), probably due to pectin lower molecular weight that enhanced gel matrix texture (Mesbahi, Jamalian et al. 2005; Kim, Kim et al. 2010).

Table III. Zn-alginate and Zn-ALM-pectin-based beads loaded with KL. Formulation code, polymeric carrier, actual drug content (ADC), encapsulation efficiency (EE), mean diameter and sphericity coefficient (SC) of optimized bead formulations manufactured by prilling.

Formulation code	Polymer (w/v)	KL/Polymer Mass ratio	ADC (%±SD)	EE (%±SD)	Dried beads diameter (µm±SD)	SC
F1	Alginate 2.0%	-	-	-	2386 ± 119	0.93±0.01
F2		1:20	1.9±0.1	39.0±1.6	2456 ± 88	0.91±0.01
F3		1:10	4.1±0.5	44.8±2.7	2210 ± 97	0.89±0.02
F4		1:5	8.3±0.2	49.7±1.5	2303 ± 107	0.91±0.01
F5	Pectin 6.0%	-	-	-	2002 ± 80	0.91±0.01
F6		1:20	3.9±0.2	81.8±4.0	2119 ± 112	0.85±0.05
F7		1:10	8.4±0.2	92.4±1.8	2018 ± 79	0.92±0.01
F8		1:5	15.6 ± 2.9	93.5±2.9	2200 ± 134	0.91±0.01

To better understand the influence of the specific polymer on gel-matrix texture, beads were cryo-fractured and analysed by SEM. Results highlighted a homogeneous and tougher inner matrix for pectin based beads compared to those produced with alginate.

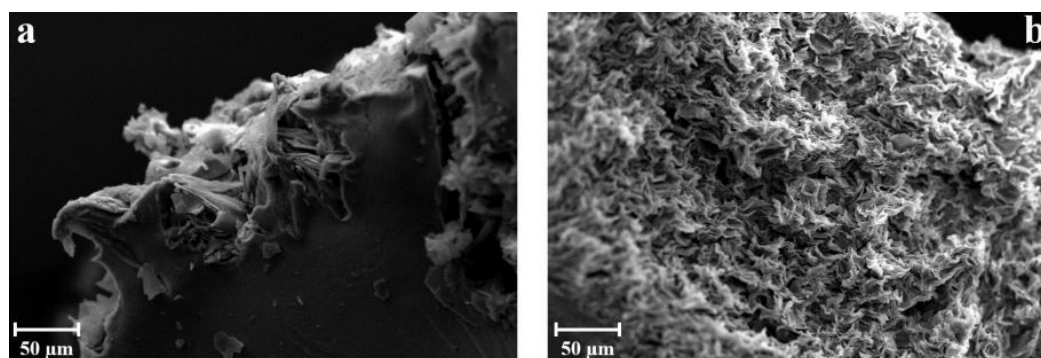


Figure 20. Zn-alginate and Zn-ALM-pectin-based beads loaded with KL. SEM microphotographs of cryo-fractured xerogel beads: F4 (a) and F8 (b).

In fact, as shown in Figure 20, KL crystals were homogeneously embedded within the Zn-ALM-pectinate matrix (Fig. 20-b) whereas they spread out on the surface for all Zn-alginate beads (Fig. 20-a). It can be assumed that this effect is due to the formation of several intermolecular hydrogen bonds and hydrophobic interactions between KL and pectin amino residues able to deeply stabilize the egg-box structure (Liu, Fishman et al. 2005; Sato and Miyawaki 2008). During the cross-linking phase, high density of the formed hydrogels can reduce the drug leaking from the hydrated beads to the gelling bath, allowing high KL entrapment (Hoffman 2002; Lin and Metters 2006). Moreover, the strong hydrogel network can determine a high shrinkage of the volume after drying process, leading to a significant reduction in mean diameter of the beads. In fact, ALM-pectin-based beads showed lower size than alginate based beads with reduction in mean diameter of 45% and 23%, respectively.

As pointed out by SEM analyses combined to image J software elaboration (Table III), mean diameters ranged from 2002 to 2200 μm for zinc-pectinate beads while zinc-alginate beads showed mean diameters between 2210 and 2456 μm . On the contrary, no significant differences were observed in terms of shape and sphericity coefficient among pectin or alginate based beads as in terms of KL polymer ratio.

SEM analyses at higher magnification showed that all KL alginate beads (F2-F3-F4) exhibited on the surface micrometric KL crystals; the amount of such crystals was not dependent on the drug-polymer ratio used to formulate the beads (Figure 21).

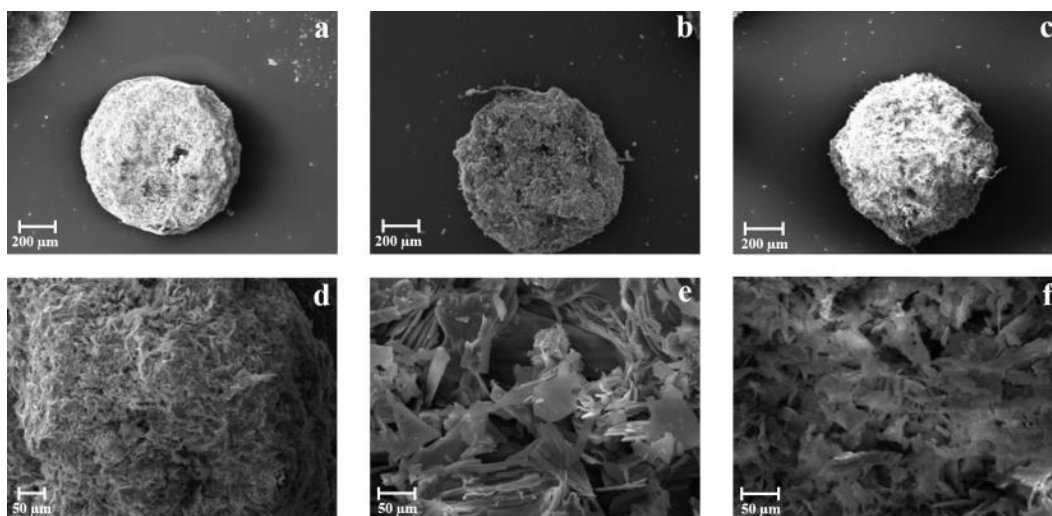


Figure 21. Zn-alginate and Zn-ALM-pectin-based beads loaded with KL. SEM microphotographs at different magnification of dried Zn-alginate beads: F2 (a–d), F3 (b–e) and F4 (c–f).

This phenomenon may be due to the incapability of zinc-alginate gel network to retain into its texture a highly soluble drug like KL that, during drying process migrates on the surface of the beads. On the contrary, analysing KL pectin-based beads, the presence of drug crystals was strictly related to KL content.

In fact, as shown in Figure 22, F6 showed only tiny spots of the drug on beads surface whereas in case of F7 and F8, in spite of a tougher polymeric matrix, drug loading enhanced KL diffusion on beads surface.

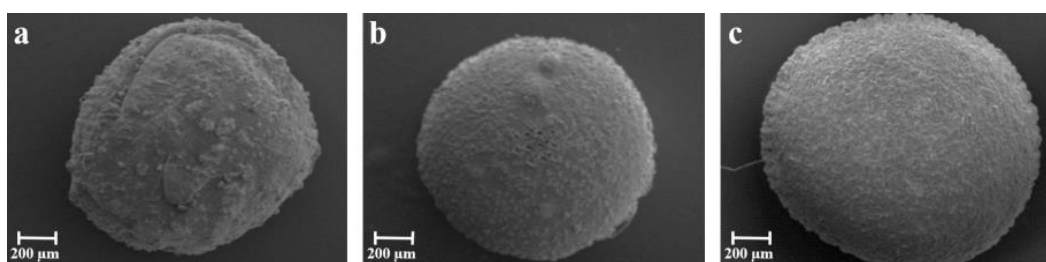


Figure 22. Zn-alginate and Zn-ALM-pectin-based beads loaded with KL. SEM microphotographs of dried Zn-pectinate beads: F6 (a), F7 (b) and F8 (c).

In order to study the effect of prilling process on the encapsulated drug as well as potential KL-polymers interactions, differential scanning calorimetric technique was used. In fact, DSC analysis is a well-known method often used to characterize physical and chemical changes in either enthalpy or heat capacity of a crystalline drug in a polymeric matrix after the encapsulation process (Manjanna, Rajesh et al. 2013). DSC thermal profiles of KL raw material, blank (F1 and F5) and KL loaded beads (F4-F8) are shown in figure 23.

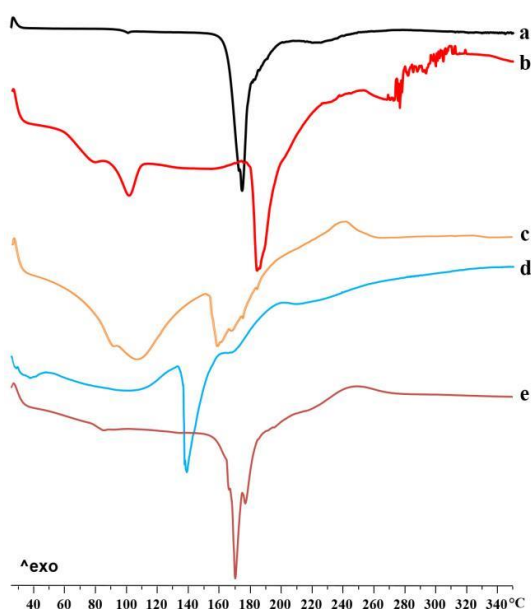


Figure 23. Zn-alginate and Zn-ALM-pectin-based beads loaded with KL. Differential scanning calorimetry thermograms: KL raw material (a) and blank Zn-alginate beads (b), F4 (c), blank Zn-pectin beads (d) and F8 (e).

KL exhibited the typical profile of a pure crystalline drug with a melting peak at 170°C. Thermograms of blank Zn²⁺-alginate beads (F1) showed two endothermic events, well separated in temperature values, at 107°C, corresponding to the loss of hydration water from the polymeric matrix (Pillay and Fassihi 1999; Cerciello, Auriemma et al. 2015); and at 190°C, corresponding to the melting of zinc-alginate matrix. These events are

followed by a ramp-like event ranging from 220°C to 300°C referable to cross-linked matrix degradation. KL loaded alginate beads, as reported for F4 (Figure 23-c), showed a thermal trend comparable to F1 beads. However, the first broad endotherm ranging from 90 to 115°C showed a higher peak intensity due to the increased water content, whereas the second endothermic peak resulted shifted at lower temperature. The last effect may be due to the presence of KL on the beads surface into the matrix as shown by SEM images and it is more evident in F4 beads formulated with the highest KL amount (drug/polymer ratio 1:5). Regarding ALM-pectin-based formulations, blank beads F5 showed an endothermic event at 145°C due to the melting of the zinc pectinate matrix and an exothermic signal at 165-220°C due to its degradation. Thermal profile of F8 (Figure 23-e), reported as example, exhibited significant shifts of these events at higher temperatures (160-180°C and 240°C), which may be attributed both to drug polymer matrix interaction and to a slower heat transfer correlated to the increase in beads hardness (Pawar, Gadhe et al. 2008).

Drug release studies

To verify whether the produced polysaccharides-based beads can be carriers able to modulate KL release in the gastrointestinal tract, dissolution tests were performed by means of the USP Apparatus II (Yang, Chu et al. 2002), using a classic pH change protocol. The main dissolution profiles are shown in Figure 24

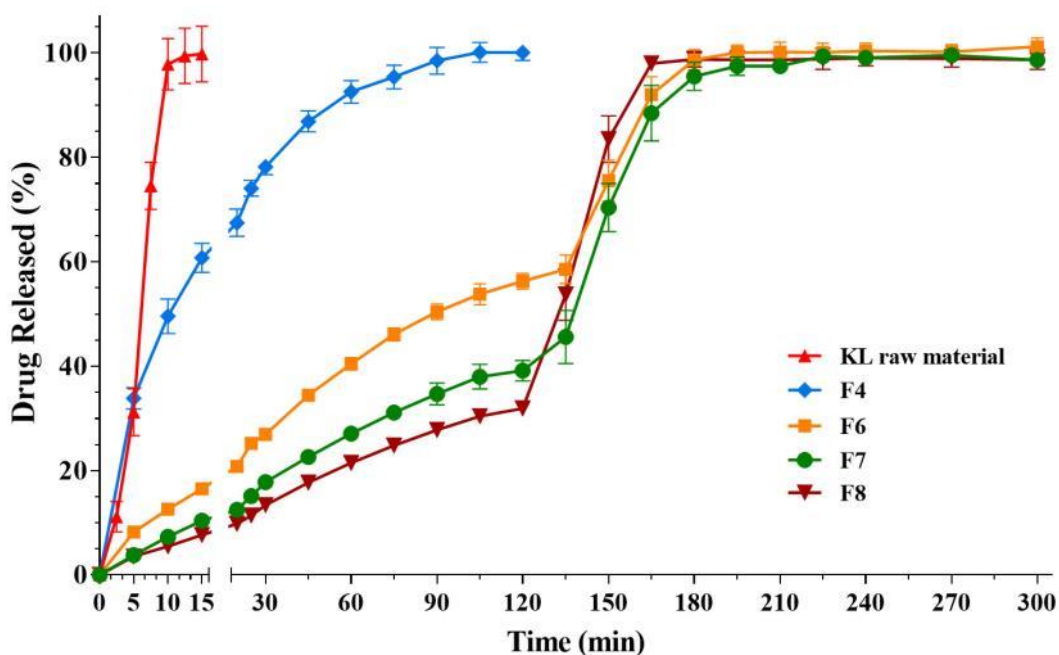


Figure 24. Zn-alginate and Zn-ALM-pectin-based beads loaded with KL. KL release profiles of formulations F4, F6, F7 and F8, compared to KL raw material.

All alginate based beads provided fast and complete drug release in acidic medium, without any lag time, in 120 min. Formulation F4, reported as example, released total KL dose at the end of the acid cycle.

On the contrary, all pectin based beads were able to achieve KL sustained release. In fact, during the permanence in acidic medium (120 min) the cumulative percent drug release was 56.2%, 39.1% and 31.9%, for F6, F7 and F8, respectively. After the pH change, drug release rate increased very rapidly, leading to KL complete delivery in about 1 h (t=180 min).

The specific drug release profile from each formulations' series perfectly matches with beads morphology and structure data obtained by SEM investigation. The F4 faster release in gastric environment was due to the presence of KL crystals on beads surface as well inside inner polymer matrix texture, which makes them highly permeable. On the contrary, the release performance of Zn²⁺-ALM-pectinate beads can be related to their structural

density which reduces swelling and erosion processes in SGF, keeping the xerogel matrix intact (Pal, Singh et al. 2013; Cerciello, Auriemma et al. 2016). Interestingly, results also showed that the amount of KL released in acidic medium decreases with drug content. Therefore, the loading of large amounts of KL in pectin based beads may promote, during the gelling phase, the formations of additional intermolecular interactions between polymer chains and KL, as also pointed out by DSC analyses, able to further stabilize the final xerogel matrix. These results are consistent with recent literature studies, confirming the higher suitability of LMP to produce xerogel beads with improved technological properties if compared to alginate (Voo, Ravindra et al. 2011; Belscak-Cvitanovic, Komes et al. 2015).

As initially planning for an highly soluble API, with the aim to further limit and delay KL release performances, F8, the most promising formulation, was selected as starting material for the preparation of a drug delivery platform made up by DR[®] capsules and F8 (F8/DR caps). Differently from conventional gelatin capsules that undergo breakdown in simulated gastric fluid in about 5 minutes, the DR[®] caps begin to disaggregate after 75-90 minutes enabling the protection of F8 formulation from the acidic environment.

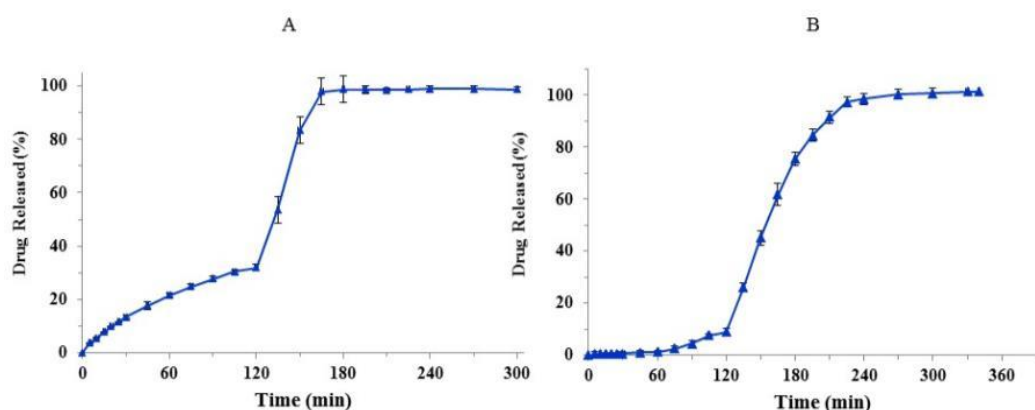


Figure 25. Zn-alginate and Zn-ALM-pectin-based beads loaded with KL. KL release profiles of F8 (A) compared to the optimized platform F8/DR caps(B).

As reported in Figure 25, F8/DR caps platform showed a strong delay of KL release in acidic environment followed by a slower release in SIF. In fact, F8/DR caps platform is a gastro-resistant formulation, reducing KL release in SGF from 31.9 to 8.8%, and prolonging its release in intestinal simulated fluid until 270 min compared to 180 min as observed for F8. Only after the disaggregation of the capsule's body, beads came into contact with the dissolution medium, starting later the dissolution process. After a lag time of about 90 min, beads are released from the capsule, start to hydrate and swell allowing a slight drug diffusion in acid medium followed by slower swelling/erosion processes in intestinal simulate fluid.

Drug release rate from the optimized platforms (ALM-pectin xerogel beads plus DR[®] capsules) may be potentially useful for the targeted release of BCS class I drugs, such as KL and theophylline, BCS class II drugs, as indomethacin, or even macromolecules, such as BSA, improving in all cases bioavailability of the loaded active pharmaceutical ingredient.

3-A 3.3 Conclusions

The present study suggests that prilling technique, conveniently optimized in terms of composition of feed solution, process parameters and gelling conditions, can be successfully used to encapsulate highly soluble drugs such as KL in polysaccharides-based hydrogels. ALM-pectin proved to be a proper polymer able to encapsulate ketoprofen lysine salt. F8 formulation was produced using 6% w/v polymer feed, drug-polymer ratio (1:5) and 10% w/v of zinc acetate (T= 4-5°C, pH= 1.5, 2 min) gelling conditions. Xerogel beads showed good morphological and size properties, high drug content and encapsulation efficiency and, finally, interesting drug release profiles. Hosting F8 in appropriate acid-resistant capsules such as DR[®] caps a new delivery platform has been obtained able to control KL release in a delayed (90 min lag time) and prolonged (270 min for complete delivery) way. The platform may

be proposed as potentially useful in the administration of highly soluble NSAIDs in the chronotherapeutic treatment of RA and /or colon targeted drug-release.

SECTION B:
Design and development of ChDDS
loaded with prednisolone as model
SAIDs

Scientific background and general aim

The first part of my PhD project, as reported in section A, was aimed to produce NSAIDs delivery systems (monolayer gel-bead and core-shell particles) with high drug entrapment and a prominent delay of drug release, satisfying the requirements of a chronotherapeutic approach for RA through the proper fine-tuning of prilling parameters.

Results showed that prilling was a suitable microencapsulation technique to produce chronotherapeutic drug delivery systems (ChDDS) of NSAIDs with different solubility features (K and KL), using polysaccharide carriers, alginate and ALM-pectin properly crosslinked with Zn ions.

In the second part of the project, our goal was to fully realize the potential of the prilling technology by creating appropriate carrier systems for SAIDs (Steroidal anti-inflammatory drugs) that would be specifically designed to improve the administration of prednisolone addressing the requirements of a chronotherapeutic treatment of RA.

SAIDs are widely used in RA management for their anti-inflammatory and immunosuppressive properties offering rapid symptomatic effects as for NSAIDs and in addition acting as “disease-modifiers” (Smolen, Aletaha et al. 2016). In fact, they have the ability to inhibit the transcription of different cytokines and chemokines responsible of RA physiopathology (IL-1, TNF- α , IL-3, IL-4, IL-5, IL-6, IL-8, IL-11, IL-12, IL-13) and macro-phage inhibitory protein (MIP) (Van der Velden 1998). However, they long-term use may lead to severe side effects like gastro-intestinal troubles, osteoporosis, muscle atrophy/myopathy, glaucoma, diabetes, cardiovascular and immune system complications (Schäcke, Döcke et al. 2002). The development of modified-release SAIDs formulations may be useful in treating the early morning symptoms of RA, reducing the well-known side-effects and improving the therapeutic efficacy (Alten, Döring et al. 2010; Alten, Holt et al. 2015).

Among different SAIDs, prednisolone and prednisone are the most widely used steroids for the oral therapy of chronic inflammation diseases because of their short half-life and relatively low side effects, compared to other SAIDs. The drugs are metabolically interconvertible, prednisolone being the pharmacologically active species. Both drugs are rapidly absorbed after oral administration with plasma half-lives of about 3.5h for prednisone and 2.8h for prednisolone. However, prednisolone bioavailability after the administration of an oral prednisone dose is approximately 80% compared to similar prednisolone dosage form. (Davis, Williams et al. 1978; Pickup 1979). Moreover, prednisolone administration seems to be preferable also in case of liver disease, because of the poor conversion of prednisone to prednisolone (Madsbad, Bjerregaard et al. 1980).

Despite the number of scientific papers on controlled-release formulation of prednisolone (Okimoto, Miyake et al. 1998; Di Colo, Baggiani et al. 2006; Lau, Johnson et al. 2012; Skowyra, Pietrzak et al. 2015), there are currently no products available on the market following a chronotherapeutic approach of the early morning pathologies.

For these reasons, engineered microparticles loaded with prednisolone as model SAIDs were produced by prilling technique, studying extensively all the formulation variables (polysaccharide concentration, drug polymer ratio, presence of other excipient) and prilling process conditions with special emphasis to the gelling process (nature of the crosslinking agent, its concentration, pH and temperature).

Results from the previous researches and the acquired know-how suggest that alginate may be the polymer of choice for prednisolone delivery acting as carrier and drug release modifier (Auriemma, Del Gaudio et al. 2011; Aquino, Auriemma et al. 2012; Auriemma, Mencherini et al. 2013; Del Gaudio, Auriemma et al. 2014; Cerciello, Auriemma et al. 2015).

To achieve our goal, three different technological strategies were followed:

- Development of basic prednisolone-loaded alginate beads produced by prilling

This part of the research comprises

- Study of the effect of divalent cations and their combination on the gelation process of alginate beads loaded with prednisolone (Part 1)
- Study of the effect of the polymer concentration and drug/polymer ratio on the performance of alginate beads (Part 2)
- *In vitro/in vivo* characterization and selection of optimized prednisolone-loaded beads (Part 2)

- Development of a more complex drug delivery technology platform

The design of a more “smart” and efficient oral platform for prednisolone delivery was based on drug-carrying beads showing the best *in vitro* performances and their charging into specific DR[®] capsules, to obtain final dosage form able to further delaying the drug release (Part 2).

- Design and formulation of floating alginate beads and their *in vitro/in vivo* characterization and performances (Part 3).

SECTION B PART1:

Study of the effect of divalent cation and their combination on alginate beads loaded with prednisolone

*Based on the article: **A. Cerciello**, P. Del Gaudio, V. Granata, M. Sala, R. P. Aquino, P. Russo. “Synergistic effect of divalent cations in improving technological properties of cross-linked alginate beads”. *Submitted 2016.**

3-B 1.1 Specific aim

Gelling solution parameters are critical variables in ionotropic gelation process and, consequently, their setting is one of the main purpose in prilling technique. The nature of the gelation bath/solvent, the selected crosslinking agent and its concentration as well as temperature and pH have functional relationship with gelling time, gel viscosity and beads strength. Moreover these key parameters may influence the technological characteristics of the final beads, such as drug entrapment, morphology and size, swelling and release behaviour as well as *in vivo* performance of the beads.

In this part of my PhD project, special attention was focused on the study of the effect of cross-linker agents on microparticles formation and characteristics, examining the possibility to use a combination of two divalent cations and aiming to exploit the positive features of individual cations, reducing their weaknesses (Ca^{2+} e Zn^{2+}).

While some papers reports on alginate beads produced with different cations (Das and Senapati 2008; Jay and Saltzman 2009), few researchers refers on the simultaneous use of two cationic crosslinkers (Chan, Jin et al. 2002).

Literature survey shows that calcium is the most used divalent cation in alginate hydrogels formation able to realize a three dimensional lattice of ionically crosslinked polymer chains. Ca^{2+} ions preferentially interact with the polyguluronic acid units (GG) of alginate in a planar two-dimensional manner, while producing the so-called “egg-box” structure (Chan, Jin et al. 2002). In contrast to the efficiency of calcium-alginate interactions, matrix swelling and drug release from Ca^{2+} -alginate beads seems to proceed rapidly in simulated biological fluids, both in gastric and in intestinal fluids, making Ca^{2+} -alginate beads not applicable as oral controlled DDS (Østberg, Lund et al. 1994; Taha, Nasser et al. 2008). In fact as reported from El-Kamel et al., the release of diltiazem hydrochloride from Ca^{2+} -alginate beads tested in simulated gastric or

intestinal fluid was very high (between 50-100% after 2h) (El-Kamel, Al-Gohary et al. 2010). This effect is probably due to the high susceptibility of calcium beads to the ions present in the dissolution fluid (Østberg, Lund et al. 1994), in fact only when pure water was used for dissolution tests Ca^{2+} -alginate beads result able to control the drug release (Aslani and Kennedy 1996).

On the contrary, as reported in the previous sections and confirmed in literature, the use of Zn^{2+} seems to be more suitable for the design of alginate hydrogels, prolonging drug release (Taha, Nasser et al. 2008; Cerciello, Auriemma et al. 2015).

For these reasons, alginate beads were prepared with Ca^{2+} and Zn^{2+} alone or blended in different ratios into the gelling solution. Their effect on hydrogel formation and properties, including particle size, morphology, and ability to encapsulate the drug were evaluated, inner matrix distribution and factors affecting drug release were also studied.

3-B 1.2 Gel-beads production and characterization

Preliminary, based on the previous experience (Aquino, Auriemma et al. 2012; Auriemma, Mencherini et al. 2013), operative parameters of the prilling apparatus were set and alginate concentration into the feed solution at 2.00 % (w/v) and drug polymer ratio at 1:5 were used.

A 600 μm nozzle was employed with a vibration frequency of 350 Hz, (100% of amplitude) and the flow rate was fixed at 6 ml/min. The droplets produced by the laminar jet break up, were collected into an aqueous solution (0.5M; pH = 1.5) of Zn^{2+} or Ca^{2+} ions or their mixtures (1:1, 4:1, 1:4), where they were gelled under gentle stirring. The beads were held into the gelling solution for 2 min at room temperature, then recovered with a sieve and thoroughly rinsed with deionized water. Finally, the hydrated gel-beads were dried to increase

product handling and stability by air exposure at room temperature (22 °C; 67% RH) for several hours (12–18 h) until constant weight was reached.

Blank (b) and P loaded alginate beads were produced (table IV), varying the cation or the blend of cations (Ca²⁺, Zn²⁺, Ca²⁺ plus Zn²⁺).

Table IV. Alginate based beads loaded with P using different crosslinking agents. (alginate 2.00 w/v; drug polymer ratio 1:5). Formulation code, gelling cation, actual drug content, encapsulation efficiency and micromeritics of dried beads obtained by prilling/inotropic gelation technique

Formulation code	Gelling Cation	ADC (%±SD)	EE (%±SD)	Dried beads diameter (mm±SD)	SC
F1	Ca ²⁺	12.9 ± 0.4	77.4 ± 2.5	1.49 ± 0.09	0.91 ± 0.02
F1_b	Ca ²⁺	/	/	1.60 ± 0.06	0.93 ± 0.02
F2	Zn ²⁺	10.9 ± 0.3	65.6 ± 1.9	2.66 ± 0.13	0.90 ± 0.02
F2_b	Zn ²⁺	/	/	2.39 ± 0.12	0.93 ± 0.01
F3	Ca ²⁺ /Zn ²⁺ (1:1)	12.0 ± 0.5	71.8 ± 3.3	2.30 ± 0.12	0.90 ± 0.02
F3_b	Ca ²⁺ /Zn ²⁺ (1:1)	/	/	1.75 ± 0.07	0.94 ± 0.01
F4	Ca ²⁺ /Zn ²⁺ (1:4)	12.0 ± 0.5	71.7 ± 3.0	2.12 ± 0.13	0.89 ± 0.03
F4_b	Ca ²⁺ /Zn ²⁺ (1:4)	/	/	1.88 ± 0.09	0.94 ± 0.01
F5	Ca ²⁺ /Zn ²⁺ (4:1)	13.8 ± 0.8	82.1 ± 4.9	2.32 ± 0.13	0.88 ± 0.03
F5_b	Ca ²⁺ /Zn ²⁺ (4:1)	/	/	1.72 ± 0.09	0.93 ± 0.02

The beads were evaluated for particle size, entrapment efficiency, *in vitro* drug release examined in simulated gastric fluid (pH 1.2) and simulated intestinal fluid (pH 6.8), swelling ability, surface and inner characterization using a scanning electron microscopy (SEM). SEM images demonstrated the structure and surface of the beads; SEM-EDS highlighted the structure and the cations distribution in cryo-fractured particles. Differential scanning calorimetry (DSC) was utilized to check the effective inclusion of the drug into the alginate matrix.

All batches showed good results in terms of encapsulation efficiency (EE >60%, table IV). In particular, Ca²⁺-alginate beads (#F1) showed the higher EE value (77.4%), compared to Zn²⁺-alginate beads (#F2, 65.6%). This effect may be related to calcium hard electrophile nature, able to quickly establish electrostatic interactions with guluronic (G) groups of alginate; the softer ions like zinc, instead tend to slowly form covalent-like bonds with carboxylate groups of G and mannuronic (M) alginate moieties (Aiedeh, Taha et al. 2007; Taha, Nasser et al. 2008).

The presence of Ca²⁺ plus Zn²⁺ into the gelling medium affected the drug encapsulation efficiency (#F3-F5 71.8-82.1%) due to a combination of the highest diffusivity of calcium ions and the highest ability of zinc ions to coordinate the polymeric chains. The high diffusivity of Ca²⁺ ($7.54 \times 10^{-6} \text{ cm}^2 \text{ s}^{-1}$) (Hazel and Sidell 1987) induces the formation of a gel layer around the falling droplets of the feed solution, able to reduce drug leaking during the formation of the gelled beads. The slower co-gelling agent (Zn²⁺), acting into the medium, was able to produce a tougher polymer matrix by increasing the coordination with carboxylate groups (G and M residues). Therefore, the ratio between the two cations may play a very important role in drug encapsulation process and derived beads properties.

In fact, when using a 1:1 or 1:4 Ca²⁺/Zn²⁺ ratio the value of EE was around 72%, whereas when Ca²⁺ quantity overcomes Zn²⁺ amount as in 4:1 ratio (#F5) the EE increased to 82% suggesting a synergistic effect of both cations.

SEM analyses, combined to image J software elaboration, allowed identifying the main characteristics in terms of structure, surface as well as mean diameter and sphericity coefficient (SC). As reported in Table IV, all beads showed satisfying SC values ranging from 0.88 to 0.94. Independently from the cation used, blank formulations exhibited better SC values compared to P loaded beads that showed higher surface roughness (Table IV).

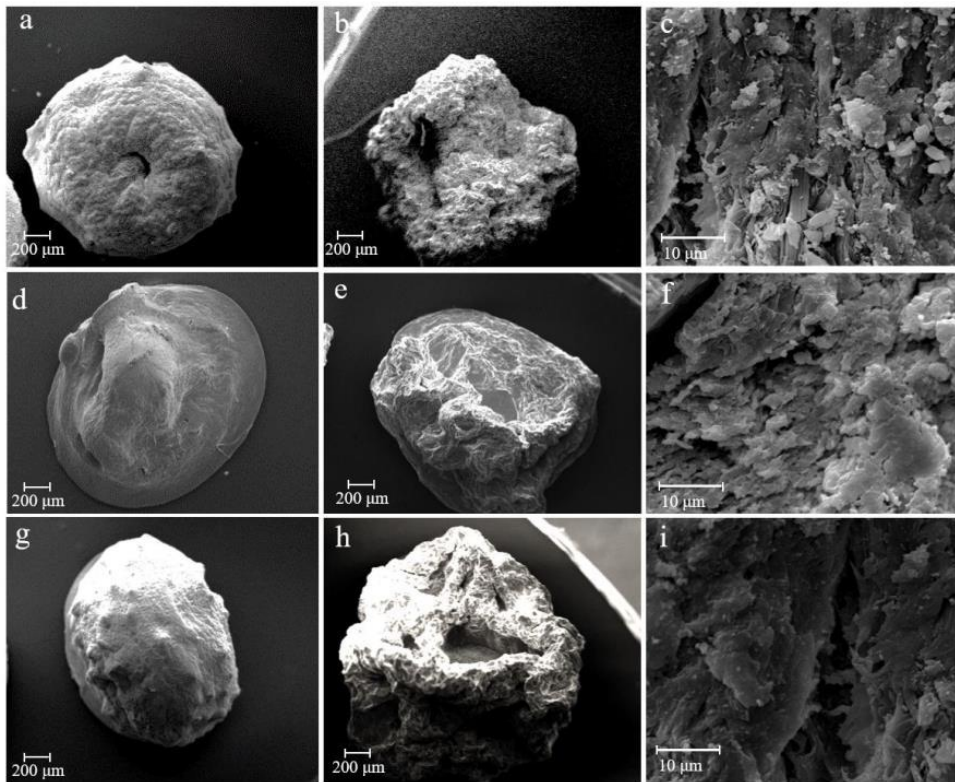


Figure 26. Alginate based beads loaded with P using different crosslinking agents. SEM microphotographs of blank beads: F1_b (a), F2_b (d), F5_b (g) and corresponding P loaded formulations (surface and cryo-fractured): F1 (b-c), F2 (e-f), F5 (h-i).

Results showed that particle size appears a cation-dependent characteristic.

Due to the higher diffusivity of Ca^{2+} , blank Ca^{2+} - beads presented a mean diameter around 1.6 mm, whereas blank Zn^{2+} -particles showed a mean diameter around 2.3 mm; the combination of the two cations, as gelling agent, produced beads with a mean diameter from 1.7 to 1.9 mm, related to the cations ratio, the higher the Zn^{2+} the larger the size.

Generally, in addition to a higher roughness, prednisolone loaded formulations exhibited larger mean diameters compared to the corresponding blank beads, confirming the cation-dependent particle sizes behaviour. In fact, #F1 (Ca^{2+} -beads) showed the lowest mean diameter (1.49 mm), whereas #F2 (Zn^{2+} -

beads) were the largest beads (about 2.7 mm). Formulations obtained using both Ca^{2+} and Zn^{2+} in different ratios (#F3-F4-#F5), displayed a reduction in mean diameter (between 2.1 and 2.3 mm) compared to Zn^{2+} alone based formulation F2 (2.7 mm), confirming that the high diffusivity of calcium ions was able to reduce droplets enlargement during gelling process.

To better understand the structure of the inner matrix, dried particles were cryo-fractured and analysed by SEM. As reported in figure 26-c-f-i, P loaded formulations showed a compact and well-organized inner texture, thanks to the interaction between sodium alginate and the cross-linkers alone or in mixture, as well as to additional hydrophobic interactions that may occur between the drug and the polymer.

SEM-EDS analysis on cryo-fractured blank beads, obtained using both Ca^{2+} and Zn^{2+} (F3_b-F4_b-F5_b), showed texture and the real cation-distribution in the cross-linked matrix.

As shown in figure 27, the cross-linkers ratio influences their distribution into the internal alginate matrix. In fact, F3_b ($\text{Ca}^{2+}/\text{Zn}^{2+}$ 1:1) and F5_b ($\text{Ca}^{2+}/\text{Zn}^{2+}$ 4:1) formulations exhibited an internal structure enriched in Ca^{2+} , due to the higher diffusivity of this cation, compared to Zn^{2+} . Only when the Zn^{2+} amount was very high, as in F4_b beads ($\text{Ca}^{2+}/\text{Zn}^{2+}$ 1:4) it was possible to observe an equilibrium between the two cations into the polymeric matrix (# F4_b).

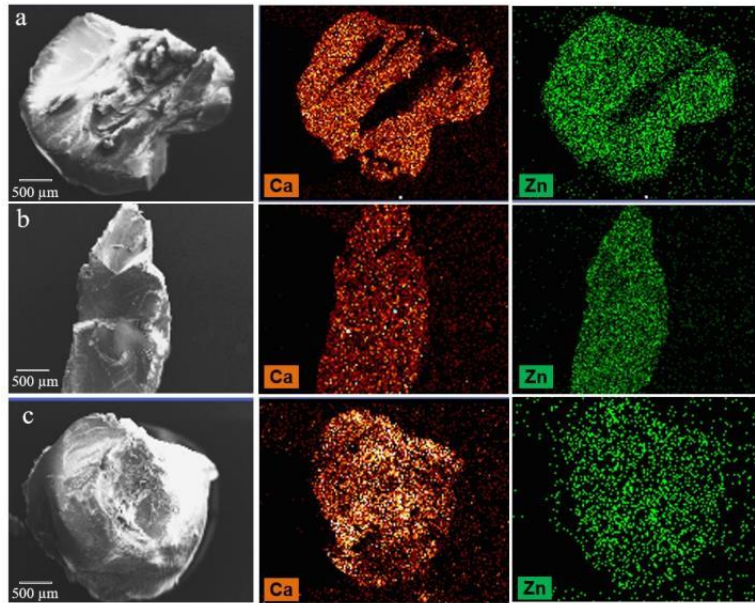


Figure 27. Alginate based beads loaded with P using different crosslinking agents. SEM and SEM-EDS microphotographs of cryo-fractured blank beads: F3_b (a), F4_b (b) and F5_b (c).

To fully characterize the beads, DSC analyses were performed on prednisolone raw material, blank and P loaded formulations.

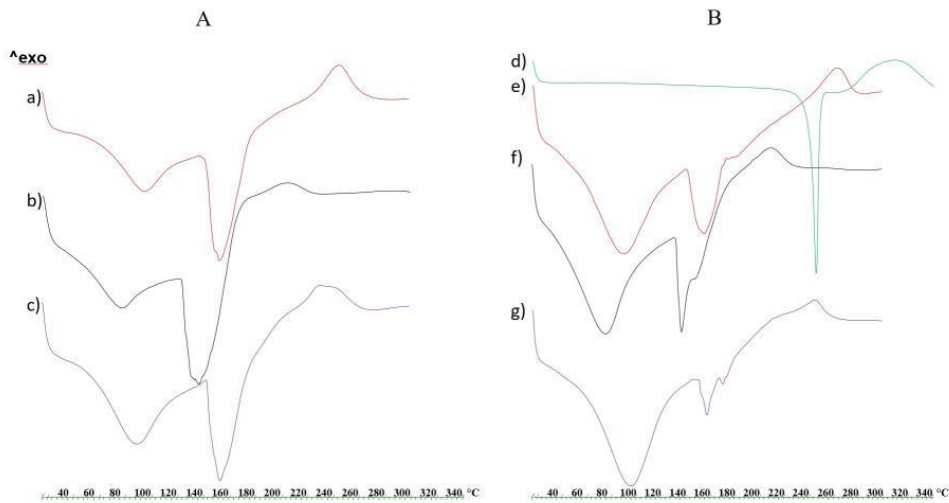


Figure 28. Alginate based beads loaded with P using different crosslinking agents. DSC thermal profile of formulations: F1_b (a), F2_b (b), F3_b (c) compared to P raw material (d) and P loaded formulations F1 (e), F2 (f), F3 (g).

As reported in figure 28-A, blank formulations showed a similar thermal behaviour: a first endothermic event between 80°C and 120°C related to the loss of water adsorbed by the hydrogel matrix, followed by a second endothermic event at 160°C for F1_b and F3_b and at 140°C for F2_b. Moreover, all formulations exhibited an exothermic event that was detected at higher temperatures in F1 and F3 (250°C - 260°C) attributable to the oxidative degradation of cross-linked matrix. Similarly, P loaded formulations (Fig. 28-B) showed the same thermal events shifted at higher temperatures close to the melting point of the active compound.

In addition, the thermal signal related to the melting point of P raw material was not detected in all P loaded formulations as effect of its effective inclusion into the alginate matrix after prilling process. Furthermore, it is interesting to point out that the encapsulation of the drug promotes an increase of the water absorbed from hydrogels, independently from the gelling agent.

Swelling behaviour and drug release studies

Swelling and dissolution experiments were conducted on P loaded formulations by means of an USP apparatus II according to the change pH protocol described in the USP 36.

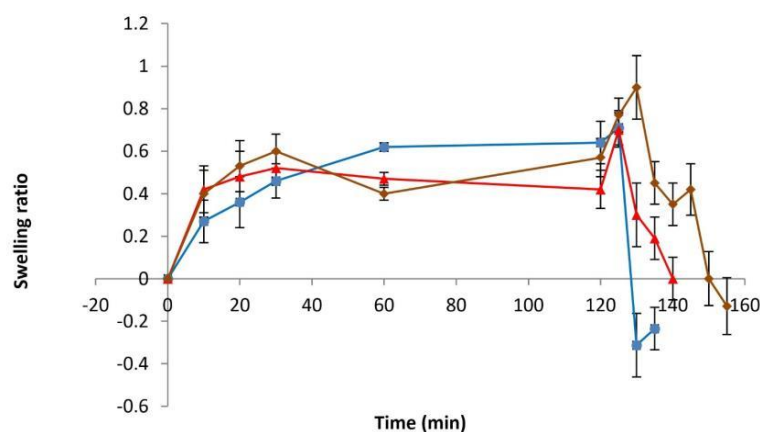


Figure 29. Alginate based beads loaded with P using different crosslinking agents. Swelling profiles of #F1 (white bars), #F2 (black bars) and #F5 (black/white bars) in SGF (up to 120 min) and in SIF (from 120 to 150 min).

As reported in figure 29, swelling profiles of beads clearly reflected alginate properties: during the transit in the acid environment, a particle swelling is observed due to the penetration of H_3O^+ ions, even if the matrix preserved its integrity, as evidenced by the low drug release in this medium (Fig 30), occurring through a diffusional/erosive mechanism. This swelling is higher for Ca-alginate (#F1, SR= 0.64 after 120 min), where the calcium is entirely substituted by H_3O^+ ions, compared to Zn-alginate (#F2, SR=0.42 after 120 min) and Ca/Zn-alginate (#F5, SR=57% after 120 min) beads. Changing the gelling agent from Ca^{2+} to Zn^{2+} , a reduced swelling for F2 and F5 compared to F1 was observed, and it may be responsible for a lower P release (Fig 30).

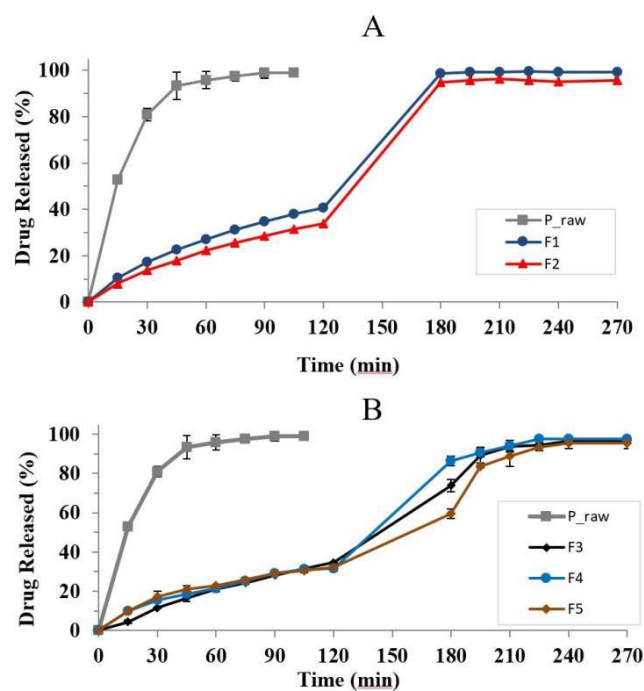


Figure 30. Alginate based beads loaded with P using different crosslinking agents. Drug release profiles from formulations F1 and F2 (A); F3, F4 and F5 (B) compared to P raw material.

These results supported some literature data, about the poor ability of calcium made systems in retaining drug release in simulated biological fluids,

compared to zinc based systems, able to create a tougher matrix thanks to a higher coordination with polymer moieties (Taha, Nasser et al. 2008; Al-Otoum, Abulateefeh et al. 2014).

However, after changing the pH, particle dimensions depend on both swelling and erosion

processes, this latter occurring for the alginate chains rapid hydrolysis in simulated intestinal fluid (SIF). The erosion process was faster for F1 and F2 microspheres, causing the complete disintegration of the beads in about 20 and 25 minutes, respectively (Fig. 29). The phosphate ions in SIF determine, in fact, the capture of cations from the cross-linked polymeric systems, causing their dissolution with consequent prompt release of P encapsulated (Caballero, Foradada et al. 2014). Therefore, as pointed out in figure 30-A, alginate microspheres crosslinked with Zn^{2+} (F2) were better able to control P release in SGF but, as Ca^{2+} -alginate particles, they failed in sustaining drug release in SIF.

Interestingly, all formulations obtained by simultaneously using Ca^{2+} plus Zn^{2+} , showed in SGF a dissolution profile similar to F2, with a lower P release respect to #F1 (about 30% vs 40%), followed by a more sustained drug release profile in SIF. In fact, after 1 hour in this medium (t=180 min), only 59.5%, 73.8 % and 86.3 % of P was released from formulations F5, F3 and F4 respectively; while at this time point the complete release of the drug was achieved from F1 and F2 microspheres.

This trend highlighted the ability of zinc and calcium ions, when properly mixed, to assemble a more resistant polymeric matrix able to prolong drug release (t= 240 min) compared with F1 or F2 pointing out a synergistic effect between Ca^{2+} and Zn^{2+} properties.

Such effect could be related to the ability of zinc and calcium to bind alginate at different sites: while Ca^{2+} preferentially interact with guluronic (G) blocks, zinc cations are less selective, interacting with both G and mannuronic (M)

sites on the alginate molecules and resulting in a huger crosslinking of the polymeric chains (Aslani and Kennedy 1996). This synergism reached its maximum when Ca^{2+} and Zn^{2+} were in the ratio 4:1.

The evaluation of release kinetics allowed to calculate P diffusion coefficient in the different formulations. In both SGF and SIF Higuchi's model (see materials and methods section) showed the poorest performance whereas good fitting capacity was demonstrated by Peppas-Korsmeyer's equation (as reported in materials and method section).

The lowest drug diffusion coefficient was found in formulation #F5 ($5.7 \times 10^{-8} \text{ cm}^2 \text{ s}^{-1}$) while #F1 and #F2 presented a diffusion coefficient of 6.9×10^{-8} and 6.3×10^{-8} , respectively. These results indicated that diffusion of P is influenced by the specific amount of Ca^{2+} and Zn^{2+} that producing a tougher matrix is able to strictly control drug diffusion. The diffusion process follows a complex non-Fickian release mechanism governed by matrix relaxation and erosion phenomena.

3-B 1.3 Conclusions

In this research, the effect of a single cation (Ca^{2+} or Zn^{2+}) or a mixture of cations (Ca^{2+} plus Zn^{2+}) in different ratios (1:1, 1:4 or 4:1) on technological properties of alginate beads loading SAID was investigated. Particularly, the crosslinkers' influence on the efficiency of encapsulation, swelling and drug release properties was studied, using prednisolone as SAID.

The addition of Ca^{2+} plus Zn^{2+} in opportune ratio evidenced a synergistic effect of the two cations, showing a series of significant improvements of the particle performance affecting positively both the encapsulation efficiency and the control of the swelling ability as well as drug release from the polymeric matrix. In fact, F5 ($\text{Ca}^{2+} / \text{Zn}^{2+}$ ratio 4:1) resulted as an interesting formulation with high P entrapment (82%) and delay of its release up to 4h.

The best formulation exploited the Ca^{2+} ability of establishing quicker electrostatic interactions with G groups of alginate and the Zn^{2+} ability to establish covalent-like bonds with both M and G blocks of alginate.

SECTION B PART 2:

Study of the effect of alginate concentration as well as drug/polymer ratio on alginate beads

- ***In vitro/in vivo* characterization of optimized microparticles and selection of prednisolone-carrying beads;**
- **Development of a more complex drug delivery technology platform**

Based on the article: A. Cerciello, G. Auriemma, S. Morello, R.P. Aquino, P. Del Gaudio, P. Russo. “Prednisolone delivery platforms: Capsules and Beads Combination for a Right Timing Therapy”, *PLoS ONE*, 2016 11(7): e0160266. doi:10.1371/journal.pone.0160266

3-B 2.1 Specific aim

The part 1 of this section pointed out that, the proper selection and combination of crosslinking agents are important parameters that profoundly characterize the technological properties of alginate carrying prednisolone microparticles (Alg.-P) produced by prilling technique.

In fact, the drug entrapment (up to 82%) as well as the drug release (delayed up to 240 min) resulted strictly influenced by the two different cross-linkers selected.

In this section, the effect of other formulation parameters as alginate concentration and P/alginate ratio, on Alg.-P technological properties and performances, was studied.

Different alginate concentrations as well as P/alginate ratios were tested to produce gel-beads by prilling; the obtained microparticles were characterized in terms of morphology, solid state characteristics swelling properties and drug release profile using well established methods (UV, SEM, DSC, FT-IR, USP-II dissolution).

Moreover, to verify whether the delayed *in vitro* drug release as effect of the particle engineering process may induce *in vivo* a delayed/prolonged activity (Cerciello, Auriemma et al. 2015) the *in vivo* anti-inflammatory effect of the optimized SAID formulation, compared to prednisolone raw, was studied using the carrageenan-induced acute oedema in rat paw (male Wistar rats) model, with a modified induction-administration protocol.

Moreover, the chance to combine the controlled release properties of SAID gel-beads with the peculiar features of DR[®] capsules was evaluated to obtain a more complex drug delivery technology platform able to further delay the drug release.

3-B 2.2 Gel beads production and characterization

Six loaded formulations, were produced by prilling using a 600 μm nozzle with a frequency of vibration of 350 Hz (amplitude 100%) with a feed solution flow rate fixed at 6.00 ml/min.

Zn was used as crosslinking agent (10% w/v) in an aqueous solution at room temperature with pH= 1.5, and the gelling time was set at 2 min.

Gel-bead formulations (#F1 – #F6) were obtained varying:

- Alginate (alg) amounts (from 2.0 % to 2.5 % w/v)
- and drug/polymer mass ratios (1:10 and 1:5 w/w),
- using a very short processing time in the selected operative conditions.

As control, blank Zn-alginate beads were also produced (F). Drying process was conducted by exposing hydrated beads to standard room conditions (22 °C; 67% RH) for 12–18 h until constant weight was reached.

Table V. Zn-alginate based beads loaded with P. Composition, actual drug content, encapsulation efficiency, mean diameter and sphericity coefficient of formulations F-F6 manufactured by prilling.

Formulation code	Alginate concentration (%w/v)	P/Alg mass ratio (w/w)	ADC (% \pm SD)	EE (% \pm SD)	Dried beads diameter (mm \pm SD)	SC
F	2.50	-	-	-	2.4 \pm 0.15	0.93 \pm 0.01
F1	2.00	1:10	6.2 \pm 0.2	67.9 \pm 2.0	2.4 \pm 0.12	0.91 \pm 0.02
F2	2.00	1:5	11.7 \pm 0.6	69.9 \pm 3.8	2.7 \pm 0.13	0.90 \pm 0.02
F3	2.25	1:10	6.6 \pm 0.3	72.8 \pm 3.4	2.4 \pm 0.12	0.90 \pm 0.01
F4	2.25	1:5	12.3 \pm 0.4	73.6 \pm 2.3	2.5 \pm 0.12	0.91 \pm 0.02
F5	2.50	1:10	6.8 \pm 0.2	74.3 \pm 2.0	2.4 \pm 0.12	0.92 \pm 0.02
F6	2.50	1:5	13.1 \pm 0.3	78.6 \pm 2.1	2.5 \pm 0.12	0.90 \pm 0.02

Actual drug content (ADC) and encapsulation efficiency (EE) values of all dried formulations ranged from 67.9 to 78.6 % (Table V) in relation to the amount (from 2 to 2.5%) of alginate used as well as to the drug/polymer ratio (from 1:10 to 1:5) selected.

In fact, the highest ADC and EE values were obtained raising drug/polymer ratio and alginate amount into the feed solutions. These data were consistent with previous observations on polysaccharides based hydrogels loaded with NSAIDs, suggesting that the loading of higher amount of drug and an increased polymer concentration may promote, during the gelation phase, intermolecular interactions able to stabilize the “egg-box” structure (Cerciello, Auriemma et al. 2015; Cerciello, Auriemma et al. 2016), reducing the leaching of the drug from the droplets into the gelling medium. Accordingly, #F6 (alg. 2.5%, drug/polymer ratio 1:5) showed the best P entrapment within the matrix (EE = 78.6 %).

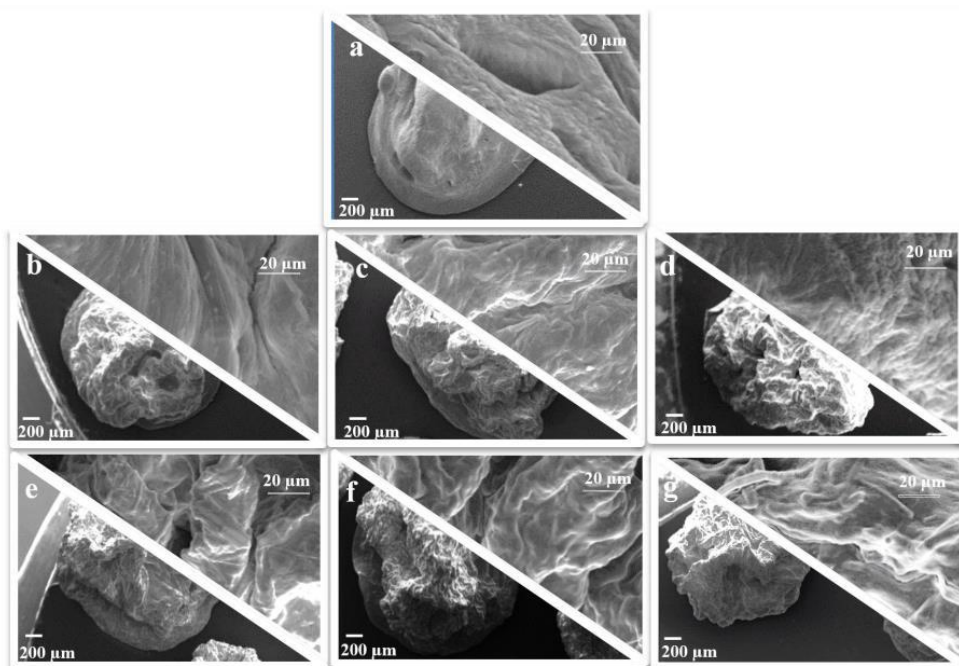


Figure 31. Zn-alginate based beads loaded with P. SEM microphotographs at different magnification of dried zinc-Alg beads: a) #F, b) #F1, c) #F2, d) #F3, e) #F4, f) #F5, g) #F6.

Polymer and drug concentration in the processed feeds influenced the surface properties of the particles: drug-free beads (#F, figure 31, a) were smoother without wrinkles, whereas P loaded beads had all an irregular surface and roughness directly related to P and polymer content. In particular, the higher the content of drug and the polymer concentration, the greater the surface roughness. Moreover, no drug crystals were observed on the particle surface (#F1-F6, figure 31 b-g) and all particles showed similar morphological characteristics in terms of sphericity coefficient (SC 0.90 - 0.92) and mean diameter values (2.4 – 2.7 mm) (Table V).

These data suggested that the optimization of operative and process variables during prilling/ionotropic gelation process (Zn^{2+} concentration, pH, temperature and curing time) was able to produce beads with almost spherical shape in a narrow dimensional range, independently from the amount of alginate or to the drug/polymer ratio selected.

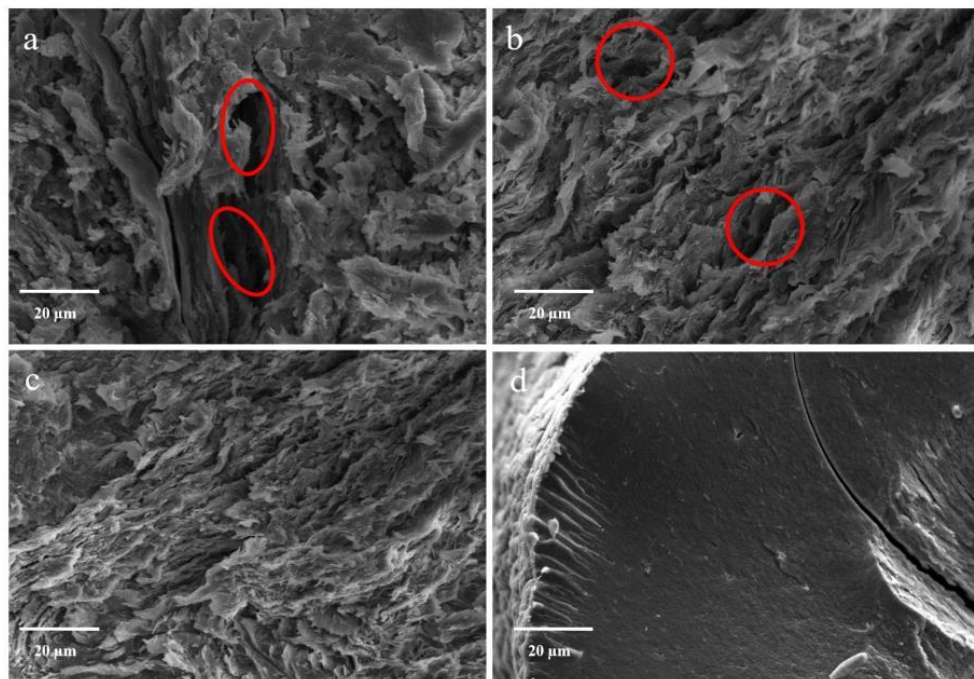


Figure 32. Zn-alginate based beads loaded with P. SEM microphotographs of cryofractured zinc-Alg beads: #F4 (a), #F5 (b) #F6 (c) and #F (d).

To better understand the influence of drug content and alginate amount on the inner structure, beads were cryo-fractured prior to SEM observation.

The blank Zn-alginate beads revealed a compact inner matrix (#F Figure 32 d). On the contrary, the internal structure of all engineered particles was less continuous and interrupted by several empty folders (Figure 32 a-b, red circles), depending on the polymer and drug concentration into the liquid feed processed.

Moreover, the images suggested that the increase of alginate (from 2.25% to 2.50%, Figure 32 a-c) and drug concentrations (from 1:10 w/w to 1:5 w/w, Figure 32 b-c) induces a higher organization of the matrix, desirable for the development of oral controlled drug delivery systems.

In order to assess the matrix resistance in biological fluids, swelling experiments were conducted in SGF and SIF, following pH change methods steps. Formulation F6 exhibited in SGF a swelling degree of about 13% after 60 min and 58% after 120 min. Beads presented at both time points smoother surface and higher particle sphericity compared to dried particles. Interestingly, drug loaded beads exhibited the maximum swelling degree (76%) at 135 min, as a result of enhanced water penetration and slow beginning of the erosion process in SIF. After this time point, the erosion overtakes the swelling, leading to a complete particle disintegration at 190 min.

In order to highlight feasible drug-polymer interaction after prilling process, thermal profiles of P raw material, blank Zn-alginate beads and drug loaded beads were studied by differential scanning calorimetry and reported in figure 33.

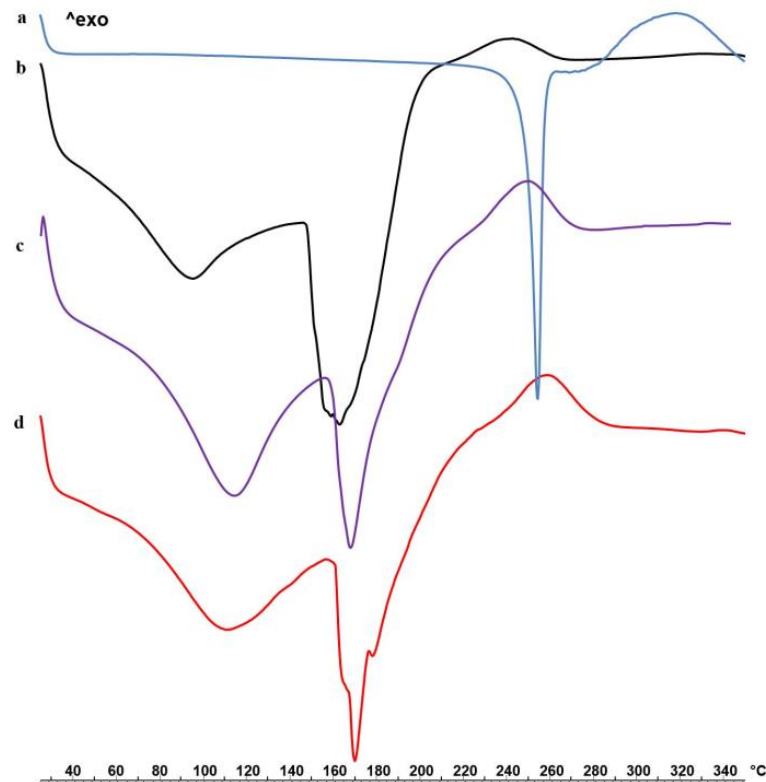


Figure 33. Zn-alginate based beads loaded with P. DSC thermograms of P raw material (a), alginate blank beads F (b) and drug loaded formulations F5 (c) and F6 (d).

P raw material exhibited a clear endothermic peak at 252°C followed by an exothermic event between 280 and 350 °C corresponding to its oxidative degradation. Both empty and P loaded formulations exhibited an opening endothermic event between 90 and 130 °C related to the loss of water adsorbed on the particle surface and entrapped into the matrix. Blank Zn-alginate beads, showed a broad endothermic signal between 150 and 182°C followed by a ramp like event up to 260 °C. The endothermic peak due to the fusion of crystalline P (252 °C) disappeared in drug loaded beads thermograms (fig. 33, c-d) suggesting a complete drug entrapment; moreover, melting as well as degradation peaks were shifted to higher temperatures in F5 and F6 thermal profiles with respect to blank Zn-alginate beads. These effects, more

pronounced in F6, suggested a physical alginate/P interaction as effect of drug loading in the polymeric matrix (Cerciello, Auriemma et al. 2016).

In order to verify the presence of such interaction suggested by DSC analysis, FT-IR studies were performed and results reported in Figure 34.

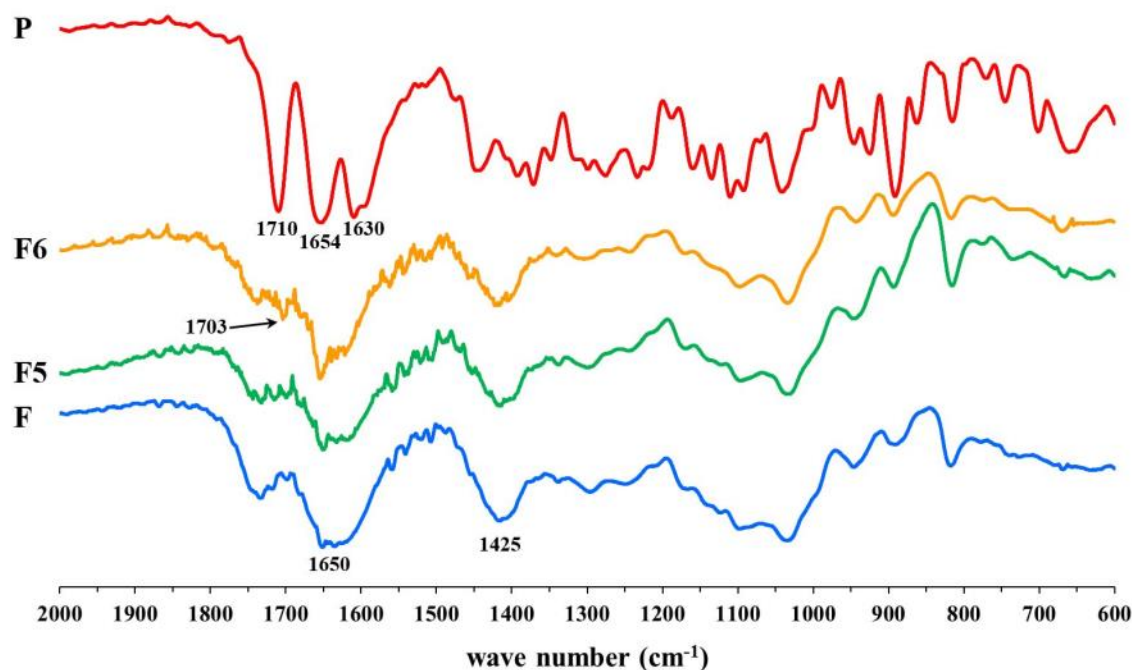


Figure 34. Zn-alginate based beads loaded with P. FTIR spectra of P raw material, formulations F5-F6 and Zn-alginate blank beads F.

P raw material exhibited two characteristic bands in the range 1590-1710 cm⁻¹ corresponding to symmetric and antisymmetric stretching of C=O aliphatic group (Palanisamy and Khanam 2011; Mazurek and Szostak 2012). The FT-IR spectrum of Zn²⁺ crosslinked alginate blank beads presented bands at 1650 and 1425 cm⁻¹ corresponding to the stretching of symmetric and antisymmetric carboxylic groups of the Zn-alginate complex and due to the coordination between the metal ion and the functional groups of the polymer (Papageorgiou, Kouvelos et al. 2010). #F5 and #F6 showed the majority of the

characteristic peaks of both Zn-alginate and prednisolone, however at 1703 cm^{-1} a new band was recognized, which could be associated to the interaction between P and alginate chains *via* Zn^{2+} coordination.

Drug release studies

Dissolution studies of prednisolone raw material and produced beads were performed using USP Apparatus 2 and a classic pH-change assay. The dissolution profiles of F2, F4 and F6 characterized by the highest drug/polymer ratio (1:5) are shown in figure 35.

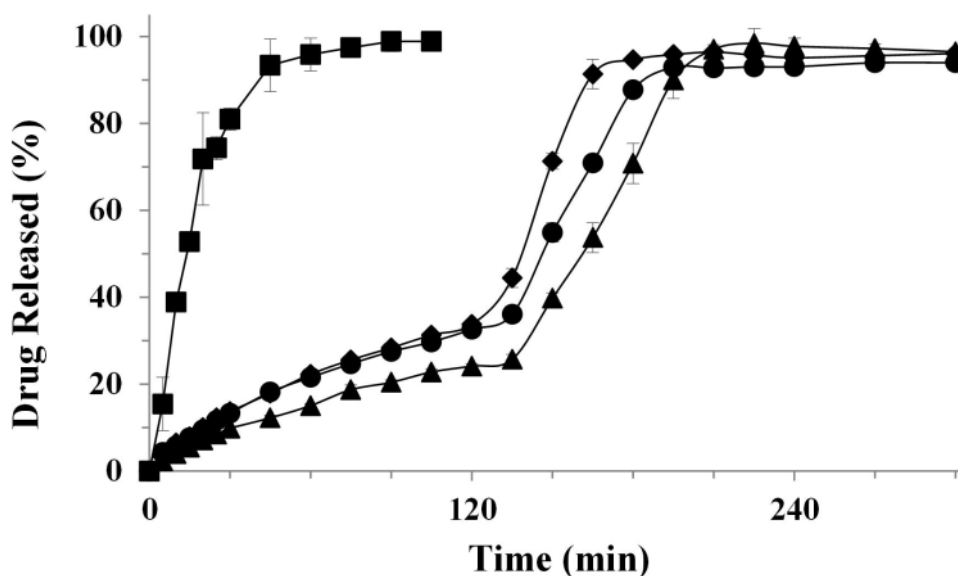


Figure 35. Zn-alginate based beads loaded with P. Release profiles of P from: raw material, square; # F2, diamond; # F4, circle and #F6, triangle. Mean \pm SD; (n=6).

As expected, the dissolution profile of P raw material was typical of compound belonging to the class I of the Biopharmaceutical Classification System (high solubility and permeability through biological membranes), the complete solubilisation was achieved in simulated gastric environment after about 90 minutes (Sugawara, Imai et al. 1994). Differently, F2, F4 and F6

showed a partial gastro-resistance. In particular, as shown in figure 35, #F6 obtained with the highest alginate amount exhibited the more interesting dissolution profile, releasing only 24.1% of the drug in simulated gastric fluid (SGF) followed after the pH change by a more sustained release in simulated intestinal fluid (SIF) with respect to #F4 and #F2 (100% of P release after about 3.5h). All formulations seem to release the drug through a diffusional/erosional mechanism. However, the greatest alginate amount as in #F6 seems to be able to better retain the drug during its exposition to simulated biological fluids. Conversely in SIF (at pH 6.8) beads started to swell and further erode due to the ion-exchange process.

Therefore, formulation F6 showing the best performances *in vitro* (drug content, inner matrix texture, drug release) was selected for the *in vivo* experiments in order to evaluate a potential delay of anti-inflammatory effect compared to reference prednisolone.

***In vivo* experiments**

As previously reported for NSAIDs, the possibility to study *in vivo* the anti-inflammatory effect of formulations showing good *in vitro* features, may be an important tool for the development of a ChDDS.

For this reason, also the more interesting SAID formulation, F6, was administered to rats by oral gavage using a modified protocol of carrageenan-induced oedema model and the anti-inflammatory activity of F6 beads was compared to the activity of reference prednisolone.

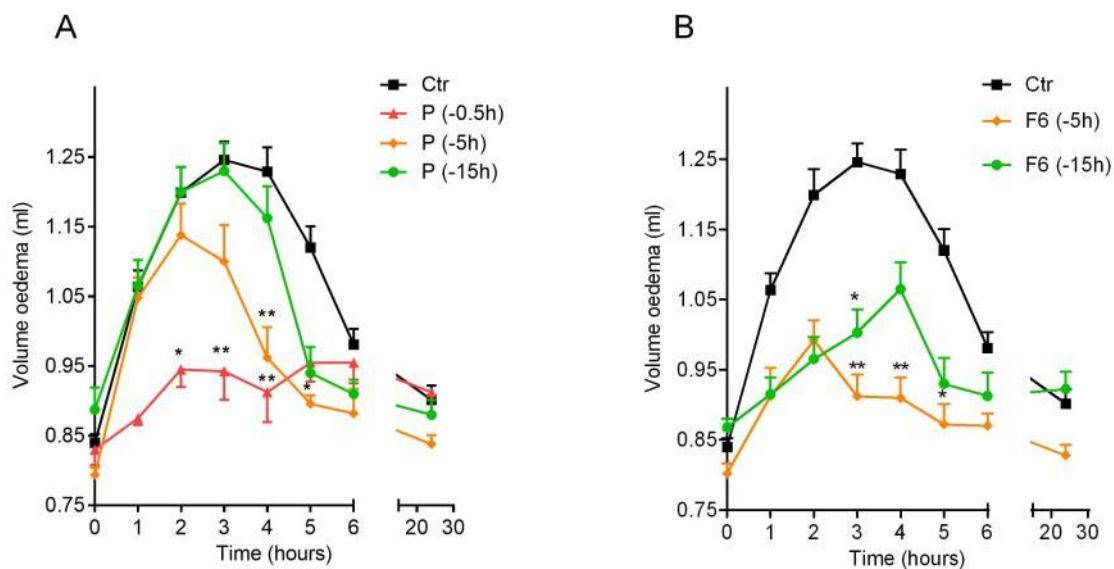


Figure 36. Zn-alginate based beads loaded with P. Oedema volume reduction obtained by administering *per os* pure prednisolone (A) and #F6 (B) at different time points (15, 5, 0.5h) to rats before carrageenan injection, compared to control; mean \pm SEM ($n = 8$). * $p < 0.05$, ** $p < 0.01$ compared to control.

Preliminary experiments were performed by using three different doses of prednisolone ($1-3-10 \text{ mg kg}^{-1}$) administered by gavage to rats 0.5h before carrageenan injection (data not shown). The dose of 3 mg kg^{-1} of prednisolone was selected as it achieved the optimal anti-inflammatory effect. The pure drug (3 mg kg^{-1} , prednisolone) was significantly efficacious in reducing rat paw oedema when administered at $t=0.5\text{h}$ before carrageenan injection (figure 36-A). The anti-inflammatory activity of prednisolone was lost when administered to rats 5h or 15 h before the phlogistic agent injection (figure 36–B).

To verify a potential delayed/prolonged *in vivo* anti-inflammatory activity, as effect of an accurate particle engineering process, F6 in dose equivalent to 3 mg kg^{-1} of prednisolone was orally administered to rats 5h and 15h before carrageenan injection. The administration time points were extended (5h and 15h) compared to those for NSAIDs (Zn-alginate beads Section A part 1)

according to the different mechanism of action and pharmacological properties of prednisolone.

Results showed that F6, significantly reduced carrageenan-induced paw oedema in rats when administered 5h before the injection of the phlogistic agent (Figure 36-B).

The anti-inflammatory activity of F6 still persisted when administered to rats 15h before carrageenan injection (Figure 36-B), in contrast to reference prednisolone (3 mg kg^{-1}) that was efficacious in reducing rat paw oedema only at $t=0.5\text{h}$ (figure 36-A). As previously reported (Cerciello, Auriemma et al. 2015), blank Zn-alginate beads (F) did not significantly affect the paw oedema when administered to rats at the same time points before oedema induction (data not shown), thus, indicating that alginate and zinc do not interfere with the inflammatory process.

***In vitro* drug release from the final dosage form**

Formulation #F6, acting as a partially gastro-resistant and sustained release formulation and able to exert the anti-inflammatory activity even if administered 15h before the phlogistic injury, was selected as core material for the development of a final dosage form suitable for a chronotherapy.

Therefore, #F6 was hosted into DR[®] capsules giving F6/DR[®] platform.

DR[®] capsules were previously used to control/delay the release of KL from ALM-pectin beads (Section A part 2), since among different capsules models, they exhibit specific feature in protecting API from acidic environment thanks to the properties of a mixture of hydroxypropyl methylcellulose (HPMC) and gellan gum.

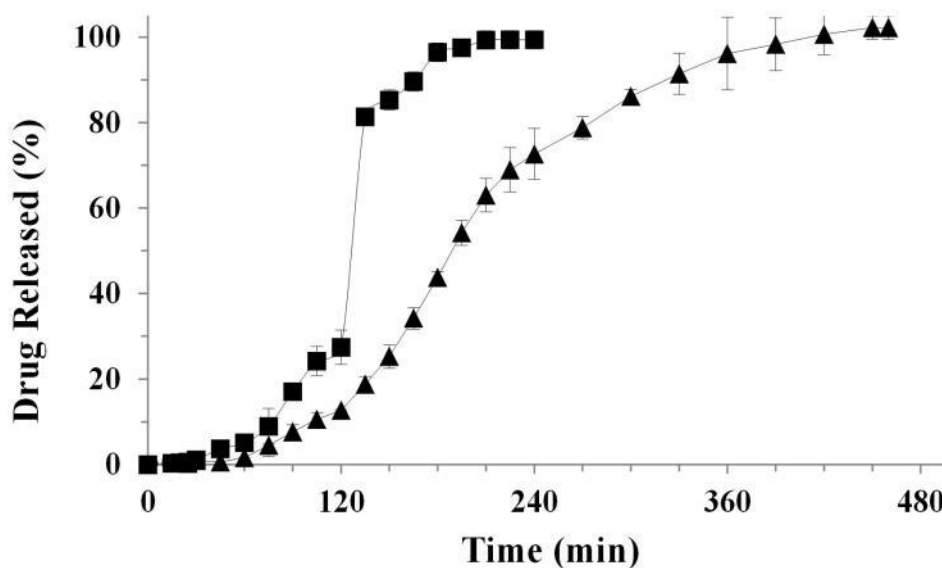


Figure 37. Zn-alginate based beads loaded with P. Release profiles of : P raw material hosted into DR[®] capsules (square) compared with optimized F6/DR[®] final dosage form (triangle). Mean \pm SD; (n=3).

The resulting dissolution profile of P from F6/DR[®] cps versus more conventional P/DR[®] cps profile showed that DR[®] caps were able *per se* to delay the dissolution profile of prednisolone (figure 37), extending its release from 90 to 180 minutes with a significant reduction in SGF (34.2%).

Interestingly, the final dosage form F6/DR[®] cps reduced significantly P release in SGF from 24.1% to 12.6%; at the same time, after pH change, P dissolution was significantly delayed up to about 390 minutes (6.5 hours).

This very interesting drug release profile was due to combination of intrinsic properties of capsules and hosted beads; only after the dissolution of the capsule body, beads are exposed to the dissolution medium, beginning later the dissolution process. Differently from gelatin capsules that normally disaggregate in simulated gastric fluid in about 5 minutes, the DR[®] capsules begin to disaggregate after 75-90 minutes protecting the formulation from the

acid environment. After this lag time, beads start to hydrate and swell, allowing a slight drug diffusion in acidic medium followed by a complete but delayed swelling and erosion processes in SIF.

3-B 2.3 Conclusions

This part of the PhD project, was aimed to study the effect of process and feed solution variables (alginate concentration and drug/polymer ratio) on particles size, morphology, solid state properties and drug release profile of prednisolone microparticles produced by prilling. Particles prepared from solution containing the highest amount of polymer and drug showed good production parameters such as high encapsulation efficiency (around 80%) and strongly crosslinked inner matrix as evidenced by SEM pictures of cryo-fractured beads. Moreover, engineered particles showed a reduced P release in gastric simulated environment and a slow release in simulated intestinal fluid, compared to conventional P.

The prolonged *in vivo* anti-inflammatory effectiveness of formulation #F6 tested by a carrageenan-induced oedema model clearly reflects its ability to release the drug in a delayed and sustained way, highlighting its potential benefits for a right chronotherapy.

Finally, the optimized formulation F6 was selected for the manufacturing of a final dosage form, using DR[®] capsules chosen for their peculiar dissolution properties. By designing a more complex platform, hosting F6 beads in DR[®] capsules, it was possible to further delay and prolong P release, up to 6.5 hours. The platform (#F6/ DR[®]) used in the present study, therefore, represents a suitable dosage form able to delay and extend SAID release in a time scale ideal for the successful treatment of early morning pathologies.

SECTION B PART 3:

Design and formulation of floating alginate beads and their *in vitro/in vivo* characterization and performances

3-B 3.1 Scientific background and specific aim

Results of the previous research (Section B part 1-2) have shown how the control/delay of prednisolone release may be obtained through engineered particles based on Zn-alginate matrix and proper selection of the polymer concentration, drug/polymer ratio above crosslinking agent. The selected variables may lead to the formation of a compact alginate matrix able to delay P release for several hours in intestinal environment (Cerciello, Auriemma et al. 2016).

Another approach to ensure drug delayed release may be the development of floating alginate beads able to act *via* an extension of the drug gastric residence time (GRT).

Generally, floating formulations are one of the most employed technological approaches to produce gastro-retentive (GR) drug delivery systems with prolonged GRT (Chaturvedi, Prabha et al. 2013; Nayak, Upadhyay et al. 2014). GR-floating formulations are low-density systems that have sufficient buoyancy to float over gastric contents and remain in the stomach for prolonged period without affecting gastric emptying rate and, at the same time, release the drug slowly (Ramteke, Jadhav et al. 2012).

In the last few years, NSAIDs or SAIDs floating formulations (i.e. diclofenac sodium, indomethacin, acetylsalicylic acid, ibuprofen, naproxen, ketorolac, prednisolone) have been successfully developed in form of single-unit dosage forms (powders, granules, capsules, tablets, laminated films) or multiple-unit formulations (Singh and Kim 2000; Badve, Sher et al. 2007; Ramteke, Jadhav et al. 2012; Ware, Tiwari et al. 2013; Gifty, Behin et al. 2015; Radwan, Abou el Ela et al. 2015).

In particular, microparticles able to float appear particularly interesting; in fact, the distribution of the multiple-unit dosage forms in the stomach is more uniform than that of single-unit dosage forms. As a result, floating microparticles may induce a more reproducible drug absorption as well as

reduce risks of local irritation (Sharma, Sharma et al.) and result potentially useful for the development of ChDDs.

To achieve this goal, floating beads were prepared adding calcium carbonate, a gas-generating agent producing CO₂ in acid conditions, to the base-formula (Zn-alginate 2.5% w/v, prednisolone/alginate 1:5_ see beads in section B part 2), which entrapment in the gel matrix may confer an increased porosity and buoyancy ability (Verma, Sharma et al. 2013).

Among different agents, producing CO₂ in acidic conditions, (sodium carbonate, potassium carbonate, sodium bicarbonate, citric acid) (Choi, Park et al. 2002; Krishnan, Sasikumar et al. 2010), calcium carbonate was selected in order to assess the potential effect of calcium interactions with G groups of alginate, combined to the presence in the gelling medium of Zn ions on the produced microparticles.

The effect of the addition of different amounts of calcium carbonate in to the feed solution on particle encapsulation efficiency, morphology as well as *in vitro* drug release profile was studied.

Moreover, the ability of the floating beads to modulate *in vivo* the anti-inflammatory response was studied using the carrageenan-induced acute oedema in rat paw (male Wistar rats) (Section B, part 2).

3-B 3.2 Floating beads production and characterization

A series of Zn-alginate formulations loaded with prednisolone was produced adding CaCO₃ in the feed solution, as gas-generating agent, in order to obtain floating-gastroretentive systems. Carbonate salts when in contact with an acid medium produced CO₂ that entrapped in a hydrogel matrix reduced the system density conferring buoyancy ability (Choi, Park et al. 2002; Verma, Sharma et al. 2013).

Alginate concentration (2.5% w/v) and drug/polymer ratio (prednisolone/alginate ratio 1:5) were fixed on the basis of previous research

(Cerciello, Auriemma et al. 2016), while different Alg/CaCO₃ ratio were studied.

Table VI. Zn-alginate/calcium carbonate based beads loaded with P. Formulation code, alginate concentration, alginate/calcium carbonate ratio and encapsulation efficiency of the produced microparticles.

Formulation code	Alginate Concentration (w/v)	Alg:CaCarb ratio (w/w)	EE (% ± SD)
F1	2.50%	/	78.6 ± 2.1
F2		1 : 0.10	88.4 ± 2.9
F3		1 : 0.25	94.5 ± 1.7
F4		1 : 0.50	87.8 ± 3.5
F5		1 : 0.75	91.1 ± 2.1
F6		1 : 1.00	91.1 ± 2.0

As reported in table VI, all formulations produced showed EE values higher than F1, obtained without calcium carbonate, in the range of 87.8 – 94.5%. This effect could be explained by the presence of calcium carbonate into the feed solutions as an insoluble dispersion in neutral pH; during the ionotropic gelation process the polymer-CaCO₃/drug droplets produced by prilling fall down into zinc acetate solution with an acidic pH (1.5) and CaCO₃ became water-soluble. The Ca²⁺ ions promoted an internal gelation, by cross-linking the alginate carboxyl group (Choi, Park et al. 2002; Verma, Sharma et al. 2013), which, in addition to the external gelation obtained by Zn²⁺ ions present in gelation medium, allowed to incorporate an higher amount of drug. Moreover, in order to evaluate the effect of calcium carbonate on the inner structure of the bead formulations, they were cryo-fractured and analysed by SEM.

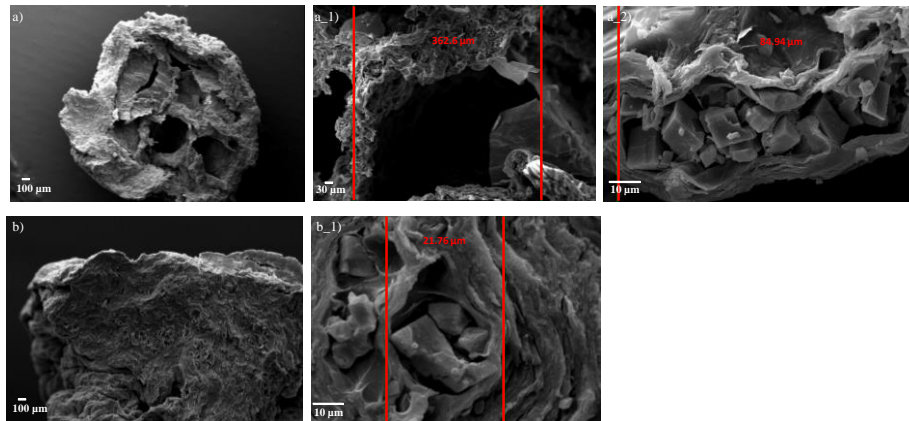


Figure 38. Zn-alginate/calcium carbonate based beads loaded with P. SEM microphotographs of cryo-fractured zinc-Alginate beads: F6 (a) and F4 (b) at different magnifications.

Particularly, in figure 38 the inner matrix of F6 and F4, obtained with a 1:1 and 1:0.5 alginate/calcium carbonate ratio, were reported. The loading of a greater amount of CaCO_3 caused the formation of a macro-porous structure (#F6, fig. 38-a-a1) due to a higher quantity of CO_2 produced during the gelling phase. At the same time together with big pores, the presence of a micro-porous structure, was detected for both formulations. In particular, porous diameter decreased significantly from F6 to F4 (84.94 μm - 21.76 μm , respectively, fig. 38 -a2 -b1) which resulted in a more compact inner structure without empty macro-porous (fig. 38 -b).

The high porous nature of the produced microparticles suggested their potential suitability to float over the gastric fluids; so, for this reason, a buoyancy test in SGF was performed.

The buoyancy ability of each formulation was evaluated by visual observation (number of floating beads/total number of beads used for the experiment*100) and expressed as floating percentage (FP). The time lag for the evaluation of FP was fixed at 2 min.

F2 and F3 (alginate/calcium carbonate ratio 1:0.1 and 1:0.25 respectively), resulted unable to float in SGF; this result, was probably related to a calcium carbonate loading too low to produce pores in the matrix.

Interestingly, F4-F5-F6 formulations resulted able to float in SGF up to 5h without any particles disintegration or erosion.

Results showed as the buoyancy ability was directly related to the concentration into the feeds of the gas generating agent, with FP of 98.3%, 84.0 and 77.3 for formulation F6-F5-F4 respectively.

Hence, as pointed out from these results, an alginate/calcium carbonate ratio $\geq 1:0.5$ was able to produce buoyant beads with a total floating time of 5h. This prolonged FT may be due to low apparent density provided by the porous nature of the beads (Fig. 38); after this time point all the microparticles tend to sink.

Dissolution experiments were, therefore, performed in SGF for 5h (corresponding to the detected floating time).

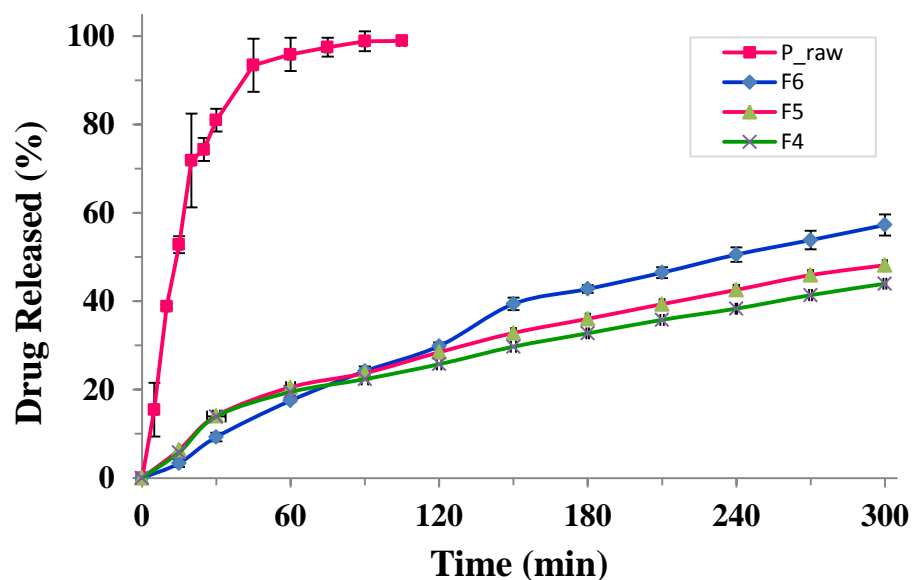


Figure 39. Zn-alginate/calcium carbonate based beads loaded with P. Release profiles of P raw material compared to formulations F4, F5 and F6 in SGF for 5h

These three formulations showed a controlled P release in SGF and particularly formulation F4 exhibited the slowest P dissolution compared to F5 and F6 (cumulative release of only 43 % $t= 300$ min). The porous alginate matrix (particularly in F4) resulted able to retain the drug during its buoyancy in SGF; this effect may be due to the high alginate crosslinking obtained with an internal gelation (Ca ions) added to an external gelation provided by Zn ions.

The produced floating microparticles showed an interesting buoyancy ability *in vitro* and resulted able to control P release in SGF for a prolonged time (5h). F4, showing an interesting floating ability and the slowest *in vitro* drug release, was selected for the *in vivo* experiments in order to evaluate the potential ability of a porous formulation to modulate the anti-inflammatory effect in rats.

***In vivo* experiments**

The potential efficacy in modulating the anti-inflammatory effect *in vivo*, of the porous formulation F4, was evaluated using the modified protocol of carrageenan-induced oedema in rat paw (male Wistar rats) used for prednisolone *non-floating* formulation (Section B, part 2) with administration time points of 0.5, 5, and 15h before oedema induction and the dose of 3.0 mg/kg.

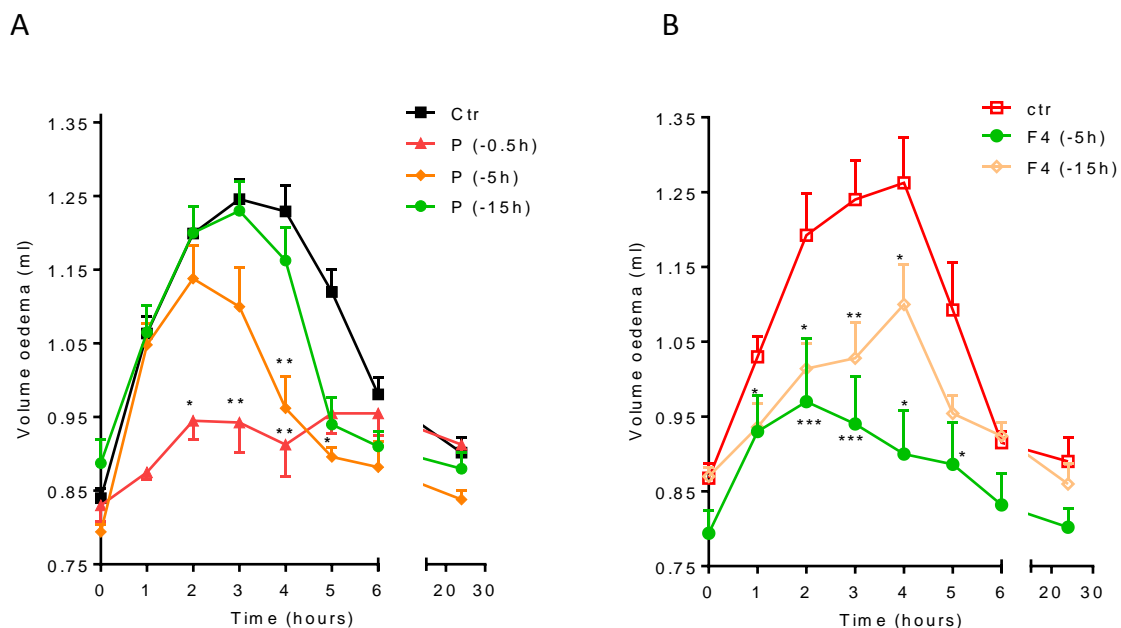


Figure 40. Zn-alginate/calcium carbonate based beads loaded with P. Oedema volume reduction obtained by administering per os pure prednisolone, P (A) and #F4 (B) at different time points (15, 5, 0.5h) to rats before carrageenan injection, compared to control; mean \pm SEM (n = 8). *p < 0.05, **p < 0.01, ***p \leq 0.001 compared to control.

As previously discussed, P raw failed to control the oedema volume when administered orally to rats 5h or 15h before carrageenan injection; on the contrary, as for *non-floating* formulation, F4 revealed still able to exert the anti-inflammatory effect *in vivo* when administered orally to rats up to 15h before oedema induction.

This result was very interesting because for an hollow matrix as F4, a fast drug release due to the high solvent penetration was expected leading to a reduced anti-inflammatory effect *in vivo*. Hence, we supposed that this delayed/prolonged *in vivo* anti-inflammatory effect of F4 was probably due to its ability to float in SGF that may reflect *in vivo* in a gastric residence time increase with a more controlled and sustained P release.

3-B 3.3 Conclusions

Hollow gel microparticles able to sustain prednisolone delivery were produced starting from an optimized Zn-alginate matrix (alginate 2.5% w/v, drug/P ratio 1:5) with the addition of calcium carbonate in the polymer/drug solution. The opportune selection of the gas generating agent, produced beads with high EE values (up to 94.0%), a porous inner matrix when alginate/calcium carbonate ratio was $\geq 1:0.5$. The hollow beads resulted able to float in SGF for 5h controlling at the same time P release. Interestingly, the best formulation F4, despite its hollow inner structure, resulted able to prolong the anti-inflammatory effect *in vivo* up to 15h compared to reference prednisolone. Thanks to its potential ability to increase the GRT *in vivo*, as well as its intrinsic controlled/delayed release properties, F4 could be proposed as an interesting formulation to be further optimized. Other studies are necessary to confirm the potentiality as a floating DDS tailored for chronotherapy.

SECTION C:
Design and development of
chronotherapeutic systems loaded
with long half-life NSAIDs

**Gastroretentive systems to sustain piroxicam release: *in vitro*
and *in vivo* characterization**

Based on the article: G. Auriemma, **A. Cerciello**, A. Pinto, S. Morello, R. P. Aquino. “Floating gastroretentive system for piroxicam sustained release: design, characterization and *in vivo* prolonged anti-inflammatory effect”.
Submitted 2016.

3-C 1.1 Scientific background and specific aims

The previous sections of my PhD thesis, focused on the design and development by prilling/ionotropic gelation technique of ChDDS loaded with anti-inflammatory drugs with different chemical and pharmacological features (NSAIDs or SAIDs) all characterized by a short half-life.

Based on the acquired know how with the formulation and process variables of the prilling technique, starting from Zn-alginate and Zn-ALM-pectin as polymeric carriers, a further challenge of my PhD project, was to design a ChDDS loaded with piroxicam (PRX) as model of long half-life NSAIDs.

PRX is commonly used in chronic inflammatory-based diseases such as rheumatoid arthritis and osteoarthritis, in controlling postoperative pain and acting as an analgesic drug. According to the biopharmaceutics classification system (BCS) and all current guidances (U.S. Department of Health and Human Services 2000; WHO 2006; European Medicines Agency EMA 2010), PRX is a BCS Class II drug with “low solubility” and “high permeability”. Being an amphoteric molecule, it is ionized under gastro-intestinal conditions, therefore its pH dependent solubility increases at low (1.2) and high (6.8) pH values and decreases in the middle pH range when the drug is in the not ionized form (Shohin, Kulinich et al. 2014). PRX is rapidly and completely absorbed after oral administration (recommended dose in adults is 20 mg daily) and exhibits a long half-life (24-48h). However, PRX elimination is impaired in some elderly people (Verbeeck, Richardson et al. 1986), who represent the majority of patients affected by rheumatic diseases, resulting in a high inter-individual variability in the steady state plasma levels. Sustained release dosage forms capable of steady release of the drug over prolonged periods may, therefore, overcome such variability due to erratic drug elimination (Joseph, Lakshmi et al. 2002).

The solution was sought in the development of a new floating/gastroretentive system able to increase the gastric residence time, thus controlling and sustaining PRX release.

Therefore, a floating gastroretentive system carrying piroxicam was designed in form of hollow microspheres, using an opportune ternary matrix made up of hydrophilic swellable polymers (alginate and ALM-pectin) opportunely mixed with Hydroxypropyl methylcellulose (HPMC). HPMC has been selected as hydrocolloid with cellulose backbone having a bulk density less than 1 (Hoffman 2002) which may act as an adjuvant in pore forming (Mukund, Kantilal et al. 2012). Interestingly, in this case the floating system was designed, without using any gas generating agent. As previously reported for alginate-calcium carbonate beads loading prednisolone (Section B part 3), it is not easy to predict and stabilize the opportune gas-generating agents amount that profoundly influences particles micromeritics, inner matrix, floating ability and dissolution rate.

Different formulation parameters of prilling technique were studied, and mainly polymers mass ratio and viscosity of the feed solutions were investigated to establish the effect of these critical process parameters on hollow particles production, micromeritics, inner structure as well as on drug loading and *in vitro* drug release.

Their potential ability to prolong the anti-inflammatory effectiveness *in vivo*, was evaluated using the consolidated model of carrageenan-induced oedema in rat paw using different induction/administration time points (0.5, 3, 5, 24 and 48h before carrageenan injection) accordingly to PRX half-life.

3-C 2.1 Gel-beads production and characterization

The floating dosage form of piroxicam was designed as hollow gel-beads based on a ternary Alginate (ALG, Pol₁), ALM-Pectin (PCT, Pol₂) and

Hydroxypropyl methylcellulose (HPMC, Pol₃) matrix using Zn as opportune cross-linker.

Several PRX hollow beads were produced by prilling and the hydrated beads were dried to the final handling and stable form. The systems were characterized to evaluate the influence of each polymer, its concentration as well as gelling conditions on hollow beads formation, their inner structure and *in vitro/in vivo* release performances.

As reported in Table VII, formulations F1-F4 were produced varying Pol₁/Pol₂/Pol₃ mass ratio and reducing progressively final polymeric concentration whereas drug-polymer ratio was fixed at 1:15 on the basis of results from preliminary experiments. As control, blank beads were also produced. Drying process of the hydrated beads was conducted by exposing them to standard room conditions (22 °C; 67% RH) for 18–24 h until constant weight was reached.

Table VII. Zn-ALG-ALM-Pct-HPMC beads loaded with PRX. Formulation code, polymeric carrier, drug content (ADC), viscosity, encapsulation efficiency (EE), mean diameter and sphericity coefficient (SC) of hollow beads manufactured by prilling.

Formulation code	Pol ₁ /Pol ₂ /Pol ₃ * mass ratio	Feed solution % (w/w)	Viscosity** (Pa*s)	ADC (%±SD)	EE (%±SD)	Dried beads Diameter (µm±SD)	SC
F1	1.75 : 4 : 1.0	6.75	114.6	5.3 ± 0.1	85.2 ± 1.8	4076 ± 85	0.53 ± 0.01
F2	1.75 : 3 : 1.0	5.75	75.8	5.0 ± 0.2	78.7 ± 2.1	3617 ± 186	0.66 ± 0.04
F3	1.75 : 3 : 0.5	5.25	74.5	5.4 ± 0.1	87.0 ± 1.3	2396 ± 129	0.86 ± 0.03
F4	1.25 : 3 : 0.5	4.75	29.4	4.7 ± 0.1	74.0 ± 2.3	2209 ± 99	0.94 ± 0.01

* Pol₁: ALG; Pol₂: ALM-Pct; Pol₃: HPMC

** spindle: R2; rotor velocity, ω: 20 rpm

Results showed good ADC and EE values; as reported in Table VII, EE was in the range between 74% (F4) and 87% (F3). The slight reduction in EE value observed for F4 may be due to the decrease in viscosity of the polymeric solution that may allow a greater drug leaking to the cross-linking solution.

Interestingly, SEM analysis of the beads highlighted significant differences in terms of shape and sphericity. Surface analysis showed that F1, F2 and F3 (6.75-5.25% w/w feed concentrations) particles have a very irregular and oblong shape correlated to the high viscosity of the feed solutions (Table VII) that may delay the break-up of the polymeric laminar-jet and, thus, droplet formation. The high entanglement existing between the chains of three different polymers makes the polymeric jet highly cohesive (viscoelastic stresses dominate) delaying drops detachment from the nozzle. At the lowest feed concentration (4.75 w/w) and viscosity (F4, 29.4 Pa*s), polymer chains are relaxed and surface tension dominates, allowing the formation of droplets that, falling in the gelation bath, give rise to spherical particles. In fact, SEM analysis of F4 showed beads spherical in shape with a SC mean value of 0.94 and a mean diameter around 2200 μm (Fig.41-d).

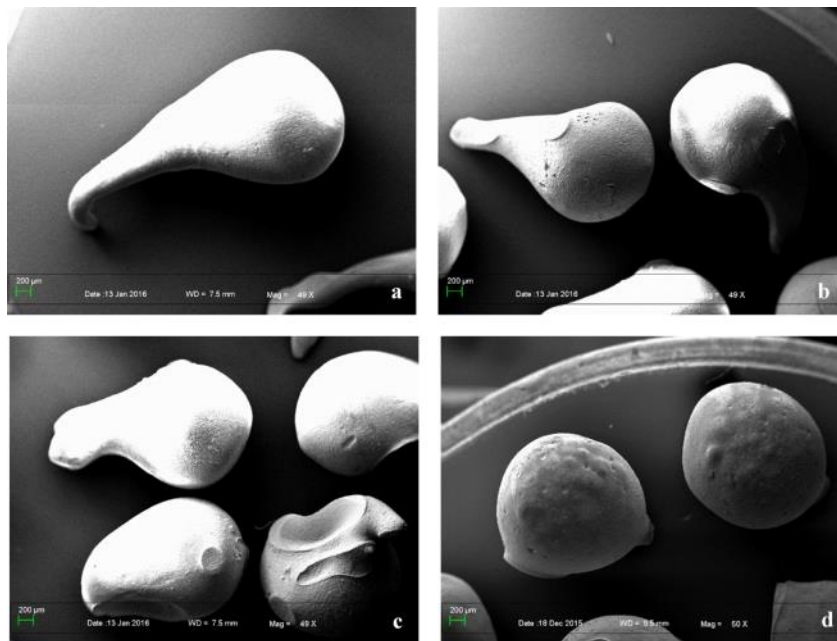


Figure 41. Zn-ALG-ALM-Pct-HPMC beads loaded with PRX. SEM microphotographs of dried beads: F1 (a), F2 (b), F3 (c) and F4 (d).

For more information about inner polymeric texture, beads were cryo-fractured and successively analysed by SEM (Fig. 42). The cross-section of beads showed either a hollow core (F1) or multiple small hollow pockets (F3-F4) of the ternary matrix. The presence of air-filled hollow spaces inside the beads may be due probably to the pore forming ability of HPMC (Mukund, Kantilal et al. 2012).

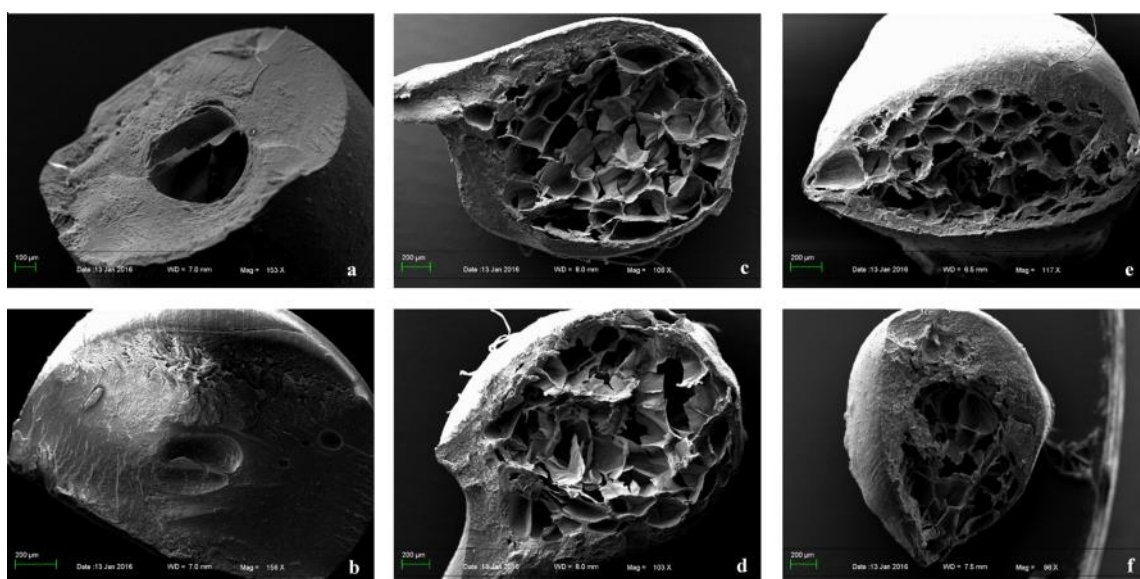


Figure 42. Zn-ALG-ALM-Pct-HPMC beads loaded with PRX. SEM microphotographs of cryo-fractured beads: F1 (a-b), F3 (b-c) and F4 (e-f).

To study piroxicam solid state after prilling process, Fluorescent Microscopy (FM) analysis on cryo-fractured beads was conducted (Fig. 43).

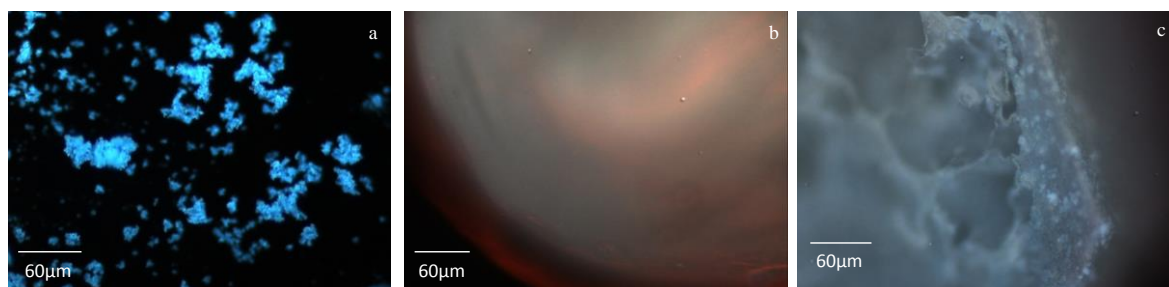


Figure 43. Zn-ALG-ALM-Pct-HPMC beads loaded with PRX. FM microphotographs of PRX raw material (a), cryo-fractured F4 blank (b) and F4 PRX loaded beads (c).

The FM images of pure PRX displayed crystalline material with blue fluorescence consisting of small crystals forming aggregates with a larger size, while images of blank particles (F4_blank) showed a reddish and off-white fluorescence in the inner and the outer, respectively. After the encapsulation process, PRX seems to keep its crystallinity and to be uniformly distributed within the hollow matrix. In fact, FM images of F4 (PRX loaded beads) displayed fluorescent spots due to PRX crystals homogeneously embedded within the hollow core.

In order to have a full technological characterization, DSC experiments were performed. The DSC thermal profiles of PRX raw material, blank (F1_b) and PRX-loaded beads (F1-F4) are shown in figure 44. According to previous observations (Vrečer, Vrbinc et al. 2003), thermal profile of pure crystalline PRX (Fig. 44-a) exhibited a very narrow melting peak at 201 °C and a broad exothermic peak at 225 °C due to the oxidative degradation. The thermogram of blank beads F1_b (Fig. 44-b) showed two endothermic events, well separated in temperature values, at 110°C corresponding to the loss of hydration water (Pillay and Fassihi 1999; Cerciello, Auriemma et al. 2015) and 160°C due to the melting of the ternary polymeric matrix, followed by an exothermic signal (ramp-like event) ranging from 227°C to 265°C and due to matrix degradation. All PRX- loaded beads (Fig.44-c-d-e-f) showed a thermal trend comparable to blank beads. After the encapsulation process, melting

peak of crystalline PRX is no longer detectable by DSC technique because, as previously reported, low-melting point polymers act as solvent for a crystalline drug embedded in a matrix (Del Gaudio, Auriemma et al. 2014). In this case, the ternary polymeric matrix begins to melt at lower temperature (160°C) than PRX (melting point 201°C), dissolving drug crystals in the melted polymers. PRX crystalline form is responsible of the exothermic signal at 312-322°C attributable to its oxidative degradation.

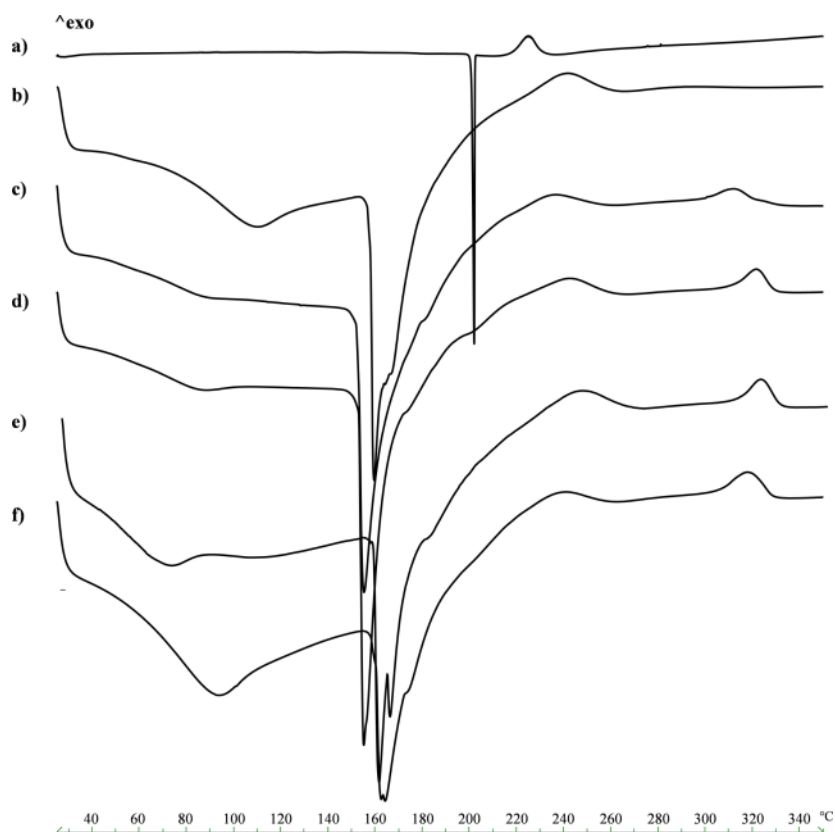


Figure 44. Zn-ALG-ALM-Pct-HPMC beads loaded with PRX. Differential scanning calorimetry thermograms: PRX raw material (a), blank beads F1_b (b) and PRX loaded beads F1 (c), F2 (d), F3 (e) and F4 (f).

***In vitro* buoyancy test**

Morphologically (Fig. 42), formulations F3 and F4, resulting from prilling of less viscous feed solutions, were the most porous. To investigate their ability

to float, buoyancy experiments were conducted through USP dissolution Apparatus II containing simulated gastric fluid – SGF and floating properties were determined by visual observation. As reported by Ishak (Ishak 2015), the time taken by beads to float on the medium surface was floating lag time (FLT). Particularly, F4 showed a significant floating ability as more than 75% of the particles float within 5 min of lag time (FLT) for all the duration of the experiment without disintegration (Fig. 45); on the contrary, F3 showed a delay in buoyancy (FLT of about 15 min) and only 25% of the beads float.

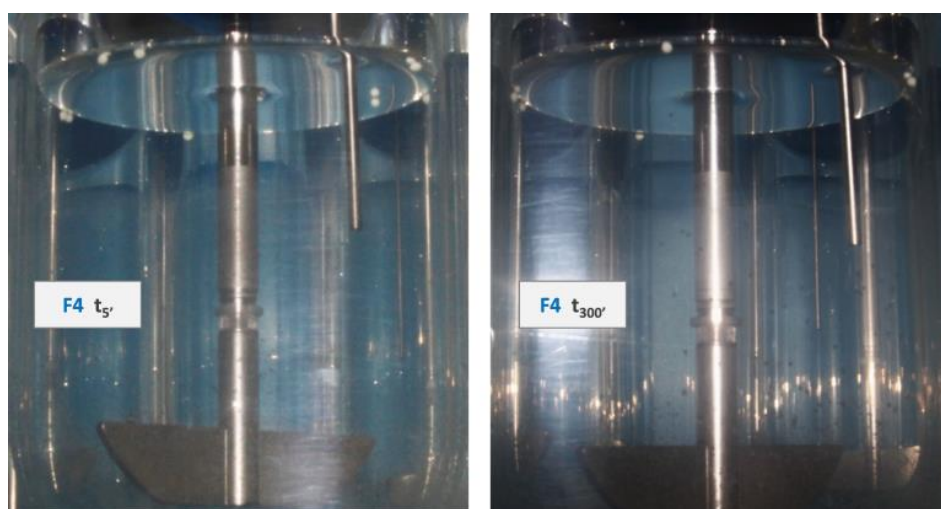


Figure 45. Zn-ALG-ALM-Pct-HPMC beads loaded with PRX. *In vitro* floating images of formulation F4.

Floating properties of F4 seem to be due to a combination of swelling of hydrocolloid particles with their low density, spongy and hollow inner structure. The hydration of the hydrocolloid beads surface in SGF results in an increased bulk volume and, at the same time, the presence of internal voids (as highlighted by SEM investigation) make beads able to entrap air acquiring bulk density less than 1, and, therefore, remaining buoyant on the acidic medium. Images obtained using transmitted (bright field) or in fluorescence (dark field) optical microscopy, were conducted on fractured particles withdrew from acidic medium. Microphotographs in figure 46 clearly

highlighted the presence of pores and air bubbles entrapped within the gel barrier.

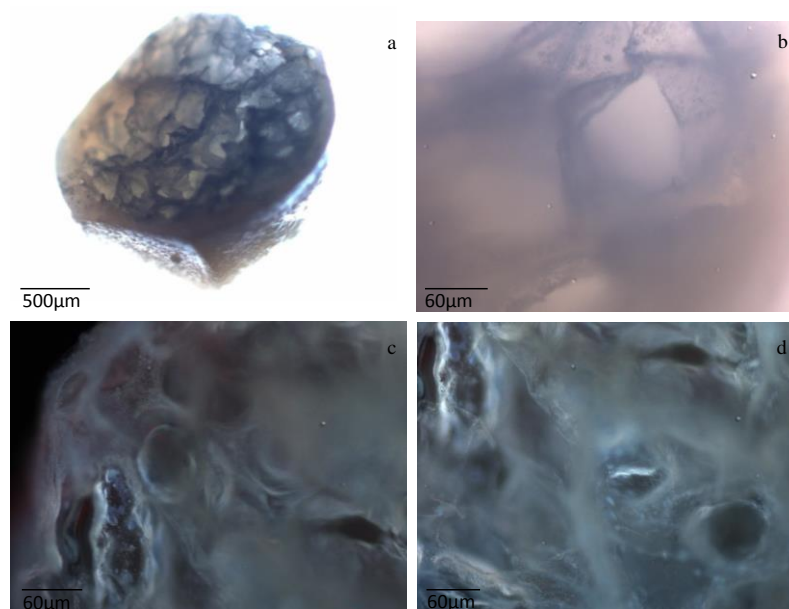


Fig.46. Zn-ALG-ALM-Pct-HPMC beads loaded with PRX .Microphotographs of hydrated fractured bead (F4) obtained using optical microscopy in bright-field (a-b) and fluorescent microscopy (c-d).

In addition, the inner cross-linked multi-polysaccharide matrix may act as reservoir for slow and sustained PRX release controlled by a diffusion mechanism process through the swollen polymers gel layer (Singh and Kim 2000).

Drug release studies

The hollow beads were tested to verify whether the porous ternary polymeric matrix is able to control and modulate PRX release in all gastrointestinal tract, by conventional dissolution test (Yang, Chu et al. 2002), using a standard pH change protocol. The main dissolution profiles are shown in figure 47.

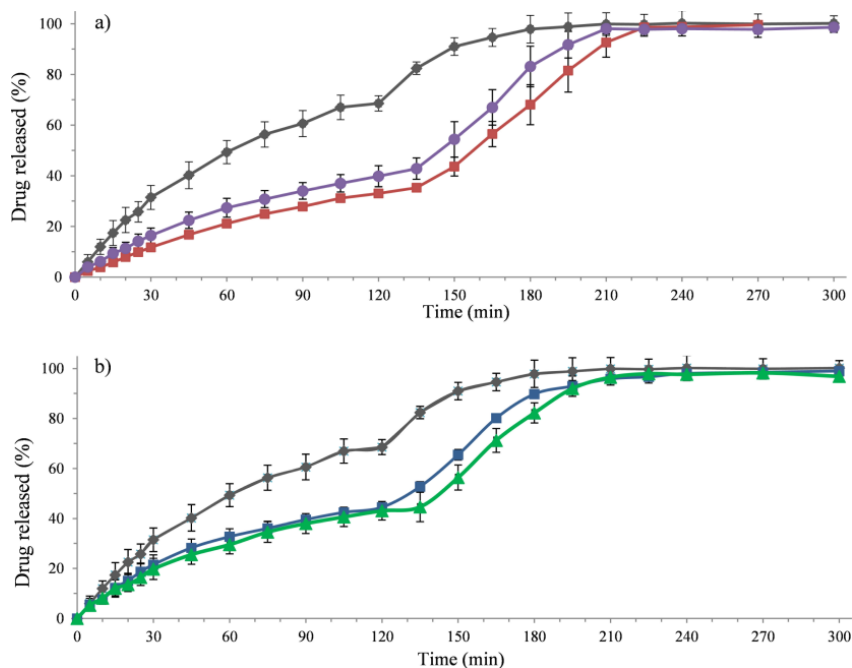


Figure 47. Zn-ALG-ALM-Pct-HPMC beads loaded with PRX. PRX release profiles of formulations: a) F1 (-■-) and F2 (-●-), b) F3 (-▲-) and F4 (-■-), with respect to pure drug (-■-).

F1-F4 showed a modulation of drug release especially in SGF at 120 min (30-40%) compared to pure PRX (68.6% of drug release). Particularly F4, the formulation most spherical in shape and with spongy inner structure, showed an interesting bimodal pattern of release. During the permanence in acidic medium F4 released 44.5% of PRX, however, about 22% of NSAID was released in the first 30 min suggesting that F4 may provide a rapid onset of anti-inflammatory/analgesic action. In SIF, after pH-change, the release was very slower (52.8, 65.5, 80.2% PRX after 135, 150, 165 min) and the total drug liberation (98.5%) was achieved at 270 min as compared to the rapid dissolving (82.4, 91 and 94.6% at the same time points) of the pure PRX. This sustained release of formulation F4 may keep the NSAID amount at the appropriate therapeutic level for a prolonged time.

***In vivo* experiments**

To verify whether the bimodal and sustained release pattern *in vitro* of F4 may correspond to an extended anti-inflammatory action *in vivo*, the anti-inflammatory effectiveness of floating formulation F4 was evaluated using a the model of carrageenan-induced oedema in rat paw as previously employed for other NSADs and SAIDs. Firstly, different doses of standard PRX were tested by administering the drug 0.5h before the carrageenan injection (Fig. 48). The control group (ctr) received 1 ml of MC at the same time point before oedema induction. The dose of 1 mg kg⁻¹ of PRX was selected as it achieved optimal anti-inflammatory effects (Fig. 48).

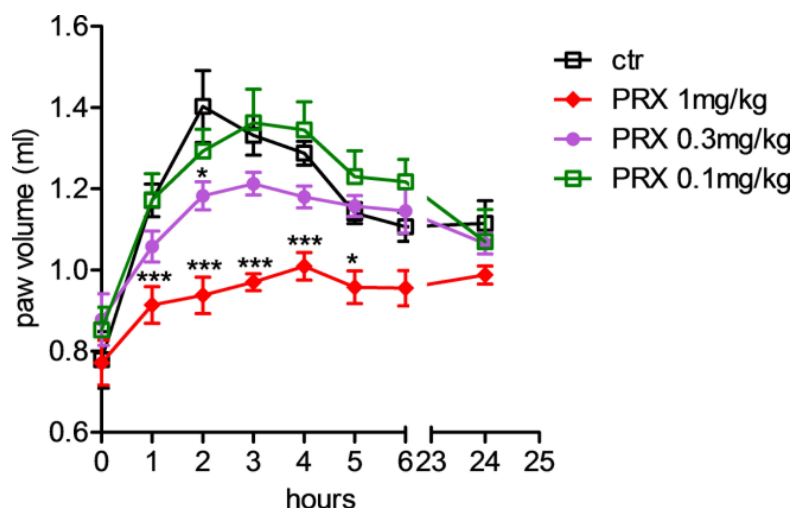


Figure 48. Zn-ALG-ALM-Pct-HPMC beads loaded with PRX. Dose-response curve of pure PRX (0.1, 0.3, and 1 mg/kg doses) administered *per os* to rats 0.5 h before carrageenan injection; mean \pm SEM ($n = 8$ per group). * $p < 0.05$, *** $p \leq 0.001$ compared to control.

To have evidence of potential prolonged *in vivo* anti-inflammatory activity of F4, as effect of its floating ability and sustained release properties, the multiple-units dosage form (PRX equivalent dose of 1 mg kg⁻¹) was tested at different time points (3-5-24h up to 48h) before carrageenan injection in comparison to pure drug. Control groups received blank beads (F) or MC. Both F and MC did not affect the paw oedema in rats (data not shown).

F4 significantly reduced carrageenan-induced paw oedema as compared to control, when administered to rats 3h or 5h before carrageenan injection with an anti-inflammatory activity similar to pure PRX (1mg kg^{-1}) (Fig. 49-A). But interestingly, F4 administered to rats 24h before oedema induction, showed a significant prolonged anti-inflammatory effect in terms of paw oedema inhibition whereas no response was observed for standard PRX. (Fig. 49-B). Additionally, F4 was still able to reduce the paw oedema in rats when administered up to 48h before the injection of the phlogistic agent (Fig 49-B). Results obtained indicated that floating and *in vitro* sustained release property of F4 is able to provide the dose fraction required to maintain an effective therapeutic plasma level of PRX for a prolonged period. In contrast, the standard drug (pure PRX 1mg kg^{-1}), due to a more rapid release, was efficacious in reducing rat paw oedema up to 5h before carrageenan injection (Fig. 49-A).

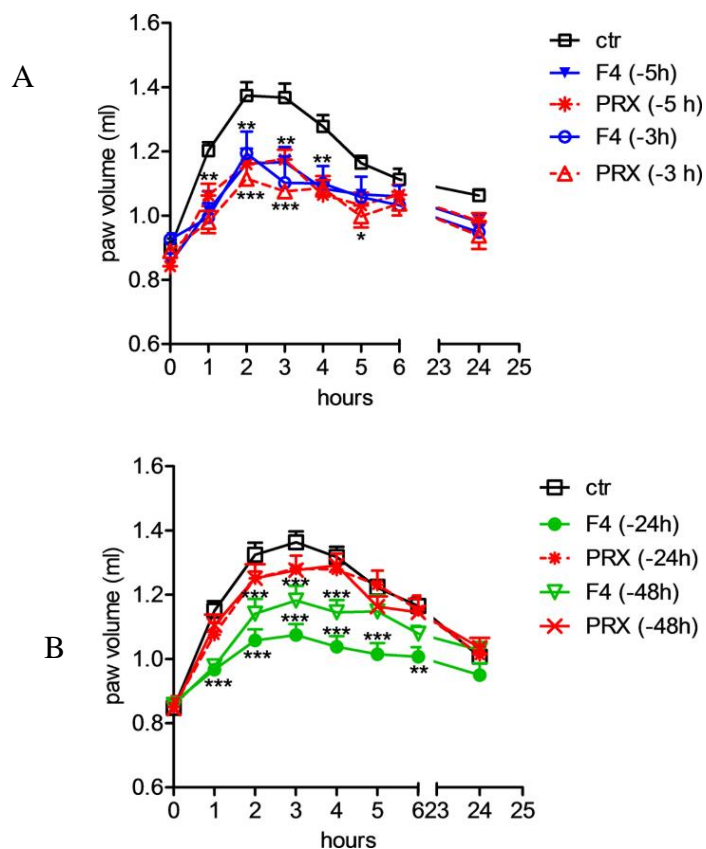


Figure 49. Zn-ALG-ALM-Pct-HPMC beads loaded with PRX. Oedema volume reduction obtained by administering F4 and pure PRX *per os* to rats 3-5h (A) and 24-48h (B) before carrageenan injection compared to control; mean \pm SEM (n = 8). *p < 0.05, **p \leq 0.01, ***p \leq 0.001 compared to control.

4.2 Conclusions

The present study suggests that prilling is a proper technique able to produce gastro-retentive (GR) delivery systems with floating ability and controlled drug release properties, using an appropriate multipolymer system based on natural and natural-derived polysaccharides (alginate, ALM-pectin and HMPC) with different key features, and without using any gas generating agent. The opportune set-up of process parameters and gelling conditions allows to produce interesting hollow gel-beads loaded with piroxicam which floating properties are based on swellable and air-entrapping ternary polymer

matrix. The final dosage form (F4) acts as a floating system in gastric medium able to control *in vitro* drug release and to extend *in vivo* the anti-inflammatory effectiveness of PRX up to 48h.

The designed floating beads with bimodal and strictly controlled NSAID release pattern may give the possibility to overcome the fluctuations in plasma drug levels, providing both a loading and a maintenance dose of NSAIDs. Such beads may be proposed as carrier system for anti-inflammatory/analgesic drugs with biopharmaceutical and pharmacokinetic properties similar to PRX and when a bimodal (rapid plus sustained) drug release profile is required as in treating chronic inflammatory diseases such as rheumatoid arthritis in elderly patients.

MATERIALS & METHODS

Materials

Sodium alginate (European Pharmacopoeia 8, MW \approx 240 KDa, mannuronic/guluronic ratio 1:2 viscosity 250-300 cP, 1% in H₂O 20°C) employed as matrix in the preparation of gel-beads was used as purchased from Carlo Erba (Milan, Italy) without further purification. ALM-pectin (viscosity \sim 30 cP, 1% in H₂O 20°C, MW \sim 150 KDa, esterification degree 24% and amidation degree 23%) was kindly donated by Herbstreith & Fox KG (Neuenburg, Germany). Hydroxypropyl methylcellulose (HPMC_ viscosity 80-120 cP, 2% in H₂O 20°C MW \sim 26 KDa), zinc acetate dehydrate (purity \geq 99.0%) and calcium chloride (purity \geq 93.0%) were supplied by Sigma- Aldrich (Sigma-Aldrich, Milan, Italy).

Calcium carbonate (purity \geq 99.0%) was acquired from J.T.Baker (Center Valley, USA).

Ketoprofen and ketoprofen lysinate were kindly donated by Dompè (Dompè s.p.a. l'Aquila, Italy), whereas piroxicam was kindly donated by Sifavitor (Sifavitor srl, Milan, Italy). Prednisolone and all other chemicals and reagents were obtained from Sigma Aldrich (Milan, Italy) and used as supplied.

Methods

Drug loaded beads preparation

Appropriate amounts of sodium alginate (2.0-2.25-2.5%) and ALM-pectin (6.00% w/w) or together with HPMC (with total polymer concentration between 4.75% - 6.75% for piroxicam beads), were dissolved in distilled water at room temperature under gentle stirring for 18 hours in order to obtain 100 ml of polymer solution. Various amounts of ketoprofen, ketoprofen lysinate, piroxicam or prednisolone were suspended into the polymer solution and stirred for 2 hours in order to obtain different drug/polymer ratios (1:20, 1:15, 1:10, 1:5). Beads were manufactured by a vibrating nozzle device (Fig. 5,

Nisco Encapsulator Var D; Nisco Engineering Inc., Zurich, CH), equipped with a syringe pump (Model 200 Series, Kd Scientific Inc. Boston, MA, USA), pumping the drug/polymer solution through a nozzle 400 μm or 600 μm in diameter. The experiments were performed at various volumetric flow rate, between 3 and 6 ml/min according to different formulations. The vibration frequency used to break up the laminar liquid jet was set between 250 and 350 Hz, amplitude of vibration 100%. The distance between the vibrating nozzle and the gelling bath was fixed at 25 cm. A stroboscopic lamp was set at the same amplitude as the frequency, in order to visualize the falling droplets.

Drug/polymer droplets fell into aqueous solutions (pH = 1.5) 0.5M or 10% w/v of calcium chloride or zinc acetate dehydrate or both of them simultaneously in different molar ratios (1:1, 1:4, 4:1), where they were gelled under gentle stirring. The beads were held into the gelling solution for 2-10 minutes, (according to the different formulations), at room temperature or at 4-5°C (for ketoprofen lysinate beads), and then recovered and thoroughly rinsed with distilled water. As a comparison, unloaded beads (blank) were produced following the same protocol. The drying process of the hydrated beads was conducted by exposing them to standard room conditions (22 °C; 67% RH) for 18–24 h until constant weight was reached.

Core-shell beads preparation

Regarding ALM-pectin-K beads, (Section A part 2) for the production of core-shell systems the enteric coating solution was prepared by dissolving Eudragit S100[®] in acetone at 6% (w/v) concentration. This solvent allowed complete dissolution of the enteric polymer while maintaining the integrity of beads. Coating was obtained by immersion of beads in the coating solution followed by solvent evaporation in a rotary evaporator. The process was repeated until the desired amount of coating was achieved. Microparticles were coated at

different levels (initial weight increase ranging from 10% to 60%). Samples of coated beads were then dried and weighed; the mean coating weight was calculated by difference with respect to the initial beads weight.

Drug content and encapsulation efficiency

Accurately weighed amounts of beads from each manufactured batch (about 10 mg each) were dissolved under vigorous stirring in PBS buffer (100 mM pH 7.0) in order to disintegrate the polymer matrix and release the encapsulated drug. Afterwards, 23 ml of ethanol (or PBS for ketoprofen lysinate evaluation) were added and the suspension was centrifuged at 6000 rpm for 15 min.

The actual drug content (ADC) was determined by UV spectroscopy (Evolution 201 UV/VIS Spectrometer; Thermo Scientific, Waltham, MA) at λ 254 nm (ketoprofen), λ 259 nm (ketoprofen lysinate), λ 244 (prednisolone) and λ 354 nm for piroxicam using the following equation:

$$ADC(\%) = \frac{\text{drug content in dry beads}}{\text{weight of dry beads}} \times 100 \quad \text{Eq. 1}$$

Encapsulation efficiency was calculated as the ratio actual to theoretical drug content (TDC) i.e. the weight of drug added (g)/weight of polymers/excipients and drug added (g) x 100. Each analysis was performed in triplicate; results were expressed in terms of mean \pm standard deviation.

Beads size and morphology

Scanning electron microscopy (SEM) was performed using a Carl Zeiss EVO MA 10 microscope with a secondary electron detector (Carl Zeiss SMT Ltd, Cambridge, UK) equipped with a LEICA EMSCD005 metallizator producing a deposition of a 200-400 Å thick gold layer. Analysis was conducted at 17 KeV.

Projection diameter was obtained by image analysis (Image J software, Wayne Rasband, National Institute of Health, Bethesda, MD, USA). At least one hundred bead images were analysed for each preparation in order to calculate length-number mean and relative standard deviation for at least three different prilling processes.

Perimeter and projection surface area obtained by image analysis were used to calculate a Sphericity Coefficient (SC) by the following equation (Almeida-Prieto, Blanco-Mendez et al. 2004):

$$SC = \frac{4\pi A}{P^2} \quad (\text{Eq.2})$$

where A is the bead surface area and P its perimeter.

Optical microscopy

For ketoprofen loaded alginate beads (Section A part 1) and piroxicam loaded alginate-ALM pectin-HPMC beads (Section C) inner structure images were obtained by the cryo-fracture of the samples and further analysis by fluorescent microscopy (FM) through a Zeiss Axiophot microscope, equipped with a 20×1.4 NA and 10×0.3 no-oil immersion plan Apochromat objective (Carl Zeiss Vision, Munchen-Hallbergmoos, Germany) using standard 4,6-diamidino-2-phenylindole optics that adsorb violet radiation (maximum 372 nm) and emit a blue fluorescence (maximum 456 nm). In brief, freeze-fracture of the beads was performed by plunging the particles into liquid nitrogen for 1 min, then fracturing the frozen beads by means of two needles. Split particles were attached to aluminium stab, covered with gold, and analysed. Other images reported in Section C were acquired from the same microscope using transmitted light microscopy (bright-field) equipped with a 2.5×0.3 and 10×0.3 no-oil immersion plan Apochromat objectives (Carl Zeiss Vision, Munchen-Hallbergmoos, Germany).

EDS analyses

For prednisolone loaded alginate beads obtained with different cross-linkers (Section B part 1), the morphology and composition of the samples were inspected by scanning electron microscopy (SEM), model LEO EVO 50, equipped with energy dispersive spectrometer (EDS), model Oxford INCA Energy 300. Elemental maps were acquired for assessing the homogeneity of the samples composition. The EDS maps were performed by operating at 20 KeV primary energy with a probe current of 100pA.

Swelling behaviour

For prednisolone loaded alginate beads (Section B, part 2), the swelling behaviour of the beads was evaluated by optical microscopy. A Leica inverted microscope equipped with a CCD camera (Leica, Milan, Italy) was employed. The beads were immersed in gastric simulated fluid for two hours and in intestinal simulated fluid until complete dissolution and observed at established time points. Swelling degree was determined as follow:

$$\%swelling = \frac{\text{bead size at time } t - \text{bead size at time zero}}{\text{bead size at time zero}} \cdot 100$$

Eq. 3

All measurements were done in triplicate and the variability expressed as S.D. For beads examined in Section B part 1, swelling behaviour in the same simulated fluids, was evaluated. At pre-determined times, beads were withdrawn from the dissolution vessel, dabbed with paper to remove the water on the bead surface and then weighted. The swelling ratio (SR) for each sample was calculated according to equation 4:

Swelling Ratio =

$$\frac{\text{bead weight at time } t - \text{bead weight at time zero}}{\text{bead weight at time zero}} \quad \text{Eq. 4}$$

Calorimetric analysis

Beads thermal characteristics were determined by differential scanning calorimetry (DSC) (Mettler Toledo DSC 822e module controlled by Mettler Star E software, Columbus, OH, USA), and compared with those obtained using both blank beads and drugs raw materials. An appropriate amount of dried beads was crimped in a standard aluminium pan that was pierced and heated from 25 °C to 350 °C at a heating rate of 10 or 20 °C/min in nitrogen atmosphere at a flow rate of 150 ml/min. Characteristic peaks were recorded and specific heat of the melting endotherm was evaluated.

Fourier Transform Infrared Spectroscopy (FT-IR) analyses

For beads discussed in Section B part 2, FT-IR spectra were detected as KBr powder dispersion (Jasco model FT/IR-410, 420 Herschel series – Jasco Corporation Tokyo, Japan) using the EasiDiff™ Diffuse Reflectance Accessory. The samples were combined with small amount of potassium bromide and pressed to 6 tons in a manual press (OMCN s.p.a., Bergamo, Italy). The thin compacts produced were analysed using 256 scans and with a 1 cm⁻¹ resolution step. Each experiment was carried in triplicate and results averaged.

***In vitro* buoyancy test**

Floating properties of prednisolone and piroxicam hollow beads (Section B part 3 and Section C) were measured in the USP dissolution Apparatus II (Sotax AT7 Smart – Sotax, Allschwil, CH) (Ishak 2015). A specific number of particles were placed in simulated gastric fluid – SGF (0.1 M hydrochloric

acid; pH 1; 75 rpm - 37°C) and the time required for the beads to rise to the surface of the medium and to float was considered as floating lag time (FLT). The percentage of floating or sinking particles was measured by visual observation (Ishak 2015) and determined after three experiments.

Drug release studies

In vitro dissolution/release tests were conducted in sink conditions on given amounts of bead formulations using a USP 27 dissolution apparatus II: paddle, 100 rpm, 37°C (Sotax AT7 Smart – Sotax, Allschwil, CH) on line with a UV spectrophotometer (Lambda 25 UV/VIS Spectrometer, Perkin Elmer, Waltham, MA, USA).

A classic pH-change assay, method A, according to <1092> monograph “The Dissolution Procedure: Development and Validation” (USP 36), was used. Briefly, dried beads were added to the dissolution medium, 750 ml 0.1M HCl (SGF) for 2 h, then 250 ml of 0.2M Na₃PO₄ was added and pH adjusted to 6.8 (SIF). While for floating beads the dissolution experiments were conducted only in SGF for all the duration of the experiment.

Data were analysed spectrophotometrically at λ 258 nm (SGF) and λ 260 nm (SIF) for ketoprofen, λ 259 nm for ketoprofen lysinate, λ 244 nm for prednisolone, whereas piroxicam was analysed at λ 333 and λ 354 nm, for gastric and intestinal simulated environment, respectively.

Ketoprofen lysinate and prednisolone optimized formulations (Section A part 3 and Section B part 2) were introduced into selected capsules (DR[®] caps) and their release from these dosage forms was evaluated using the USP-II apparatus equipped with mesh basket (USP Standard Size Mesh, 40) and the experimental protocol previously reported.

Dissolution tests were conducted on six different batches of particles; mean values and standard deviation were reported.

Kinetic of drug release

In order to evaluate prednisolone diffusion coefficient when released through the different crosslinked alginate matrix (Section B part 1), the analysis of released amount of the drug was performed, splitting the release into two phases corresponding to gastric and intestinal environments. Two common kinetic models were used to fit the release data. The Higuchi's model (Eq. (5)) that is the most used to investigate pure Fickian transport:

$$M_t = A\sqrt{D(2C_0 - C_s)t} \quad (5)$$

where M_t is the drug cumulative amount released at time t , t is time, A is the surface area, D the diffusivity of the drug through the matrix, and C_0 and C_s are the initial drug concentration and drug solubility, respectively. This model is applicable when drug solubility is higher than drug concentration, and when pure diffusion is the leading release mechanism (Higuchi 1961). The second model employed to fit release data was the Peppas-Korsmeyer's equation (Eq. 6):

$$\frac{M_t}{M_\infty} = kt^n \quad (6)$$

where M_∞ is the drug amount released at infinity, k is a constant, and n is a diffusion coefficient, which depends on geometry and release mechanism of the formulation (Ritger and Peppas 1987).

Since Eq. 5 and 6 are usually limited to the description of the first 60% of release whereas in the study we compared the fitting performed over 60% of release to that over 100% of the profile to address adequacy of the procedure employed, Levenberg–Marquardt method was applied in order to evaluate the lack of fit correlation coefficient normalized to the degree of freedom of the system (Marquardt 1963; Del Gaudio, De Cicco et al. 2015).

Animals and carrageenan oedema induction

Male Wistar rats (180-220g) were purchased from Charles River (Charles River Laboratories, Calco, Italy). Rats were anaesthetized with isoflurane and oedema was induced by injecting in the right hind paw 100µl of carrageenan 1% (w/v) as previously reported (Cicala, Morello et al. 2007). Paw volume (ml) was measured plethysmographically (2Biological-Instruments, Italy) at the time zero, each hour for 6h, and at 24h after carrageenan injection. Data were expressed as mean \pm S.E.M. Statistical differences were evaluated by two-way analysis of variance (ANOVA). P value of <0.05 was considered statistically significant. All the experiments were approved by Italian Health Ministry (authorization n° 805/2015-PR) and conducted according to institutional animal care guidelines, Italian Law 26/2014 based on the European Community Law for Animal Care 2010/63/UE.

***In vivo* experiments**

Dose-response curves of standard ketoprofen (K) and prednisolone (P) (dose *per os* 1.0, 3.0 and 10.0 mg/kg) or piroxicam (dose *per os* 0.1, 0.3 and 1 mg/kg) were performed by oral administration of the drug to rats 0.5h before the carrageenan injection, using an aqueous solution of methylcellulose, MC (0.5% w/v) as vehicle (Chakraborty, Khandai et al. 2010).

To assess the *in vivo* anti-inflammatory effectiveness of best formulations in comparison with the reference drugs, rats were treated by oral gavage with the formulations (K and P equivalent dose 3 mg kg⁻¹; PRX equivalent dose 1 mg kg⁻¹) or raw with reference K, P, PRX in 0.5% (w/v) methyl cellulose (Chakraborty, Khandai et al. 2010) using the same doses. Samples were administered to rats at different times before the injection of the phlogistic agent accordingly with formulation type (0.5, 3, 5, 15, 24, 48h). Control groups received 1 mL of MC or blank beads in 0.5% (w/v) MC.

REFERENCES

- Abbas, S. S., M. F. Schaalán, et al. (2014). "Possible potentiation by certain antioxidants of the anti-inflammatory effects of diclofenac in rats." The Scientific World Journal **2014**.
- Agarwal, T., S. N. G. H. Narayana, et al. (2015). "Calcium alginate-carboxymethyl cellulose beads for colon-targeted drug delivery." International Journal of Biological Macromolecules **75**: 409-417.
- Ahirrao, S. P., P. S. Gide, et al. (2014). "Ionotropic gelation: a promising cross linking technique for hydrogels." Res Rev J Pharm Nanotechnol **2**: 1-6.
- Aiedeh, K. M., M. O. Taha, et al. (2007). "Effect of ionic crosslinking on the drug release properties of chitosan diacetate matrices." J Pharm Sci **96**(1): 38-43.
- Al-Otoum, R., S. R. Abulateefeh, et al. (2014). "Preparation of novel ionotropically crosslinked beads based on alginate-terephthalic acid composites as potential controlled release matrices." Pharmazie **69**(1): 10-18.
- Almeida-Prieto, S., J. Blanco-Mendez, et al. (2004). "Image analysis of the shape of granulated powder grains." J Pharm Sci **93**(3): 621-634.
- Alten, R., G. Döring, et al. (2010). "Hypothalamus-pituitary-adrenal axis function in patients with rheumatoid arthritis treated with nighttime-release prednisone." The Journal of rheumatology **37**(10): 2025-2031.
- Alten, R., R. Holt, et al. (2015). "Morning stiffness response with delayed-release prednisone after ineffective course of immediate-release prednisone." Scandinavian journal of rheumatology.
- Alvarez-Lorenzo, C., B. Blanco-Fernandez, et al. (2013). "Crosslinked ionic polysaccharides for stimuli-sensitive drug delivery." Advanced drug delivery reviews **65**(9): 1148-1171.
- Ambekar Sunil, S., M. Venkata Srikanth, et al. (2013). "Chronotherapeutic drug delivery from indomethacin compression coated tablets for early morning pain associated rheumatoid arthritis." Current drug delivery **10**(1): 109-121.
- Aquino, R. P., G. Auriemma, et al. (2012). "Piroxicam loaded alginate beads obtained by prilling/microwave tandem technique: Morphology and drug release." Carbohydrate Polymers **89**(3): 740-748.
- Aquino, R. P., G. Auriemma, et al. (2013). "Design and production of gentamicin/dextran microparticles by supercritical assisted atomisation for the treatment of wound bacterial infections." International Journal of Pharmaceutics **440**(2): 188-194.
- Arvidson, N. G., B. Gudbjörnsson, et al. (1994). "Circadian rhythm of serum interleukin-6 in rheumatoid arthritis." Annals of the rheumatic diseases **53**(8): 521-524.

- Arvidson, N. G., B. Gudbjörnsson, et al. (1994). "Circadian rhythm of serum interleukin-6 in rheumatoid arthritis." Annals of the Rheumatic Diseases **53**(8): 521-524.
- Aslani, P. and R. Kennedy (1996). "Effect of gelation conditions and dissolution media on the release of paracetamol from alginate gel beads." Journal of microencapsulation **13**(5): 601-614.
- Atassi, F., C. Mao, et al. (2010). "Solid-state characterization of amorphous and mesomorphous calcium ketoprofen." Journal of pharmaceutical sciences **99**(9): 3684-3697.
- Auriemma, G., P. Del Gaudio, et al. (2011). "A combined technique based on prilling and microwave assisted treatments for the production of ketoprofen controlled release dosage forms." International journal of pharmaceutics **415**(1): 196-205.
- Auriemma, G., T. Mencherini, et al. (2013). "Prilling for the development of multi-particulate colon drug delivery systems: Pectin vs. pectin–alginate beads." Carbohydrate Polymers **92**(1): 367-373.
- Badve, S. S., P. Sher, et al. (2007). "Development of hollow/porous calcium pectinate beads for floating-pulsatile drug delivery." European journal of pharmaceutics and biopharmaceutics **65**(1): 85-93.
- Belscak-Cvitanovic, A., D. Komes, et al. (2015). "Improving the controlled delivery formulations of caffeine in alginate hydrogel beads combined with pectin, carrageenan, chitosan and psyllium." Food Chem **167**: 378-386.
- Berkland, C., K. Kim, et al. (2001). "Fabrication of PLG microspheres with precisely controlled and monodisperse size distributions." Journal of Controlled Release **73**(1): 59-74.
- Berkland, C., D. W. Pack, et al. (2003b). " Microparticles, US Patent 6,669,961 B2."
- Bethke, T. D., A. Huennemeyer, et al. (2010). "CHRONOPHARMACOLOGY OF ROFLUMILAST: A COMPARATIVE PHARMACOKINETIC STUDY OF MORNING VERSUS EVENING ADMINISTRATION IN HEALTHY ADULTS." Chronobiology International **27**(9-10): 1843-1853.
- Bohadana, A. B., B. Hannhart, et al. (2002). "Nocturnal worsening of asthma and sleep-disordered breathing." Journal of Asthma **39**(2): 85-100.
- Brandau, E., . US (1995). "US Patent no 54726485."
- Brandau, T. (2002). "Preparation of monodisperse controlled release microcapsules." International Journal of Pharmaceutics **242**(1–2): 179-184.
- Brandenberger, H. and F. Widmer (1998). "A new multinozzle encapsulation/immobilisation system to produce uniform beads of alginate." Journal of Biotechnology **63**(1): 73-80.

- Brejnholt, S. M. (2009). Pectin. Food Stabilisers, Thickeners and Gelling Agents, Wiley-Blackwell: 237-265.
- Buseti, C. and T. Crimella (2006). Methods for treating early morning pathologies, Google Patents.
- Buttgereit, F., G. Doering, et al. (2008). "Efficacy of modified-release versus standard prednisone to reduce duration of morning stiffness of the joints in rheumatoid arthritis (CAPRA-1): a double-blind, randomised controlled trial." The Lancet **371**(9608): 205-214.
- Buttini, F., P. Colombo, et al. (2012). "Particles and powders: tools of innovation for non-invasive drug administration." J Control Release **161**(2): 693-702.
- Caballero, F., M. Foradada, et al. (2014). "Characterization of alginate beads loaded with ibuprofen lysine salt and optimization of the preparation method." International Journal of Pharmaceutics **460**(1): 181-188.
- Caballero, F., M. Foradada, et al. (2014). "Characterization of alginate beads loaded with ibuprofen lysine salt and optimization of the preparation method." International Journal of Pharmaceutics **460**(1-2): 181-188.
- Cerciello, A., G. Auriemma, et al. (2016). "Natural polysaccharides platforms for oral controlled release of ketoprofen lysine salt." Drug development and industrial pharmacy **42**(12): 2063-2069.
- Cerciello, A., G. Auriemma, et al. (2016). "A novel core-shell chronotherapeutic system for the oral administration of ketoprofen." Journal of Drug Delivery Science and Technology **32**: 126-131.
- Cerciello, A., G. Auriemma, et al. (2016). "Prednisolone Delivery Platforms: Capsules and Beads Combination for a Right Timing Therapy." PLoS One **11**(7): e0160266.
- Cerciello, A., G. Auriemma, et al. (2015). "Design and In Vivo Anti-Inflammatory Effect of Ketoprofen Delayed Delivery Systems." J Pharm Sci **104**(10): 3451-3458.
- Chakraborty, S., M. Khandai, et al. (2010). "Preparation, in vitro and in vivo evaluation of algino-pectinate bioadhesive microspheres: An investigation of the effects of polymers using multiple comparison analysis." Acta Pharm **60**(3): 255-266.
- Chan, L., Y. Jin, et al. (2002). "Cross-linking mechanisms of calcium and zinc in production of alginate microspheres." International Journal of Pharmaceutics **242**(1): 255-258.
- Chaturvedi, S., K. Prabha, et al. (2013). "Approaches to increase the gastric residence time: floating drug delivery systems-a review." Asian Journal of Pharmaceutical and Clinical Research **6**(3): 1-9.
- Chikanza, I., P. Petrou, et al. (1993). "Excessive and dysregulated secretion of prolactin in rheumatoid arthritis: immunopathogenetic and therapeutic implications." Rheumatology **32**(6): 445-448.

- Cho, C.-H. (2015). "Molecular mechanism of circadian rhythmicity of seizures in temporal lobe epilepsy." Neuronal mechanisms of epileptogenesis.
- Choi, B., H. J. Park, et al. (2002). "Preparation of alginate beads for floating drug delivery system: effects of CO₂ gas-forming agents." International Journal of Pharmaceutics **239**(1): 81-91.
- Cicala, C., S. Morello, et al. (2007). "Haemostatic imbalance following carrageenan-induced rat paw oedema." Eur J Pharmacol **577**(1-3): 156-161.
- Cimini, A., L. Brandolini, et al. (2015). "Gastroprotective effects of L-lysine salification of ketoprofen in ethanol-injured gastric mucosa." J Cell Physiol **230**(4): 813-820.
- Clements, J. N. (2011). "Treatment of rheumatoid arthritis: A review of recommendations and emerging therapy."
- Cohen-Mansfield, J., D. Garfinkel, et al. (2000). "Melatonin for treatment of sundowning in elderly persons with dementia—a preliminary study." Archives of Gerontology and Geriatrics **31**(1): 65-76.
- Cutolo, M. (2016). "Glucocorticoids and chronotherapy in rheumatoid arthritis." RMD open **2**(1): e000203.
- Dai, W., Y. Guo, et al. (2015). "Sylysia 350/Eudragit S100 solid nanomatrix as a promising system for oral delivery of cyclosporine A." International Journal of Pharmaceutics **478**(2): 718-725.
- Dalmoro, A., A. A. Barba, et al. (2012). "Intensifying the microencapsulation process: Ultrasonic atomization as an innovative approach." European Journal of Pharmaceutics and Biopharmaceutics **80**(3): 471-477.
- Das, M. and P. Senapati (2008). "Furosemide-loaded alginate microspheres prepared by ionic cross-linking technique: Morphology and release characteristics." Indian journal of pharmaceutical sciences.
- Das, S., K.-Y. Ng, et al. (2010). "Formulation and Optimization of Zinc-Pectinate Beads for the Controlled Delivery of Resveratrol." AAPS PharmSciTech **11**(2): 729-742.
- Davis, M., R. Williams, et al. (1978). "Prednisone or prednisolone for the treatment of chronic active hepatitis? A comparison of plasma availability." Br J Clin Pharmacol **5**(6): 501-505.
- de Arce Velasquez, A., L. M. Ferreira, et al. (2014). "Novel Pullulan-Eudragit(R) S100 blend microparticles for oral delivery of risedronate: formulation, in vitro evaluation and tableting of blend microparticles." Mater Sci Eng C Mater Biol Appl **38**: 212-217.
- Del Gaudio, P., G. Auriemma, et al. (2013). "Design of alginate-based aerogel for nonsteroidal anti-inflammatory drugs controlled delivery systems using prilling and supercritical-assisted drying." Journal of pharmaceutical sciences **102**(1): 185-194.
- Del Gaudio, P., G. Auriemma, et al. (2014). "Novel co-axial prilling technique for the development of core-shell particles as delayed drug delivery

- systems." European Journal of Pharmaceutics and Biopharmaceutics **87**(3): 541-547.
- Del Gaudio, P., P. Colombo, et al. (2005). "Mechanisms of formation and disintegration of alginate beads obtained by prilling." International Journal of Pharmaceutics **302**(1-2): 1-9.
- Del Gaudio, P., F. De Cicco, et al. (2015). "Alginate beads as a carrier for omeprazole/SBA-15 inclusion compound: A step towards the development of personalized paediatric dosage forms." Carbohydr Polym **133**: 464-472.
- Del Gaudio, P., P. Russo, et al. (2009). "Encapsulation of ketoprofen and ketoprofen lysinate by prilling for controlled drug release." Aaps Pharmscitech **10**(4): 1178-1185.
- Della Porta, G., P. Del Gaudio, et al. (2013). "Supercritical drying of alginate beads for the development of aerogel biomaterials: optimization of process parameters and exchange solvents." Industrial & Engineering Chemistry Research **52**(34): 12003-12009.
- Devdhawala Mehul, G. and K. Seth Avinash (2010). "Current status of chronotherapeutic drug delivery system: An overview." J Chem Pharm Res **2**(3): 312-328.
- Dhalleine, C., A. Assifaoui, et al. (2011). "Zinc-pectinate beads as an in vivo self-assembling system for pulsatile drug delivery." International Journal of Pharmaceutics **414**(1-2): 28-34.
- Di Colo, G., A. Baggiani, et al. (2006). "A new hydrogel for the extended and complete prednisolone release in the GI tract." Int J Pharm **310**(1-2): 154-161.
- Dumas, H., M. Tardy, et al. (1992). "Prilling process applied to collagen solutions." Drug Development and Industrial Pharmacy **18**(13): 1395-1409.
- Durazzo, T., S. Spencer, et al. (2008). "Temporal distributions of seizure occurrence from various epileptogenic regions." Neurology **70**(15): 1265-1271.
- El-Gibaly, I. (2002). "Oral delayed-release system based on Zn-pectinate gel (ZPG) microparticles as an alternative carrier to calcium pectinate beads for colonic drug delivery." International Journal of Pharmaceutics **232**(1): 199-211.
- El-Kamel, A., O. Al-Gohary, et al. (2010). "Alginate-diltiazem hydrochloride beads: optimization of formulation factors, in vitro and in vivo availability." Journal of microencapsulation.
- El-Nawawi, S. A. and Y. A. Heikal (1995). "Factors affecting the production of low-ester pectin gels." Carbohydrate Polymers **26**(3): 189-193.
- European Medicines Agency EMA, C. f. M. P. o. H. U. C. (2010). "Guidance on the Investigation of Bioequivalence (2010)."

- Ferrell, J. M. and J. Y. L. Chiang (2015). "Circadian rhythms in liver metabolism and disease." Acta Pharmaceutica Sinica B **5**(2): 113-122.
- Fotaki, N. (2011). "Flow-Through cell apparatus (usp apparatus 4): operation and features." Dissolution Technol **18**(4): 46-49.
- Gao, Z. (2009). "In vitro dissolution testing with flow-through method: a technical note." Aaps Pharmscitech **10**(4): 1401-1405.
- García-González, C., M. Alnaief, et al. (2011). "Polysaccharide-based aerogels—Promising biodegradable carriers for drug delivery systems." Carbohydrate Polymers **86**(4): 1425-1438.
- Gaumann, A., M. Laudes, et al. (2000). "Effect of media composition on long-term in vitro stability of barium alginate and polyacrylic acid multilayer microcapsules." Biomaterials **21**(18): 1911-1917.
- Gaweł, M., T. Librowski, et al. (2013). "Influence of zinc hydroaspartate on the anti-inflammatory and gastric activity of ketoprofen in rats." Pharmacological Reports **65**(1): 214-219.
- Gazzaniga, A., L. Palugan, et al. (2008). "Oral pulsatile delivery systems based on swellable hydrophilic polymers." European Journal of Pharmaceutics and Biopharmaceutics **68**(1): 11-18.
- Gentile, M., L. Boltri, et al. (1999). Parenteral pharmaceutical compositions containing ammoniomalkyl salts of 2-arylpropionic acids, Google Patents.
- Gibbs, J. E. and D. W. Ray (2013). "The role of the circadian clock in rheumatoid arthritis." Arthritis research & therapy **15**(1): 1.
- Gift, M., S. Behin, et al. (2015). "Formulation and Evaluation of Floating Pulsatile Drug Delivery System of Ibuprofen and Ranitidine Combination."
- Goh, C. H., P. W. S. Heng, et al. (2012). "Alginates as a useful natural polymer for microencapsulation and therapeutic applications." Carbohydrate Polymers **88**(1): 1-12.
- Grant, G. T., R. E. Morris, et al. (1973). "Biological interactions between polysaccharides and divalent cations: the egg-box model." FEBS Letters **32**(1): 195-198.
- Hazel, J. R. and B. D. Sidell (1987). "A method for the determination of diffusion coefficients for small molecules in aqueous solution." Analytical Biochemistry **166**(2): 335-341.
- Hermida, R. C., D. E. Ayala, et al. (2007). "Chronotherapy of hypertension: Administration-time-dependent effects of treatment on the circadian pattern of blood pressure." Advanced Drug Delivery Reviews **59**(9–10): 923-939.
- Higuchi, T. (1961). "Rate of release of medicaments from ointment bases containing drugs in suspension." Journal of pharmaceutical sciences **50**(10): 874-875.

- Hoffman, A. S. (2002). "Hydrogels for biomedical applications." Advanced Drug Delivery Reviews **54**(1): 3-12.
- Hoffman, A. S. (2012). "Hydrogels for biomedical applications." Advanced drug delivery reviews **64**: 18-23.
- Hu, J., A. Kyad, et al. (2005). "A comparison of dissolution testing on lipid soft gelatin capsules using USP apparatus 2 and apparatus 4." Dissolution Technol **12**(2): 6-9.
- Hu, K., E. J. Van Someren, et al. (2009). "Reduction of scale invariance of activity fluctuations with aging and Alzheimer's disease: Involvement of the circadian pacemaker." Proceedings of the National Academy of Sciences **106**(8): 2490-2494.
- Ishak, R. A. (2015). "Buoyancy-generating agents for stomach-specific drug delivery: an overview with special emphasis on floating behavior." J Pharm Pharm Sci **18**(1): 77-100.
- Jay, S. M. and W. M. Saltzman (2009). "Controlled delivery of VEGF via modulation of alginate microparticle ionic crosslinking." Journal of Controlled Release **134**(1): 26-34.
- Joseph, N. J., S. Lakshmi, et al. (2002). "A floating-type oral dosage form for piroxicam based on hollow polycarbonate microspheres: in vitro and in vivo evaluation in rabbits." J Control Release **79**(1-3): 71-79.
- Kamada, M., F. Hirayama, et al. (2002). "Cyclodextrin conjugate-based controlled release system: repeated-and prolonged-releases of ketoprofen after oral administration in rats." Journal of Controlled Release **82**(2): 407-416.
- Khan, S., A. Ullah, et al. (2016). "Insight into hydrogels." Designed Monomers and Polymers **19**(5): 456-478.
- Kim, I.-Y., S.-J. Seo, et al. (2008). "Chitosan and its derivatives for tissue engineering applications." Biotechnology Advances **26**(1): 1-21.
- Kim, Y., Y.-S. Kim, et al. (2010). "Molecular differences of low methoxy pectins induced by pectin methyl esterase I: Effects on texture, release and perception of aroma in gel systems." Food Chemistry **123**(2): 451-455.
- Krishnan, V., S. Sasikumar, et al. (2010). "Effect of pore forming agents on the physical characteristics and release kinetics of levofloxacin hemihydrate from floating alginate drug delivery system—an in vitro study." Trends Biomater Artif Organs **24**(3): 139-145.
- Lau, E. T., S. K. Johnson, et al. (2012). "Preparation and in vitro release of zein microparticles loaded with prednisolone for oral delivery." J Microencapsul **29**(7): 706-712.
- Lee, K. Y. and D. J. Mooney (2012). "Alginate: Properties and biomedical applications." Progress in Polymer Science **37**(1): 106-126.
- Lemmer, B. (1991). "Circadian rhythms and drug delivery." Journal of Controlled Release **16**(1-2): 63-74.

- Lévi F and O. A. (2011). "Circadian clocks and drug delivery systems: impact and opportunities in chronotherapeutics." **8**(12): 1535-1541.
- Levi, F., C. L. Louarn, et al. (1985). "Timing optimizes sustained-release indomethacin treatment of osteoarthritis." Clinical Pharmacology & Therapeutics **37**(1): 77-84.
- Lin, C.-C. and A. T. Metters (2006). "Hydrogels in controlled release formulations: Network design and mathematical modeling." Advanced Drug Delivery Reviews **58**(12–13): 1379-1408.
- Litinski, M., F. A. Scheer, et al. (2009). "Influence of the circadian system on disease severity." Sleep medicine clinics **4**(2): 143-163.
- Liu, L., M. L. Fishman, et al. (2005). "Interaction of various pectin formulations with porcine colonic tissues." Biomaterials **26**(29): 5907-5916.
- Liu, W. and R. Guo (2006). "Interaction between flavonoid, quercetin and surfactant aggregates with different charges." Journal of colloid and interface science **302**(2): 625-632.
- Liu, Z., Y. Jiao, et al. (2008). "Polysaccharides-based nanoparticles as drug delivery systems." Advanced drug delivery reviews **60**(15): 1650-1662.
- Lotlikar, V., U. Kedar, et al. (2010). "pH-responsive dual pulse multiparticulate dosage form for treatment of rheumatoid arthritis." Drug development and industrial pharmacy **36**(11): 1295-1302.
- Madsbad, S., B. Bjerregaard, et al. (1980). "Impaired conversion of prednisone to prednisolone in patients with liver cirrhosis." Gut **21**(1): 52-56.
- Maestroni, G., A. Sulli, et al. (2002). "Melatonin in rheumatoid arthritis: a disease-promoting and modulating hormone?" Clinical and experimental rheumatology **20**(6): 872.
- Maghsoodi, M. (2014). "Floating-pulsatile release multiparticulate system for chronopharmacotherapy: effect of some hydrophobic additives on the buoyancy and release behavior of particles." Drug Res **64**(1): 10-16.
- Mandal, S., S. S. Kumar, et al. (2010). "Development and evaluation of calcium alginate beads prepared by sequential and simultaneous methods." Brazilian journal of pharmaceutical sciences **46**(4): 785-793.
- Manjanna, K. M., K. S. Rajesh, et al. (2013). "Formulation and Optimization of Natural Polysaccharide Hydrogel Microbeads of Aceclofenac Sodium for Oral Controlled Drug Delivery." American Journal of Medical Sciences and Medicine **1**(1): 5-17.
- Maroni, A., M. D. Del Curto, et al. (2012). "Polymeric coatings for a multiple-unit pulsatile delivery system: Preliminary study on free and applied films." International Journal of Pharmaceutics(0).
- Marquardt, D. W. (1963). "An algorithm for least-squares estimation of nonlinear parameters." Journal of the society for Industrial and Applied Mathematics **11**(2): 431-441.

- Mazurek, S. and R. Szostak (2012). "Quantitative Determination of Prednisone in Tablets by Infrared Attenuated Total Reflection and Raman Spectroscopy." Journal of AOAC International **95**(3): 744-750.
- Mazzitelli, S., A. Tosi, et al. (2008). Production and Characterization of Alginate Microcapsules Produced by a Vibrational Encapsulation Device, Journal of Biomaterials Applications **23**: 123-145.
- McInnes, I. B. and G. Schett (2011). "The pathogenesis of rheumatoid arthritis." New England Journal of Medicine **365**(23): 2205-2219.
- Medina, J. R., D. K. Salazar, et al. (2014). "Comparative in vitro dissolution study of carbamazepine immediate-release products using the USP paddles method and the flow-through cell system." Saudi Pharmaceutical Journal **22**(2): 141-147.
- Mesbahi, G., J. Jamalian, et al. (2005). "A comparative study on functional properties of beet and citrus pectins in food systems." Food Hydrocolloids **19**(4): 731-738.
- Moogooee, M., H. Ramezanzadeh, et al. (2011). "Synthesis and in vitro studies of cross-linked hydrogel nanoparticles containing amoxicillin." Journal of pharmaceutical sciences **100**(3): 1057-1066.
- Mormont, M.-C., J. Waterhouse, et al. (2000). "Marked 24-h rest/activity rhythms are associated with better quality of life, better response, and longer survival in patients with metastatic colorectal cancer and good performance status." Clinical Cancer Research **6**(8): 3038-3045.
- Mukund, J. Y., B. R. Kantilal, et al. (2012). "Floating microspheres: a review." Brazilian Journal of Pharmaceutical Sciences **48**(1): 17-30.
- Nayak, K. P., P. Upadhyay, et al. (2014). "Gastroretentive drug delivery systems and recent approaches: A review." Journal of pharmaceutical research & opinion **2**(1).
- Neeharika, M. and B. J. Jyothi (2015). "CHRONOTHERAPEUTICS: AN OPTIMIZING APPROACH TO SYNCHRONIZE DRUG DELIVERY WITH CIRCADIAN RHYTHM." Journal of Critical Reviews **2**(4): 31-40.
- Ohdo, S., S. Koyanagi, et al. (2010). "Chronopharmacological strategies: Intra- and inter-individual variability of molecular clock." Advanced Drug Delivery Reviews **62**(9-10): 885-897.
- Okimoto, K., M. Miyake, et al. (1998). "Design and evaluation of an osmotic pump tablet (OPT) for prednisolone, a poorly water soluble drug, using (SBE)7m-beta-CD." Pharm Res **15**(10): 1562-1568.
- Orr, W. C., M. L. Allen, et al. (1994). "The pattern of nocturnal and diurnal esophageal acid exposure in the pathogenesis of erosive mucosal damage." American Journal of Gastroenterology **89**(4).

- Østberg, T., E. M. Lund, et al. (1994). "Calcium alginate matrices for oral multiple unit administration: IV. Release characteristics in different media." International Journal of Pharmaceutics **112**(3): 241-248.
- Pal, K., V. K. Singh, et al. (2013). "Hydrogel-based controlled release formulations: designing considerations, characterization techniques and applications." Polymer-Plastics Technology and Engineering **52**(14): 1391-1422.
- Palanisamy, M. and J. Khanam (2011). "Solid dispersion of prednisolone: solid state characterization and improvement of dissolution profile." Drug development and industrial pharmacy **37**(4): 373-386.
- Papageorgiou, S. K., E. P. Kouvelos, et al. (2010). "Metal-carboxylate interactions in metal-alginate complexes studied with FTIR spectroscopy." Carbohydrate Research **345**(4): 469-473.
- Patil, J., M. Kamalapur, et al. (2010). "Ionotropic gelation and polyelectrolyte complexation: the novel techniques to design hydrogel particulate sustained, modulated drug delivery system: a review." Digest Journal of Nanomaterials and Biostructures **5**(1): 241-248.
- Pavlova, M. K., S. A. Shea, et al. (2004). "Day/night patterns of focal seizures." Epilepsy & Behavior **5**(1): 44-49.
- Pawar, A. P., A. R. Gadhe, et al. (2008). "Effect of core and surface cross-linking on the entrapment of metronidazole in pectin beads." Acta Pharm **58**(1): 78-85.
- Peppas, N. A. and W. Leobandung (2004). "Stimuli-sensitive hydrogels: ideal carriers for chronobiology and chronotherapy." Journal of Biomaterials Science, Polymer Edition **15**(2): 125-144.
- Perry, M. G., J. Kirwan, et al. (2009). "Overnight variations in cortisol, interleukin 6, tumour necrosis factor α and other cytokines in people with rheumatoid arthritis." Annals of the rheumatic diseases **68**(1): 63-68.
- Pickup, M. E. (1979). "Clinical pharmacokinetics of prednisone and prednisolone." Clin Pharmacokinet **4**(2): 111-128.
- Pillay, V. and R. Fassihi (1999). "In vitro release modulation from crosslinked pellets for site-specific drug delivery to the gastrointestinal tract. I. Comparison of pH-responsive drug release and associated kinetics." J Control Release **59**(2): 229-242.
- Pillay, V. and R. Fassihi (1999). "In vitro release modulation from crosslinked pellets for site-specific drug delivery to the gastrointestinal tract: II. Physicochemical characterization of calcium-alginate, calcium-pectinate and calcium-alginate-pectinate pellets." Journal of Controlled Release **59**(2): 243-256.
- Prajapati, C. V., R. P. Patel, et al. (2012). "Formulation, optimization and evaluation of sustained release microsphere of ketoprofen." J Pharm Bioallied Sci **4**(Suppl 1): 0975-7406.

- Radwan, M. A., A. E. S. F. Abou el Ela, et al. (2015). "Pharmacokinetics and analgesic effect of ketorolac floating delivery system." Drug Delivery **22**(3): 320-327.
- Rafnsson, V., H. Tulinius, et al. (2001). "Risk of breast cancer in female flight attendants: a population-based study (Iceland)." Cancer Causes & Control **12**(2): 95-101.
- Ramteke, K., V. Jadhav, et al. (2012). "Microspheres: As carriers used for novel drug delivery system." IOSRPHR **2**(4): 44-48.
- Ritger, P. L. and N. A. Peppas (1987). "A simple equation for description of solute release I. Fickian and non-Fickian release from non-swellable devices in the form of slabs, spheres, cylinders or discs." Journal of Controlled Release **5**(1): 23-36.
- Rockville, M. (1997). FDA Guidance for Industry: extended release oral dosage forms: development, evaluation and application of in vitro/in vivo correlation.
- Roy, P. and A. Shahiwala (2009). "Statistical optimization of ranitidine HCl floating pulsatile delivery system for chronotherapy of nocturnal acid breakthrough." European Journal of Pharmaceutical Sciences **37**(3-4): 363-369.
- Sajan, J., T. Cinu, et al. (2009). "Chronotherapeutics and chronotherapeutic drug delivery systems." Tropical Journal of Pharmaceutical Research **8**(5).
- Sato, Y. and O. Miyawaki (2008). "Analysis of intermolecular interaction among pectin molecules in aqueous sugar solutions." Food science and technology research **14**(3): 232-238.
- Schäcke, H., W.-D. Döcke, et al. (2002). "Mechanisms involved in the side effects of glucocorticoids." Pharmacology & therapeutics **96**(1): 23-43.
- Sharma, D., S. K. Sharma, et al. "A REVIEW ON MULTIPARTICULATE FLOATING DRUG DELIVERY SYSTEM."
- Shea, S. A., M. F. Hilton, et al. (2007). Day/Night Pattern of Myocardial Infarction and Sudden Cardiac Death. Blood pressure monitoring in cardiovascular medicine and therapeutics, Springer: 253-291.
- Shohin, I. E., J. I. Kulinich, et al. (2014). "Biowaiver Monographs for Immediate Release Solid Oral Dosage Forms: Piroxicam." Journal of Pharmaceutical Sciences **103**(2): 367-377.
- Singh, A., P. K. Sharma, et al. (2011). "Release behavior of drugs from various natural gums and polymers." Polimery w medycynie **41**(4): 73-80.
- Singh, B. N. and K. H. Kim (2000). "Floating drug delivery systems: an approach to oral controlled drug delivery via gastric retention." Journal of Controlled Release **63**(3): 235-259.

- Singh, B. N. and K. H. Kim (2000). "Floating drug delivery systems: an approach to oral controlled drug delivery via gastric retention." J Control Release **63**(3): 235-259.
- Singh, M., K. Hemant, et al. (2011). "Microencapsulation: A promising technique for controlled drug delivery." Research in pharmaceutical sciences **5**(2): 65-77.
- Skowrya, J., K. Pietrzak, et al. (2015). "Fabrication of extended-release patient-tailored prednisolone tablets via fused deposition modelling (FDM) 3D printing." Eur J Pharm Sci **68**: 11-17.
- Smith, D. H., J. M. Neutel, et al. (2001). "A new chronotherapeutic oral drug absorption system for verapamil optimizes blood pressure control in the morning." American journal of hypertension **14**(1): 14-19.
- Smolen, J. S., D. Aletaha, et al. (2016). "Rheumatoid arthritis." The Lancet **388**(10055): 2023-2038.
- Smolensky, M. H. and N. A. Peppas (2007). "Chronobiology, drug delivery, and chronotherapeutics." Advanced drug delivery reviews **59**(9): 828-851.
- Sriamornsak, P. (2003). "Chemistry of pectin and its pharmaceutical uses: A review." Silpakorn University International Journal **3**(206-228).
- Sriamornsak, P. and J. Nunthanid (1998). "Calcium pectinate gel beads for controlled release drug delivery:: I. Preparation and in vitro release studies." International Journal of Pharmaceutics **160**(2): 207-212.
- Stigliani, M., R. P. Aquino, et al. (2013). "Non-steroidal anti-inflammatory drug for pulmonary administration: design and investigation of ketoprofen lysinate fine dry powders." International Journal of Pharmaceutics **448**(1): 198-204.
- Straub, R. H. and M. Cutolo (2007). "Circadian rhythms in rheumatoid arthritis: implications for pathophysiology and therapeutic management." Arthritis & Rheumatism **56**(2): 399-408.
- Sugawara, S., T. Imai, et al. (1994). "The controlled release of prednisolone using alginate gel." Pharm Res **11**(2): 272-277.
- Sulli, A., G. Maestroni, et al. (2002). "Melatonin serum levels in rheumatoid arthritis." Annals of the New York Academy of Sciences **966**(1): 276-283.
- Surve, S. B., A. D. Sapkal, et al. (2013). "CHRONOTHERAPY-A NEW VISTA IN NOVEL DRUG DELIVERY: An Overview."
- Tagde, P., N. Jain, et al. (2012). "Formulation & Evaluation of Bilayer Floating Tablets Of Metoprolol Tartrate." International Journal of Biomedical and Advance Research **3**(2): 122-128.
- Taha, M. O., W. Nasser, et al. (2008). "Sodium lauryl sulfate impedes drug release from zinc-crosslinked alginate beads: Switching from enteric coating release into biphasic profiles." International Journal of Pharmaceutics **350**(1): 291-300.

- Tavares, R., G. A. Wells, et al. (2010). "Classification of rheumatologic opinion on early inflammatory arthritis: Harmonization of a heterogeneous standard." Arthritis Care & Research **62**(10): 1407-1414.
- Tiwari, G., T. R., et al. (2012). "Drug delivery systems: An updated review." Int J Pharm Investig. **2**(1): 2–11.
- To, H. (2016). "Chronotherapy for rheumatoid arthritis: current perspectives." Dovepress **2016:6**: 47-53.
- Tous, S., M. Fathy, et al. (2014). "Preparation and evaluation of ketoprofen-loaded calcium alginate beads." Int J Pharm Tech Res **6**(3): 1100-1112.
- Tran, V.-T., J.-P. Benoît, et al. (2011). "Why and how to prepare biodegradable, monodispersed, polymeric microparticles in the field of pharmacy?" International Journal of Pharmaceutics **407**(1): 1-11.
- U.S. Department of Health and Human Services, F. a. D. A., Center for Drug Evaluation and Research (CDER) (2000). Guidance for industry: Waiver of in vivo bioavailability and bioequivalence studies for immediate-release solid oral dosage forms based on a Biopharmaceutics Classification System. Accessed December 20, 2010.
- Van der Velden, V. (1998). "Glucocorticoids: mechanisms of action and anti-inflammatory potential in asthma." Mediators of inflammation **7**(4): 229-237.
- Verbeeck, R., C. Richardson, et al. (1986). "Clinical pharmacokinetics of piroxicam." The Journal of rheumatology **13**(4): 789-796.
- Verma, A., M. Sharma, et al. (2013). "Floating alginate beads: studies on formulation factors for improved drug entrapment efficiency and in vitro release." Farmacia **61**(1): 143-161.
- Vino, S., P. Paryani, et al. (2012). "Formulation and evaluation of chitosan beads of levocetirizine dihydrochloride." Journal of Applied Pharmaceutical Science **2**(8): 221.
- Voo, W. P., P. Ravindra, et al. (2011). "Comparison of alginate and pectin based beads for production of poultry probiotic cells." J Biosci Bioeng **111**(3): 294-299.
- Vrečer, F., M. Vrbinc, et al. (2003). "Characterization of piroxicam crystal modifications." Int J Pharm **256**(1-2): 3-15.
- Wagh, V. D. and P. Kalshetti (2011). "Chronopharmaceutics: Dosage form design to rhythms in disease state." JChrDD **2**(1): 23-29.
- Walker, S. E. and J. D. Jacobson (2000). "Roles of prolactin and gonadotropin-releasing hormone in rheumatic diseases." Rheumatic Disease Clinics of North America **26**(4): 713-736.
- Ware, M., S. P. Tiwari, et al. (2013). "New insights into gastro-retentive floating drug delivery systems." World J Pharma Sci **3**(1): 252-270.

- Wen, H. and K. Park (2011). Oral controlled release formulation design and drug delivery: Theory to practice, John Wiley & Sons.
- White, R. J., V. Budarin, et al. (2009). "Tunable porous carbonaceous materials from renewable resources." Chemical Society Reviews **38**(12): 3401-3418.
- WHO, W. H. O. (2006). Proposal to waive in vivo bioequivalence requirements for WHO Model List of Essential Medicines immediate-release, solid oral dosage forms, Technical Report Series.
- Yang, L., J. S. Chu, et al. (2002). "Colon-specific drug delivery: new approaches and in vitro/in vivo evaluation." International Journal of Pharmaceutics **235**(1-2): 1-15.
- Youan, B.-B. C. (2004). "Chronopharmaceutics: gimmick or clinically relevant approach to drug delivery?" Journal of Controlled Release **98**(3): 337-353.
- Zhang, Z., R. Zhang, et al. (2016). "Encapsulation of β -carotene in alginate-based hydrogel beads: Impact on physicochemical stability and bioaccessibility." Food Hydrocolloids **61**: 1-10.
- Zvonar, A., J. Kristl, et al. (2009). High celecoxib-loaded nanoparticles prepared by a vibrating nozzle device, Journal of Microencapsulation. **26**: 748-759.